

2004

Building a comprehensive energy model for off-highway vehicles with emphasis on vehicle thermal control systems

Ayhan Zora
University of Northern Iowa

Let us know how access to this document benefits you

Copyright ©2004 Ayhan Zora

Follow this and additional works at: <https://scholarworks.uni.edu/etd>



Part of the [Automotive Engineering Commons](#), and the [Heat Transfer, Combustion Commons](#)

Recommended Citation

Zora, Ayhan, "Building a comprehensive energy model for off-highway vehicles with emphasis on vehicle thermal control systems" (2004). *Dissertations and Theses @ UNI*. 506.

<https://scholarworks.uni.edu/etd/506>


This Open Access Dissertation is brought to you for free and open access by the Student Work at UNI ScholarWorks. It has been accepted for inclusion in Dissertations and Theses @ UNI by an authorized administrator of UNI ScholarWorks. For more information, please contact scholarworks@uni.edu.

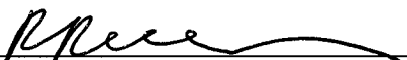
Offensive Materials Statement: Materials located in UNI ScholarWorks come from a broad range of sources and time periods. Some of these materials may contain offensive stereotypes, ideas, visuals, or language.

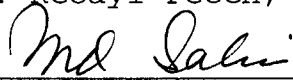
BUILDING A COMPREHENSIVE ENERGY MODEL
FOR OFF-HIGHWAY VEHICLES
WITH EMPHASIS ON VEHICLE THERMAL CONTROL SYSTEMS

A Dissertation
Submitted
in Partial Fulfillment
of the Requirements for the Degree
Doctor of Industrial Technology

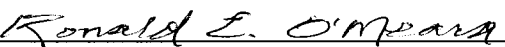
Approved:


Dr. Mohammed Fahmy, Chair


Dr. Recayi Pecen, Co-Chair


Dr. MD Salim, Committee Member


Dr. John W. McCormick, Committee Member


Dr. Ronald E. O'Meara, Committee Member

Ayhan Zora

University of Northern Iowa

December 2004

UMI Number: 3153975

INFORMATION TO USERS

The quality of this reproduction is dependent upon the quality of the copy submitted. Broken or indistinct print, colored or poor quality illustrations and photographs, print bleed-through, substandard margins, and improper alignment can adversely affect reproduction.

In the unlikely event that the author did not send a complete manuscript and there are missing pages, these will be noted. Also, if unauthorized copyright material had to be removed, a note will indicate the deletion.

UMI[®]

UMI Microform 3153975

Copyright 2005 by ProQuest Information and Learning Company.

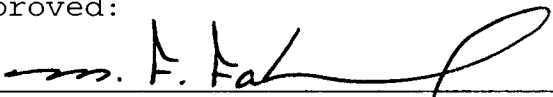
All rights reserved. This microform edition is protected against unauthorized copying under Title 17, United States Code.

ProQuest Information and Learning Company
300 North Zeeb Road
P.O. Box 1346
Ann Arbor, MI 48106-1346

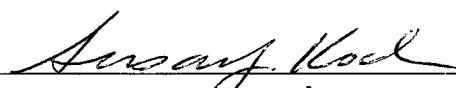
BUILDING A COMPREHENSIVE ENERGY MODEL
FOR OFF-HIGHWAY VEHICLES
WITH EMPHASIS ON VEHICLE THERMAL CONTROL SYSTEMS

An Abstract of a Dissertation
Submitted
in Partial Fulfillment
of the Requirements for the Degree
Doctor of Industrial Technology

Approved:



Dr. Mohammed Fahmy, Committee Chair



Dr. Susan J. Koch,
Interim Dean of the Graduate College

Ayhan Zora
University of Northern Iowa
December 2004

ABSTRACT

Utilizing machine and thermal system simulations (vehicle energy models) can be very helpful for vehicle manufacturing companies to develop a machine with acceptable component temperatures, less heat loads to the vehicle cooling systems, and reduced emissions that will also reduce overall product development cycle.

Energy models of vehicles were developed mostly in the automotive industry, and most of these studies were based on partial energy models.

The aim of this research study was to create a comprehensive energy model for agricultural machinery, which will be a basis for future work on similar products. A tractor model from a Midwest off-road machinery manufacturing company was selected as a starting point for modeling. The work in creating the model has been presented in detail. Verification of the simulation model has been carried out using the results from three different wind tunnel tests that have been conducted by the Midwest company; namely the PTO test, the AXLE test, and the high-speed wind tunnel transport test.

The critical parameters were selected to be analyzed for each test were the top tank Temperature, the intake

manifold temperature, the oil cooler inlet temperature, the oil cooler outlet temperature, the fuel cooler inlet temperature, the fuel cooler outlet temperature, the fan speed, the engine speed, the PTO torque and the axle torque.

Based on the analysis of data, it was concluded that the comprehensive energy model is adequately representing the selected tractor model from the energy distribution and the component temperatures point of view. Therefore, it can be used for specific field missions that are not easy to conduct in a wind tunnel set up to acquire data for the critical parameters.

ACKNOWLEDGEMENTS

First of all, I express my deepest appreciation to my committee members for their continuous support, help and guidance throughout my course of study and the completion of this research. The discussions with Dr. Mohammed Fahmy, my advisor, were always the greatest help in my study with his invaluable experience in academic and nonacademic life. He really proved that he cares about his students with his outstanding guidance, and affectionate authority. Dr. Pecen, my co-advisor, has provided a great support through discussions and recommendation in a friendly manner that students would always like to have with their advisors. Dr. MD Salim, Dr. John W. McCormick and Dr. Ronald E. O'Meara helped me through suggestions on validation of the model and proof reading.

I want to thank to Mr. Ron Burk and Mr. Boris Volfson for their indisputably needed contributions to this study. Besides supplying a comfortable working environment in the company, Mr. Burk has facilitated the understanding the physics of components in off-highway vehicles for the author with his extraordinary experience. Mr. Volfson has enabled transferring this understanding into the simulation-modeling world. Without having his directives

and always questioning character, the research would not be this much inspirational.

I would like to thank with deep gratitude to my wife Yıldız K. Zora, who made many personal sacrifices to ensure a stable household and a positive studying environment for me. Additionally, to our children, Betül, Alparslan and Reyhan, who all tolerated my late night classes, weekend studying, and most of all, their understanding as to why Dad could not attend some of their school and after school activities. My heart goes to all of you.

Special thanks to my parents Leman and Ruhi Zora for their life long support and love. They instilled within me the drive and persistence necessary to complete a task. I love you both.

In closing, I want to recognize the intellectual and spiritual support of M. Fethullah Gülen Hocaefendi. Without his encouragement I would not even think to pursue an academic life beyond my bachelors degree. His ideas have been the light for my life.

TABLE OF CONTENTS

	PAGE
LIST OF TABLES	viii
LIST OF FIGURES	x
LIST OF EQUATIONS	xiii
CHAPTER 1. INTRODUCTION	1
Background	1
Statement of Need	3
Statement of Problem	3
Statement of the Purpose	3
Research Questions	4
Assumptions	4
Limitations	5
Definition of Terms	5
Summary	9
CHAPTER 2. REVIEW OF LITERATURE	10
Introduction	10
Existing Simulation Programs	10
An overview on EASY5	11
Energy Models	16
Benefits of Vehicle Simulation	19
CHAPTER 3. METHODOLOGY AND DESIGN	21
Introduction	21

Model Development	21
Missions	22
High speed transport mission	22
Primary tillage mission	23
Selected Tests	24
PTO test	24
Axle test	25
Wind tunnel high-speed transport test	25
Development Strategy	25
Verification of Model	27
CHAPTER 4. RESULTS AND DISCUSSIONS	28
Developing the Components of Simulation	28
Engine	28
Simulation model in WAVE	29
Running the WAVE engine model.	34
An alternative model for engine.	36
Approximations in alternative CAC circuit.	40
Transmission	41
Easy5 model for the transmission.	42
PTO Drive	44
Vistronic Fan Drive	44
Transmission Oil Circuit	47
Implement Hydraulic Circuit	49
Heat calculations for pumps	50

Heat rejection calculation for the oil cooler	52
Fuel Cooler Circuit	55
Heat calculations for pumps	57
Heat rejection calculation for the fuel cooler	57
Recirculation of Air Effect	59
Controlled Torque Applied to PTO Shaft and Rear Axles	63
PTO torque generator	63
Rear AXLE torque generator	65
Theory for the rotating inertia	67
Front and Rear Differentials	68
Final Drives	68
Vehicle Dynamics	69
Ground and Terrain	73
Tires	75
Implement Load	77
Verification of the Developed Model	79
Comparison with PTO Test Data	80
Comparison with AXLE Test Data	87
Comparison with High Speed Wind Tunnel Transport Test Data	94
CHAPTER 5. CONCLUSIONS, RECOMMENDATIONS AND SUMMARY	102
Research Questions of the Study	102
Recommendations for Future Work	104

Summary of the Study	106
REFERENCES	108
APPENDIX A: HELP DOCUMENT FOR RS LIBRARY USED CONNECTING WAVE AND EASY5	112
APPENDIX B: POWER SHIFT TRANSMISSION AND PTO	115
APPENDIX C: OVERALL STRATEGY DIAGRAM OF THE VARIABLE SPEED FAN CONTROL	119
APPENDIX D: TRANSMISSION AND HYDRAULIC OIL CIRCUIT	121

LIST OF TABLES

TABLE	PAGE
1 EPA Emission Standards for Off-highway Vehicles	1
2 Some Standard Libraries in Easy5	12
3 Groups of Components in General Purpose Library	13
4 Selected Tests and Missions and Their Required Components	26
5 Target Toptank Temperature If PTO is Engaged	46
6 Target Toptank Temperature If PTO is not Engaged ...	46
7 Volumetric Flow Rates of Hydraulic Pumps	48
8 Heat Rejection (kW) Specification for the Oil Cooler	52
9 Heat Rejection per ETD for the Fuel Cooler	54
10 Heat Rejection (kW) for the Fuel Cooler	58
11 Heat Rejection per ETD for the Fuel Cooler	58
12 Temperature Difference from the Ambient Because of Recirculation of Air Effect	61
13 Efficiencies and Gear Ratios for the Final Drives ..	69
14 Geometric Dimension and Physical Inputs to M3 Component	72
15 Cone Index for Different Soil Types	75
16 Tire Selection Codes and Tire Dimensions for the Tractor	77
17 The PTO Test Data for Selected Parameters	81
18 Percentage Errors of the Simulation Results from the PTO Test Data	86
19 The AXLE Test Data for Selected Parameters	88

20	Percentage Errors of the Simulation Results from the AXLE Test Data	93
21	The High-speed Wind Tunnel Transport Test Data for Selected Parameters	95
22	Percentage Errors of the Simulation Results from the AXLE Test Data	101

LIST OF FIGURES

FIGURE	PAGE
1 A schematic for connecting components in Easy5	14
2 Hierarchical structure of vehicle model	22
3 Ground profile for high speed transport test	23
4 A schematic for the turbocharged diesel engine	29
5 WAVE engine model for diesel engine	31
6 Demonstrating application of WAVE model in Easy5 ...	33
7 Inputs to WV component	34
8 A snapshot from the WAVE engine model running	35
9 Alternative charge air cooler (CAC) circuit schematic	36
10 A schematic of energy balance for diesel engines ...	37
11 Easy5 model for the alternative CAC circuit	39
12 Power shift transmission for the tractor	41
13 Easy5 model for power shift transmission	42
14 Easy5 model for PTO drive	44
15 The Easy5 model for vistronic fan drive	47
16 The Easy5 model for oil cooler hydraulic circuit ...	49
17 The Easy5 model for implement hydraulic circuit	50
18 Easy model for the fuel circuit	56
19 The schematic for recirculation of air effect	60
20 Recirculation Effect on Air Temperature at Grill Screen	62

21	PTO torque generator connected to torque summing junction	64
22	Rear AXLE connected with tires	65
23	Axle torque generator is connected to the rear axle	66
24	The usage of M3 and GT in the CEM	70
25	The schematic of planar vehicle dynamics	71
26	The schematic for ground and terrain model	73
27	An overall view to comprehensive energy model the tractor	76
28	A schematic for three-point hitch for tractor	78
29	Comparing the simulation against the PTO test for Toptank temperature	82
30	Comparing the simulation against the PTO test for intake manifold temperature	83
31	Comparing the simulation against the PTO test for oil cooler inlet temperature	83
32	Comparing the simulation against the PTO test for oil cooler outlet temperature	84
33	Comparing the simulation against the PTO test for fuel cooler inlet temperature	84
34	Comparing the simulation against the PTO test for fuel cooler outlet temperature	85
35	Comparing the simulation against the PTO test for fan speed	85
36	Comparing the simulation against the PTO test for PTO torque	86
37	Comparing the simulation against the AXLE test for Toptank temperature	89
38	Comparing the simulation against the AXLE test for intake manifold temperature	90

39	Comparing the simulation against the AXLE test for oil cooler inlet temperature	90
40	Comparing the simulation against the AXLE test for oil cooler outlet temperature	91
41	Comparing the simulation against the AXLE test for fuel cooler inlet temperature	91
42	Comparing the simulation against the AXLE test for fuel cooler outlet temperature	92
43	Comparing the simulation against the AXLE test for fan speed	92
44	Comparing the simulation against the AXLE test for axle torque	93
45	Comparing the simulation against the high-speed wind tunnel transport test for Toptank temperature	96
46	Comparing the simulation against the high-speed wind tunnel transport test for intake manifold temperature	97
47	Comparing the simulation against the high-speed wind tunnel transport test for oil cooler inlet temperature	97
48	Comparing the simulation against the high-speed wind tunnel transport test for oil cooler outlet temperature	98
49	Comparing the simulation against the high-speed wind tunnel transport test for fuel cooler inlet temperature	98
50	Comparing the simulation against the high-speed wind tunnel transport test for fuel cooler outlet temperature	99
51	Comparing the simulation against the high-speed wind tunnel transport test for fan speed	99
52	Comparing the simulation against the high-speed wind tunnel transport test for the engine speed ..	100

LIST OF EQUATIONS

EQUATION	PAGE
1 Equation for simulation speed	34
2 Energy balance for the control volume in diesel engine	37
3 Equation of heat due to inefficiency in gear	43
4 Equation of heat due to windage losses	43
5 Calculation of the heat generation due to pump inefficiency by using pump power	51
6 Calculation of power of a pump	51
7 Calculation of the heat generation due to pump inefficiency	51
8 Conversion of ambient air speed to air mass flow rate	53
9 Conversion of volumetric flow rate to mass flow rate	53
10 Heat rejection from an heat exchanger per entrance temperance difference	53

CHAPTER 1

INTRODUCTION

Background

The off-highway sector has been under increasing pressure to lessen operating costs and emissions ("A Joint Venture," 2001). The main reason of the pressure stems from the regulation of the U.S. Environmental Protection Agency (EPA). In 1990 amendments to the Clean Air Act authorized the EPA to regulate off-highway diesel engine emissions for new engines. The regulations on particulate matter (PM) and oxides of nitrogen (NOx) emissions for the engines between 50 and 750 hp (37.5 - 562.5 kW) are listed in Table 1.

Table 1

EPA Emission Standards for Off-highway Vehicles

Tier	Year	NOx
Tier 1	1996-1999	Reduce 35%
Tier 2	2001-2004	Reduce 30% over Tier 1
Tier 3	2006-2008	Reduce 35% over Tier 2
Tier 4	2010+	-

Recognizing the need for the off-highway vehicle industry, the Society of Automotive Industry and U.S.

Department of Energy (DOE) organized a joint meeting to determine critical research and development (R&D) areas for minimizing off-highway vehicle emissions while maintaining or improving system performance ("A Joint Venture," 2001). Their meeting report stated "using machine and thermal system simulations and various types of cooling system models is increasingly important to develop a machine with acceptable component temperatures, emissions control, and the sound levels within increasingly shorter product development cycles."

Companies are expected to run numerous tests on prototypes to validate their products before selling them to customers. "In general, prototype testing is an expensive tool for the design as there are many applicable component configurations as well as a large number of physical variables that need to be measured during testing and validation" (Joshi & Jayan, 2002). Ability to predict heat loads and critical temperatures without conducting expensive and time-consuming prototype tests can help companies to reduce cost and to be more competitive.

Therefore a comprehensive energy simulation model, which has the ability to predict heat loads and critical temperatures in off-highway vehicles, can be a useful tool

for vehicle manufacturing companies in the competitive market.

Statement of Need

The need for this study was based on the importance of reducing the high testing costs and impracticality of testing and measuring the critical parameters on off-highway machinery during field runs. There was also a need for a comprehensive energy model to reach the emission requirements of EPA by improving thermal management in such vehicles ("A Joint Venture," 2001). Although there have been studies on developing partial energy models in the automotive industry (Valeo, 2002), a limited number of studies were published in this area for off-highway machinery.

Statement of Problem

The problem of this research study was to calculate design parameters (e.g. critical temperatures, pressures, and velocities) of off-highway vehicles for specified tests and missions.

Statement of the Purpose

The purpose of this study was to develop a comprehensive energy simulation model, which can be applied to other vehicles using similar components, for off-highway

vehicles with emphasis on thermal control systems, so that it can accurately calculate critical design parameters.

Research Questions

The following research questions will provide direction for this study:

1. Is EASY5 simulation package adequate to create a comprehensive energy model for off-highway vehicles?
2. With what accuracy the comprehensive energy model represents the off-highway machines?

Assumptions

In this study, the following assumptions were made as a basis for the subsequent analysis:

1. It was assumed that incorporation in between Easy5 and WAVE software packages is possible.
2. It was assumed that there are enough numbers of tests that were conducted to validate the model.
3. It was assumed that the comprehensive energy model can be used in design processes to reduce the production cost?
4. It was assumed that the comprehensive energy model can be used in design processes to reduce

heat loads to the cooling systems of the vehicle, and hence to improve emissions?

Limitations

The following limitations were innate in this research study:

1. This study was limited to agricultural vehicles classified as off-highway machinery.
2. This study used a limited number of missions in its accomplishment.
3. The model created in this study can run only in Unix operating system and Windows operating system with Exceed XWindow emulator (Johnson, 2000).

Definition of Terms

In order to bring the reader to a common base, some of the terms are defined, even though they are not unique to this study.

Aftercooler: Look definition of Charge Air Cooler.

Charge Air Cooler (CAC): A heat exchanger utilized to cool the heated intake air due to compression. It can be also called as intercooler or aftercooler.

Cone index (CI): "The force per unit basal area required to push a cone penetrometer through a specified increment of soil" ("Soil Science Society," 2004).

Cone penetrometer: "An instrument in the form of a cylindrical rod with a cone-shaped tip designed for penetrating soil and for measuring the end-bearing component of penetration resistance. The resistance to penetration developed by the cone equals the vertical force applied to the cone divided by its horizontally projected area" ("Soil Science Society," 2004).

CPUSEC: Central Processing Unit (CPU) time in seconds

Dyno: A torque generator used to apply torque on PTO and/or axle shafts.

EASY5 (Engineering Analysis Systems): An engineering analysis simulation software package originally created by Boeing Inc. and currently owned by MSC Software Inc.

Entrance Temperature Difference (ETD): The temperature difference of inlet inner circulating fluid and inlet outer cooling air.

Exceed: XWindow terminal software. Exceed provides the ability for the user to run and display UNIX applications (X clients) from the familiar Microsoft Windows environment.

Final Drive: A gearbox between tires and differential.

Grill Screen: The screen in front of the tractor that the ambient air goes through and reaches to heat exchangers.

Grill Screen Restriction: Because of the work condition the grill screen is blocked out with dirt and applies additional pressure restriction to ambient air.

Head Wind: The wind blows from the front to the rear of the tractor.

Intake manifold temperature: The temperature of air at the intake manifold of engine.

Intercooler: Look definition of Charge Air Cooler.

Off-highway vehicles: According to U.S. Environmental Protection Agency's (EPA) definition "the off-highway includes outdoor power equipment, recreational vehicles, farm and construction machinery, lawn and garden equipment, marine vessels, locomotives, aircraft, and other applications" ("A Joint Venture," 2001). In this study the definition of off-highway, or non-road, term will be restricted to only surface-based agriculture vehicles.

Oil cooler inlet temperature: The temperature of lubricating oil at the inlet of oil cooler.

Power-Take-Off (PTO): a shaft mechanism in the back of a tractor, which is used for driving implements.

Product development cycle: the time of how long it will take to produce a specific product through the manufacturing cycle.

Proportional and Integral (PI) Controller: A controller that generates the output depending on the input and feedback parameters with the use of integral and proportional constant.

Rated Speed: "EPA proposes that the rated speed of any engine shall be defined at the single point on an engine's maximum-power versus speed curve that lies farthest away from the zero-power, zero-speed point on a normalized maximum-power versus speed plot" ("Federal Register," 1998, p. 68529)

RPM: Rotation per minute.

Tail Wind: The wind blows from the rear to the front of the tractor.

Toptank temperature: A radiator consists of two tanks (top and bottom) with pipes and fins in between. The direction of the flow of coolant is from top to bottom. The temperature of coolant in the tank at the top is called Toptank temperature.

Vistronic Fan Drive: A fan drive that generates fan speed electronically depending on critical input temperatures.

WAVE: One-dimensional engine simulation package developed by Ricardo Inc.

Windage: "the retarding force of air friction on a moving object" ("HyperDictionary," 2003).

Summary

The aim of this research study was to create a comprehensive energy model for agricultural machinery, which will be a basis for future work on similar products. A tractor model from a Midwest off-road machinery manufacturing company was selected as a starting point for modeling. The work in creating the model will be presented in detail. Verification and validation of the simulation model will be carried out using the results from tests that have been already conducted by the Midwest company. Finally results will be demonstrated based on outcomes of two complete missions, namely high-speed transport mission and primary tillage mission.

CHAPTER 2

REVIEW OF LITERATURE

Introduction

In the review of literature a variety of simulation models and laboratory tests were examined. The summary of this review of literature has been divided into five categories: (a) Simulation programs, (b) An overview on Easy5, (c) Applications of Easy5, (d) Energy models, and (e) Benefits of vehicle simulation.

Existing Simulation Programs

"Standardized software techniques exist for modeling the dynamics of off-highway machinery. There exists several commercial modeling and simulation program such as Dymola, Dynasty, Easy5, Hydraulics Block-Set, and others which have hydraulic system capability along with the capability to model other types of systems such as linkages and electrical systems" (Fales, 2004). Another widely used simulation program for system development is MatLab/Simulink.

WAVE engine simulation program has been developed by Ricardo Software. "WAVE is a leading engine performance and 1-D gas dynamics simulation software with licenses in truck, agricultural, locomotive, marine and power

generation. WAVE enables performance simulations to be carried out based on virtually any intake, combustion and exhaust system design" (Diesel & Gas Turbine Publications, 2000). It deserves the leading position not only by its functionality letting the user to analyze any combination of system design, but also its connectivity to other industry-standard commercial programs such as Easy5 and MatLab/Simulink.

A simplified energy model (SEM) was previously developed in Deere and Company for tractors in Easy5. Considering convenience of using a lot of components, which was modeled for SEM, and availability of licenses, Easy5 has been selected as development environment for this study. Hence, in this review of literature, only Easy5 simulation package will be investigated further.

An overview on EASY5

"EASY5 is a graphics-based software tool used to model, simulate, and design dynamic systems characterized by differential, difference, and algebraic equations." ("EASY5 Overview," n.d.). Boeing Inc developed it for use within the Aerospace Industry. Under its new owner, MSC.Software, it has grown to be a full-featured simulation package (Favate, 2002).

Diaz-Calderon (2000) combines commercial simulation packages under three major categories: (1) block-diagrams, (2) object-oriented modeling and (3) bond graphs. He places Easy5 in the first category by stating that Easy5 is "based on an interactive environment for modeling where the user defines the system as a network of interconnected." He also points out that "Easy5 takes the modeling approach a step further in which the system is modeled by defining the interactions between components instead of between simulation blocks as with the block-diagram approach" (Diaz-Calderon, 2000).

Table 2

Some Standard Libraries in Easy5

Libraries	
General Purpose	Interactive Simulation
Ricardo Engine	Ricardo Planetary Kit
Gas Dynamics	Aerospace Vehicle
Basic Hydraulic	Ricardo Powertrain Advanced
Thermal Hydraulic	Ricardo Electric Systems

In EASY5, models are built from basic mathematical blocks, such as summers, dividers, and integrators, and

special systems-level components such as engines, transmissions, differentials, gears, pipes, orifices, actuators, heat exchangers, clutches, etc. All of these blocks are contained in the standard libraries (Society of Automotive Engineers, 1992). Some of the libraries are listed in Table 2.

Components are even grouped further within the libraries. The groups for general purpose library are listed in Table 3.

Table 3

Groups of Components in General Purpose Library

Groups	
Cont. Xfer Functions	Nonlinear Effects
Discrete Functions	Tabular Functions
Sum/Multiply/Divide	Logic
Integrators	Data Analysis
Controllers	Special Purpose
Switches	Math Functions
Function Generators	Struct./Forces

For example, the Sum/Multiply/Divide group contains Divider, Gain Block, Product, Multiply and Add

(Multiplexed), and Summing Junction. Besides having standard libraries, Easy5 allows the modeler to create and build up user-defined libraries. Moreover, FORTRAN and C programming language code can be embedded to models.

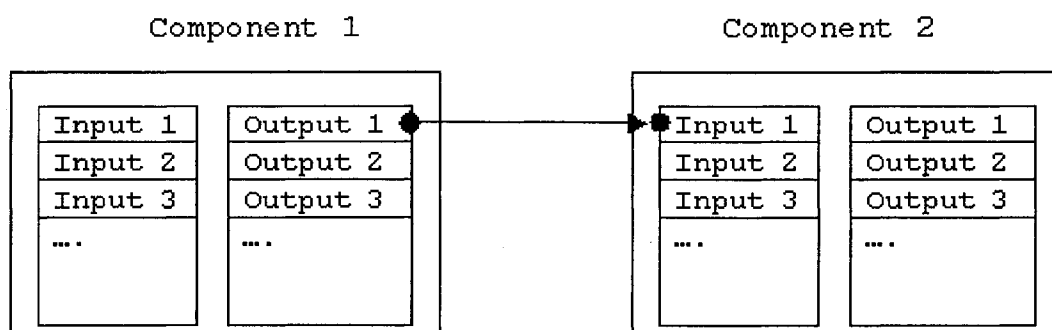


Figure 1. A schematic for connecting components in Easy5

Components and program codes are designed to have inputs and outputs, which are used to connect them to each other as it is depicted in Figure 1.

After the network is completed by connecting components together, Easy5 creates an executable for the model. According to Miller (1997), simulation packages consist of three major parts: the graphical user interface (GUI), the simulation engine, and the network of objects to be simulated. "In Easy5 the simulation engine and network of the objects to be simulated are tightly coupled" (Miller, 1997). Therefore, creating an executable of the

model means compiling and linking the network with Easy5 simulation engine. However, the GUI part of Easy5 is maintained by a separate library called interactive simulation.

In most of the standard programming languages, an executable of the program can be operated independent of the programming environment. Whereas, the executable of an Easy5 model can only be run together with the simulation package, however, the same executable can be run for variety of different inputs.

Easy5 is used for modeling a variety of physical components in mechanical systems and vehicles, such as hydraulics, drivetrain (transmission, differential, gearbox, etc.), pneumatics, engine, and so on. In order to model different components several libraries are available at certain additional costs. The modeler may also choose to develop their own library, which requires very good engineering and physical science skills, deep product knowledge, and advanced modeling experience.

Fritz (1999) and his colleagues introduced a simulation approach to analyze the dynamics of planar mechanism by using Easy5. "The analysis is based on the equations of motion of the mechanism linkages. The chosen

methodology allows the modeling of a variety of possible mechanisms" (Fritz, ElSawy, Modler & Goldhahn, 1999).

Dvorak (2003) has discussed modeling fluid-power systems by demonstrating several examples with Easy5. He has used thermal hydraulic advanced library developed by MSC.Software. He stated that, "Hydraulic systems have been difficult to simulate because they include complex and diverse components with highly nonlinear and discontinuous dynamics." (Dvorak, 2003). He has also discussed the linearization, which leads to inaccuracy in representation of physical systems, could be one way to get around this problem. However, he claimed that, "the latest ideas embodied in MSC.Easy5, a simulation and modeling program, provide a solution by letting engineers build accurate physics-based models of hydraulic systems, as well as multidisciplinary systems. These can include mechanical, electrical, thermal, pneumatic powertrain components controlled by digital and analog systems" (Dvorak, 2003).

Energy Models

Energy models of vehicles are developed mostly in the automotive industry. However most of these studies were partial energy models. For example, the Thermal System that Valeo has developed for the Chrysler Group vehicle included

only engine cooling, and heating, ventilation and air conditioning (HVAC) (Valeo, 2002). The main goal of his research was to keep engine and passengers at optimum desired temperatures in the studied vehicle. Their system did not include mechanical systems such as the transmission, the differential and other essential components of powertrain.

Sandberg (2001) investigated the effect of different powertrain combinations on fuel consumption for heavy trucks. He has concentrated his research on studying fuel consumption rather than complete vehicle. He has developed a vehicle simulation in Dymola, and used MatLab to manage exchangeable data sets and to create Graphical User Interface (GUI), (Sandberg, 2001).

Another limited energy model study was conducted for GKN Westland Helicopters Limited (Harbach, 1999). Harbach (1999) has investigated the fuel delivery system and main gearbox oil system of helicopters. He has developed the system with MatLab/Simulink.

General Motors (GM) and Delphi Corporation engineers have conducted a joint research to explore the impact of different placement orders of condenser, fan, and radiator (Yang, Bozeman, Shen, & Acre, 2003). They have primarily

investigated the efficiency of condenser-fan-radiator order combination against condenser-radiator-fan order combination. Their study was "a vehicle level thermal system analysis, in which the thermal fields due to each of the vehicle segments (front end, underhood, and underbody) are calculated and analyzed together as one thermal system" (Yang et al., 2003). In their study, they have used the commercial Computational Fluid Dynamics (CFD) software Fluent.

Another study on an energy model for vehicles was carried out by Assanis (1999) and his colleagues in Automotive Research Center (ARC) at the University of Michigan. In their study, they integrated diesel engine, driveline and vehicle dynamics (Assanis et al., 1999). They only have a charge air cooler (which they call intercooler) model needed for diesel engine, however, they did not have a radiator circuit or a fan control system which are essential for comprehensive energy models of vehicles. As they have stated "linking high fidelity engine simulation module with a detailed multi-body vehicle dynamics module presented challenges due to different time steps required for the solution of the differential equations inherent in those module" (Assanis et al., 1999). One of the biggest

challenges they have faced was long simulation time. High fidelity engine simulation models require very small simulation time steps (e.g. usually much smaller than 0.001 seconds) as opposed to other portions of vehicle model, which can usually be solved with bigger time steps. Since differential equation solver picks the minimum time step, simulation slows down dramatically. They have overcome this problem by introducing a wait state algorithm.

Benefits of Vehicle Simulation

In his article exploring the transition of simulation programs from the Aerospace Industry to the Automotive Industry, Gould (2003) conferred that the simulation "work paid off for Boeing 777, resulting in these benefits:

- 90% reduction in engineering change requests (6000 to 600)
- 50% reduction in cycle time for engineering change request
- 90% reduction in material rework
- 50 times improvement in assembly tolerances" (Gould, 2003).

Gould cited Richard Smith, director of CAD/CAM products and services for The Boeing Commercial Airplanes, as stating that "Physical models have gone down in significance. We produce a number of aerodynamics test cycles digitally, and one cycle physically. The physical

model, measuring three to four feet in wingspan, validates the simulation, to see if the simulation is giving us the right answers" (Gould, 2003).

CHAPTER 3

METHODOLOGY AND DESIGN

Introduction

A tractor model from a Midwest off-road machinery manufacturing company has been selected as a basis of this study, because of the availability of abundance of test data. Model development has been planned in such a way that it can be applied to other tractor models and other agricultural vehicles that consist of similar components.

Easy5 computer simulation package will be employed in developing the energy model of a tractor. Existence of a variety of components in available standard libraries, feature of creating models for non-standard components, and characteristic of its compatibility and connectivity with existent simulation packages (such as WAVE for engine simulation), gives us confidence that Easy5 is a powerful development tool in creating comprehensive energy models for off-highway machinery.

Model Development

The hierarchical structure for the tractor is shown in Figure 2. Each box represents either a component or a group of components.

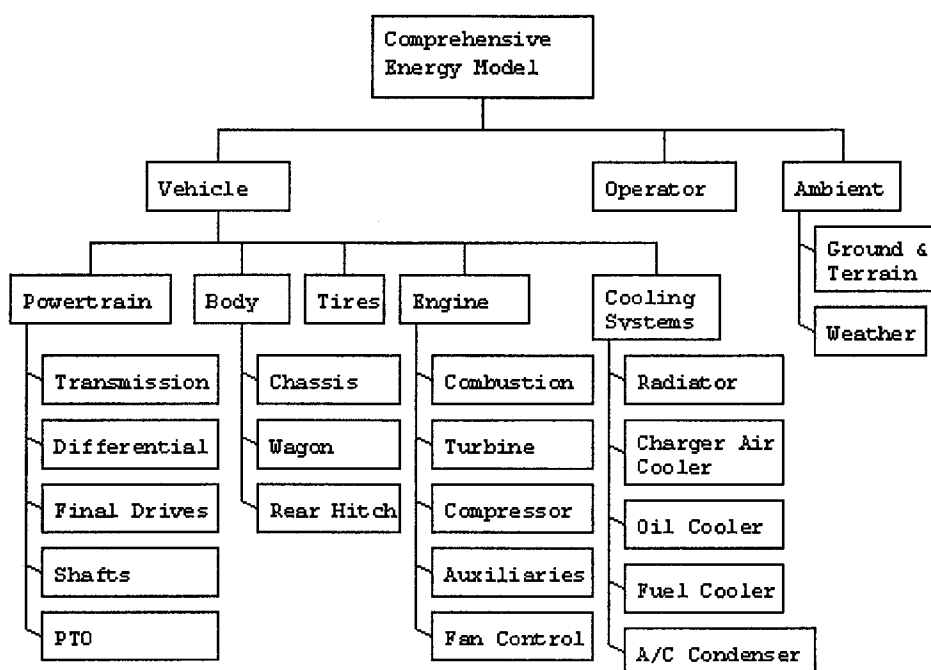


Figure 2. Hierarchical structure of vehicle model

Missions

Two main missions are determined for the Comprehensive Energy Model (CEM) to accomplish: (1) High Speed Transport and (2) Primary Tillage.

High speed transport mission. The set of conditions for primary tillage mission are:

- The engine will be operated with full throttle.
- The transmission will be set to 16th gear.
- Single tires will be used for each axle.
- With 40 metric tons of load including tractor weight, the model tractor will be run uphill

with different slopes for one mile (See Figure 3). The goal is to determine the angle of the hill to maintain 2000 engine rpm.

- Then the model will be run downhill for one mile with the same angle.
- The road surface is asphalt.
- Ambient temperature is 75 °F
- Wind speed is 0 mph.

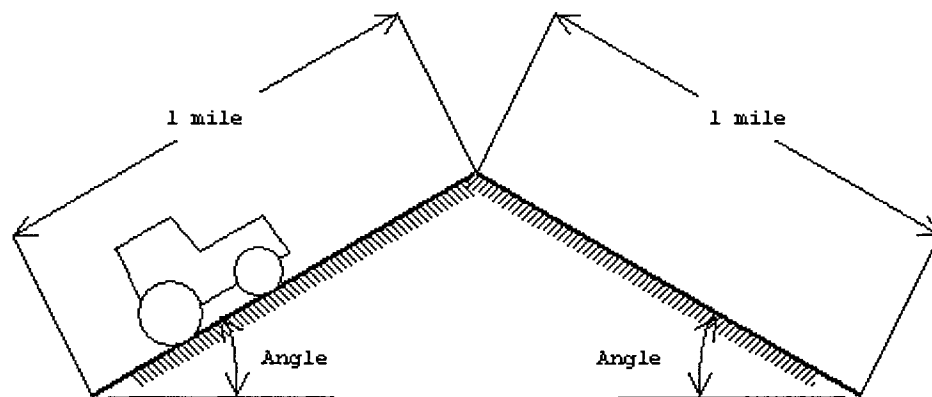


Figure 3. Ground profile for high speed transport test

Primary tillage mission. The set of conditions for primary tillage mission are:

- The engine will be run with full throttle.
- The transmission will be set to 8th gear.
- Draft load will be applied to maintain 2200 rpm.

- Cone index (CI) of soil is set to 1500 kPa and slope of ground is zero.
- Dual tires will be used for each axle.
- The length of the field is 0.5 miles.
- At the end of the field, implement is raised and lowered for in 10 seconds.
- Ambient temperature is 75 °F
- Wind speed is 0 mph.

The goal of this mission is to determine the constant amount of grill screen restriction that results in overheating when reaching end of field (0.5 miles).

Selected Tests

Available tests are determined for the tractor as PTO test, axle test, and wind tunnel high-speed transport test.

PTO test. In this test, the tires are removed from tractor, PTO clutch is engaged and then a torque applied to PTO shaft with an instrument called Dyno. The engine is kept running at 2200 rpm for 2 hours to make sure all components have reached to steady-state, this is called warm-up session. Finally six sets measurements are taken for selected parameters with one-minute interval. Some of the parameters measured are: Engine rpm, Fan rpm, PTO rpm, PTO torque, Toptank temperature, Intake manifold

temperature, Oil cooler inlet temperature, Fuel cooler inlet temperature.

Axle test. Axle test is similar to PTO test with the only difference that Dyno torque is applied to rear axle final drive shafts instead of PTO shaft. In order to apply torque to rear axles the rear tire are disassembled from the tractor. PTO clutch is disengaged to make sure no additional torque applied. Transmission can be set any desired gear, however for the AXLE test in this study the transmission gear is set to 9th gear. The A/C is turned on. The wind speed is set to 11 km/h. The engine speed is set to 2200 rpm.

Wind tunnel high-speed transport test. Similar to the AXLE test, the transmission is set 16th Gear and Dyno torque is applied to rear axle to maintain 2200 engine rpm. The wind speed is set to 21.9 km/h in the wind tunnel. Ambient temperature is set to 40 °C. To maintain constant inlet fuel temperature at 40 °C, the fuel is supplied to engine from fuel housing not from the fuel tank. The A/C is turned on.

Development Strategy

The necessary components for three selected tests and two missions for the tractor model are listed in Table 4.

Table 4

Selected Tests, Missions and Their Required Components

Stage	Tests and Missions	Needed Components
1	PTO Test	<ul style="list-style-type: none"> - Engine - Transmission with PTO only - PTO drive - Vistronic Fan Drive - Radiator Circuit - Charge Air Cooler Circuit - Transmission Oil Circuit - Fuel Cooler Circuit - Recirculation of Air Effect - Controlled Torque Applied to PTO shaft
2	Hot Point Axle Test	<ul style="list-style-type: none"> - Transmission completed - Rear/Front Axle - Final Drives - AC Loop - Controlled Torque Applied to Rear Axle Final drives
3	Wind Tunnel High-Speed Transport Test	<ul style="list-style-type: none"> - Vehicle
4	High Speed Transport Mission	<ul style="list-style-type: none"> - Ground and Terrain - Tires
5	Primary Tillage Mission	<ul style="list-style-type: none"> - Implement load - Implement hydraulics circuit

Table 4 shows the needed components for a model build up from top to bottom. Thus the test, which needs the minimum number of components to be added, is the PTO Test. Accordingly, the primary tillage mission requires that the maximum number of components added, as it requires

implement load and implement hydraulic circuit components in addition to all the components listed in previous four categories. This strategy enables the modeler to validate the model at the end of each stage.

Verification of Model

The completed comprehensive energy model will be verified by conducting sample runs to compare with the PTO test, the axle test and the wind tunnel high-speed transport test.

CHAPTER 4

RESULTS AND DISCUSSIONS

Developing the Components of SimulationEngine

The engine used in the tractor is 8.1 liter, 6-cylinder, turbocharged and air-to-air aftercooled Diesel Engine. Rated speed of the engine is 2200 rpm. Compression ratio is 16.5 to 1. A simplified schematic for air circulation of the engine is given in Figure 4. Fuel and coolant circuits are neglected since they will be modeled separately.

After combustion, exhaust gases reach about 500 °C temperature with almost 3 bar of pressure. Part of this heat energy is converted to mechanical rotational energy and transmitted to the compressor through a shaft, and the remaining of energy is thrown to the atmosphere exhaust gas. The compressor sucks the air from ambient and compresses it to about 2.5 bar. Increase in the pressure results in increase in temperature to about 200 °C. This hot air is cooled down by charge air cooler to almost 50 °C.

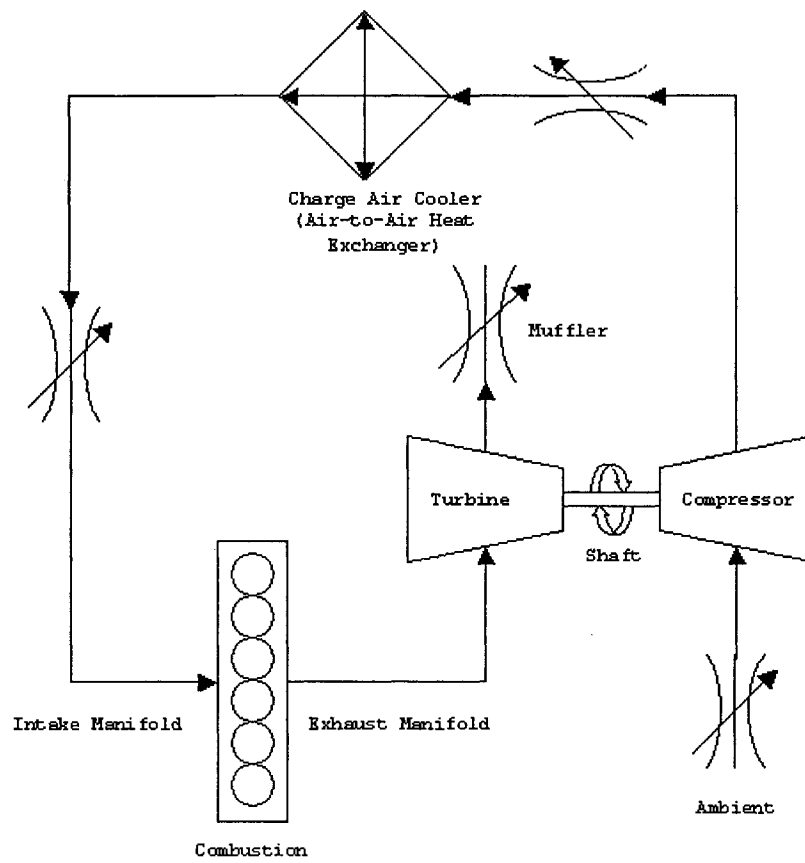


Figure 4. A schematic for the turbocharged diesel engine

Simulation model in WAVE. A complete high fidelity simulation model for this engine has been developed by engineers in Midwest off-road machinery manufacturing company. Inputs and outputs required for incorporating WAVE engine model and Easy5 Comprehensive Energy model are listed as follows:

Inputs:

- Throttle setting - Lets the driver to decide how much power needed for operations

- Torque to Flywheel - The torque needed to drive the drivetrain

- Air temperature inlet to Filter
- Ambient temperature and pressure

Outputs:

- Engine RPM
- Engine Torque
- Fuel mass flow
- Air/Fuel ratio
- Inlet Air mass flow
- Temperatures and Pressures (of gases) at inlet and outlet of Charge Air Cooler, Compressor and Turbine
- Temperature and pressure at intake manifold
- Temperature and pressure at exhaust manifold
- Heat rejected through Charge Air Cooler (CAC)
- Heat rejected to the radiator coolant

Among these desired parameters, only heat rejection from CAC output could not be satisfied, instead it had to be an estimated input to WAVE.

WAVE engine model for 6-cylinder 8.1 liter diesel engine is demonstrated in Figure 5.

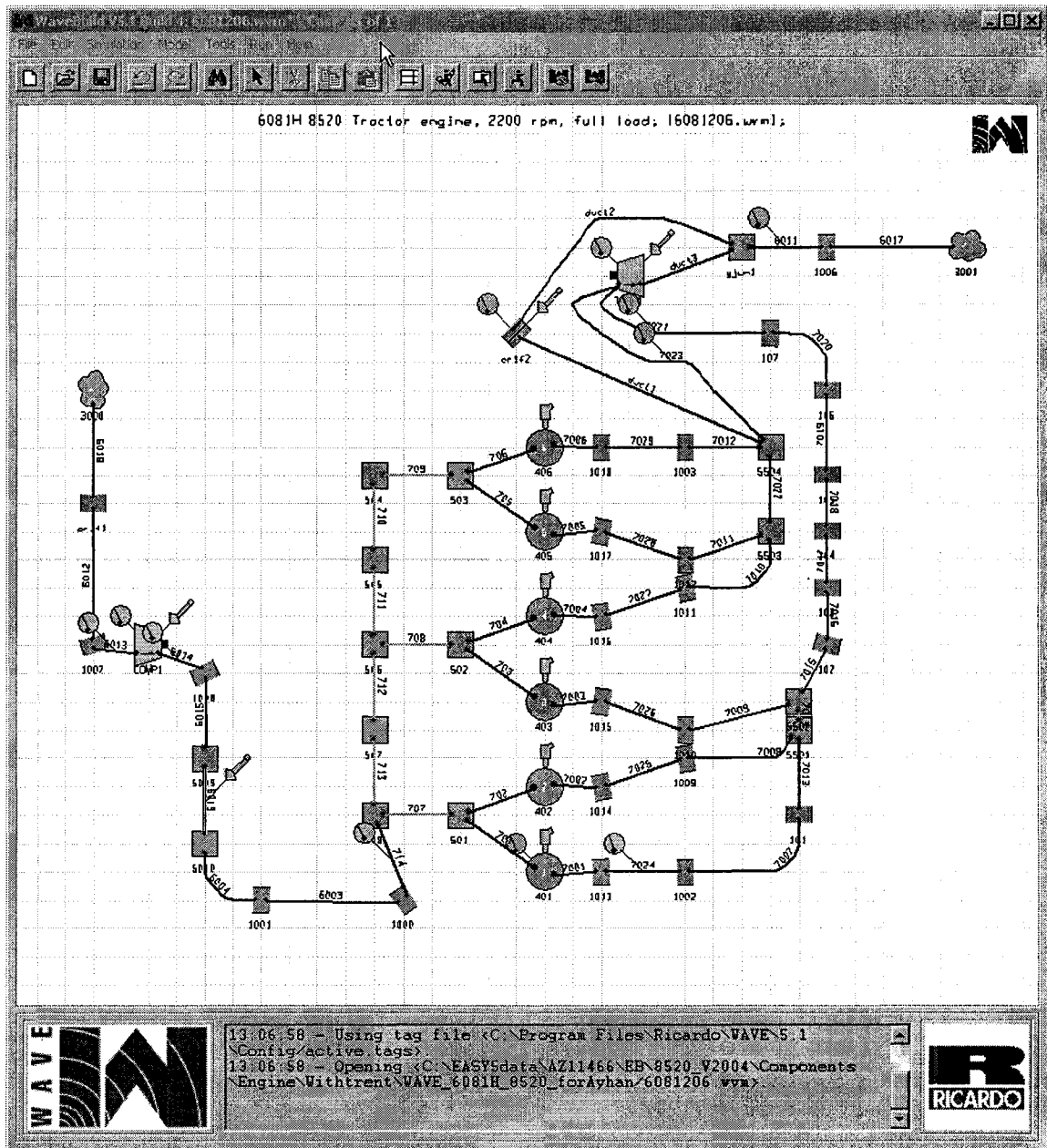


Figure 5. WAVE engine model for the diesel engine

The model is built on WaveBuild canvas. The components in this canvas are placed in such a way that the flow can be from left to right. Six circular shapes in the middle

represent combustion. The left of the combustion is intake manifold, and the compressor is placed before intake. The right of the combustion is exhaust manifold, and the turbine is placed after exhaust manifold. The connecting shaft in between turbine and compressor is maintained programmatically. Cloud shapes represent the ambient conditions. Finally, the name of the file can be seen from the title bar as well as from the header of the canvas as '6081206.wvm'.

Interaction between the WAVE engine model and Easy5 simulation model is provided with 'rs'- Ricardo Software Co-simulations Library (rs-library) and 'rx' - Multiplex Component Library (rx-library). The rx-library has only one component, namely RX-Multiplex Scalars to Vector, which converts scalar inputs into an output vector. The rs-library has also one component, namely WV-WAVE Link. The help manual for WAVE Link component is given in Appendix A.

Figure 6 demonstrates how the WAVE engine model can be incorporated with an Easy5 model.

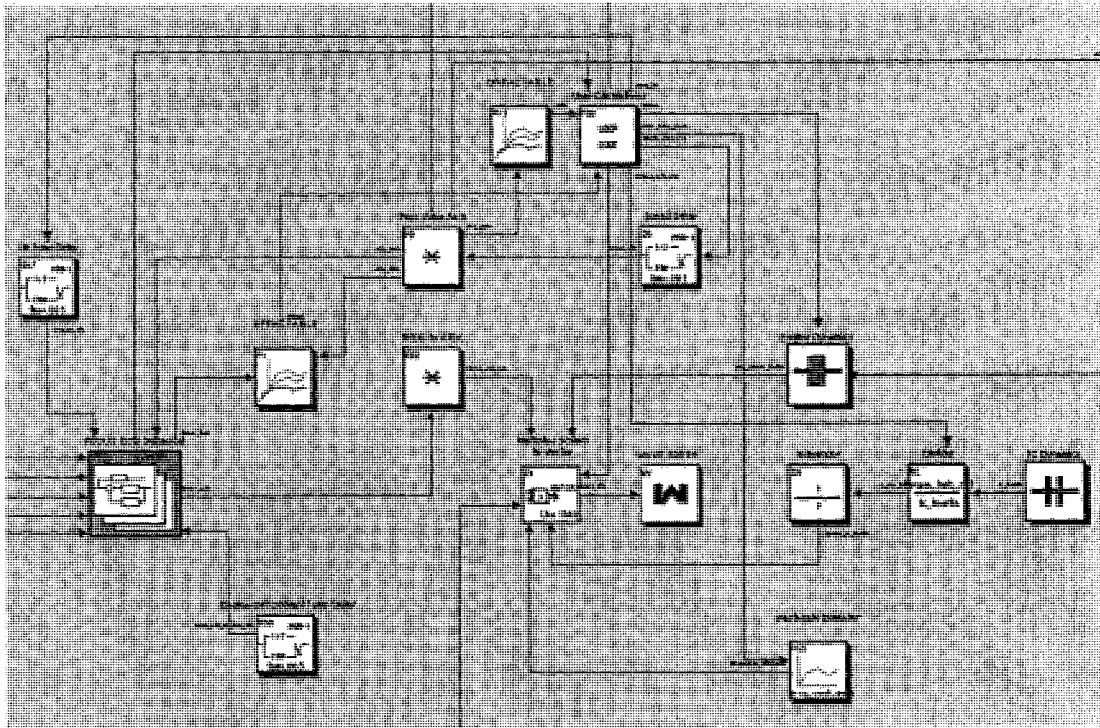


Figure 6. Demonstrating application of WAVE model in Easy5

WV component has an input named WIF_WV (WAVE Input File Prefix) to specify the name of the WAVE engine model file (see Figure 7). The name of the WAVE input file is restricted to be a number (6081206) since the inputs in Easy5 can only accept numerical data types.

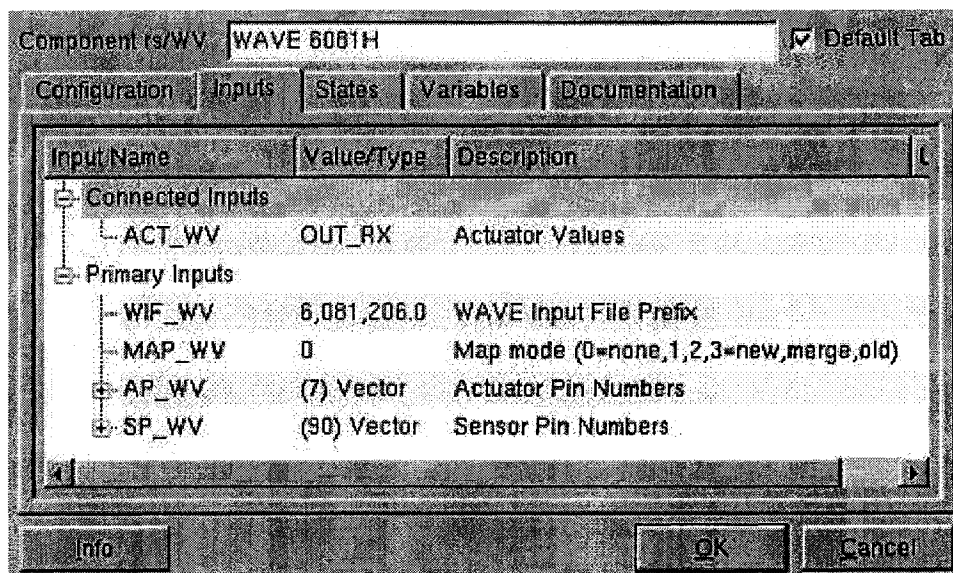


Figure 7. Inputs to WV Component

Running the WAVE engine model. Figure 8 represents a snap shot of CPUSEC vs. time form the sample run. The WAVE engine model could generate simulation results for 450 seconds of test in 70000 seconds of CPU time. Simulation speed is calculated by using equation 1 as 1/155. In another words, the WAVE model is 155 times slower than real-time.

$$\text{Simulation Speed} = \frac{\text{Time}}{\text{CPUSEC}} \quad (1)$$

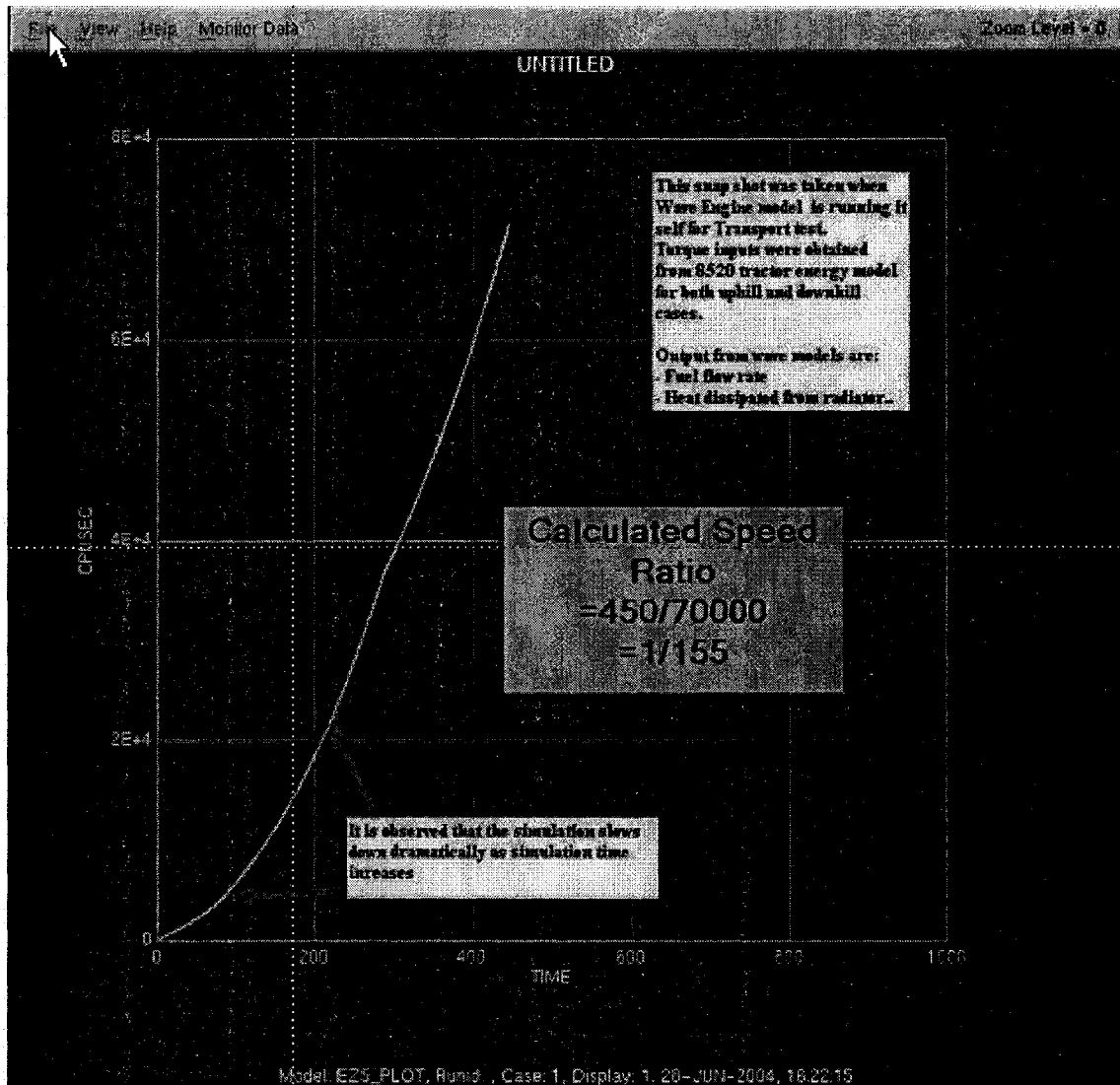


Figure 8. A snapshot from the WAVE engine model running

Since the WAVE Engine Model is a high fidelity model, when it was incorporated with the comprehensive energy model, the simulation speed of the complete model is observed to be 500 times slower than real-time. This makes the development of the simulation model incredibly inefficient.

An alternative model for engine. An innovative approach has been developed to avoid the inconvenience due to the slow simulation. First, a new charge air cooler circuit (see Figure 9) has been developed in Easy5 by taking the schematic in Figure 4 as a basis.

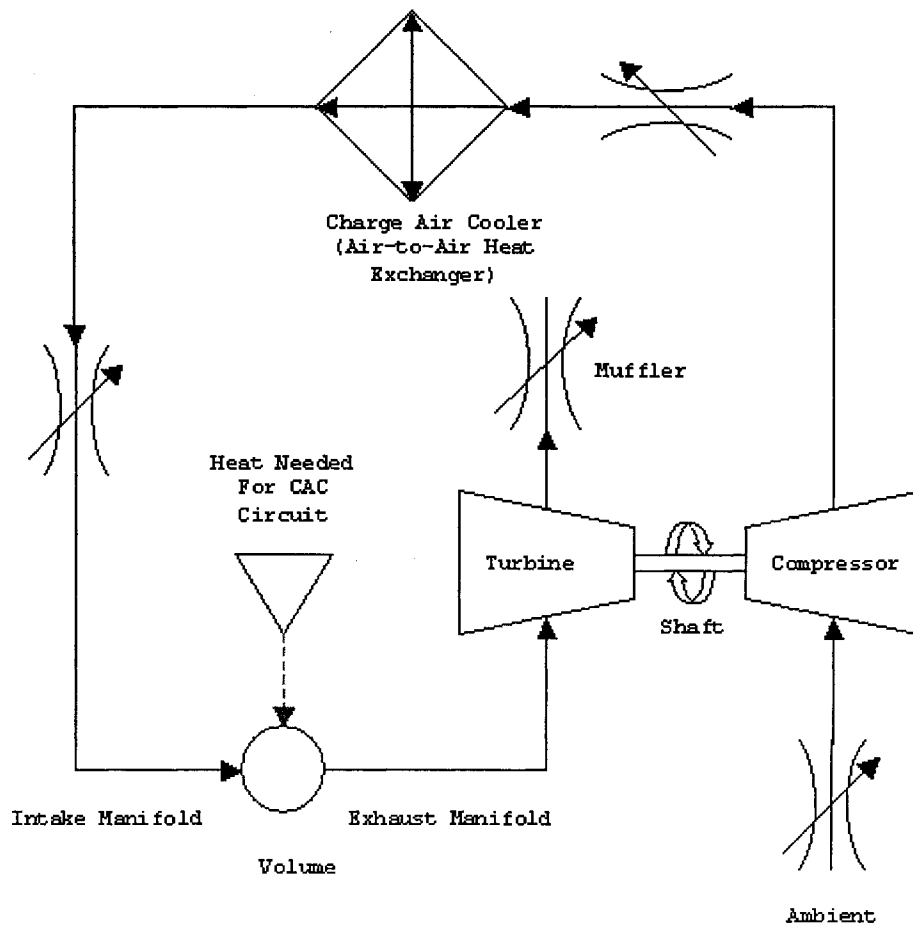


Figure 9. Alternative Charge Air Cooler (CAC) Circuit Schematic

The main difference in these two schematics is that the combustion module is replaced by a simple volume. In order to energize the turbine in this circuit, some heat (Heat Needed for CAC Circuit) should be applied to the volume.

Calculation of heat needed for CAC circuit. Figure 10 demonstrates the input and output energies for a diesel engine on a simplified schematic of piston-cylinder mechanism.

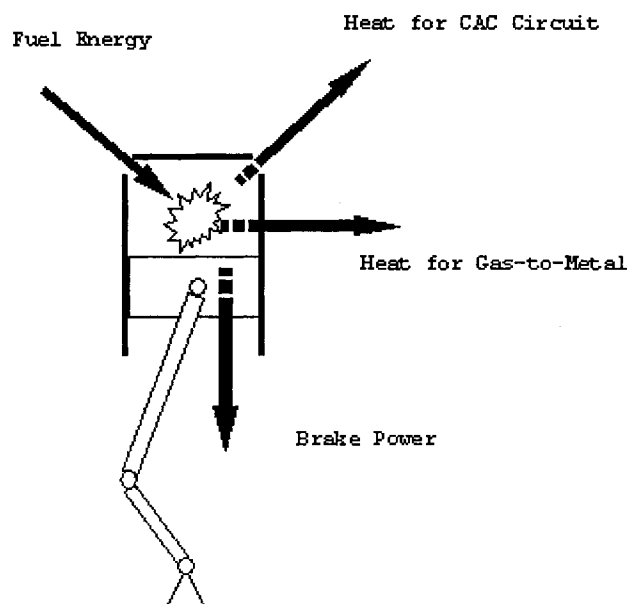


Figure 10. A schematic of energy balance for diesel engines

From conservation of energy by taking the volume cylinder and piston encloses as a control volume:

$$Q_{\text{Fuel}} = Q_{\text{CAC-circuit}} + Q_{\text{Gas-to-metal}} + P_{\text{Brake}} \quad (2)$$

where,

Q_{Fuel} : Fuel Energy
 $Q_{\text{CAC-circuit}}$: Heat for CAC Circuit
 $Q_{\text{Gas-to-metal}}$: Heat for Gas-to-Metal
 P_{Brake} : Brake Power

The fuel energy is calculated as mass flow rate (kg/s) times the lower heating value of diesel fuel (J/kg). The lower heating value for the No. 2 diesel fuel used in the tests is 42,550,560 [J/kg]. The fuel mass flow rate is obtained by running the WAVE Engine model.

The WAVE engine model also provides a good estimate for the heat for Gas-to-Metal that represents the heat rejected through radiator.

Brake power is defined as the power obtained from the engine after all the losses and can be calculated as the torque delivered to drivetrain (Nm) times the angular velocity of the flywheel (radian/s).

Since all the other variables are known, equation 2 can be utilized in calculating the heat needed for CAC circuit. This heat directly is applied to volume replacing

combustion and energizes the turbine. An Easy5 model of the alternative charge air cooler circuit is shown in Figure 11. A check valve is placed before the volume (the node component NO) to ensure no reverse flow from the volume to the heat exchanger.

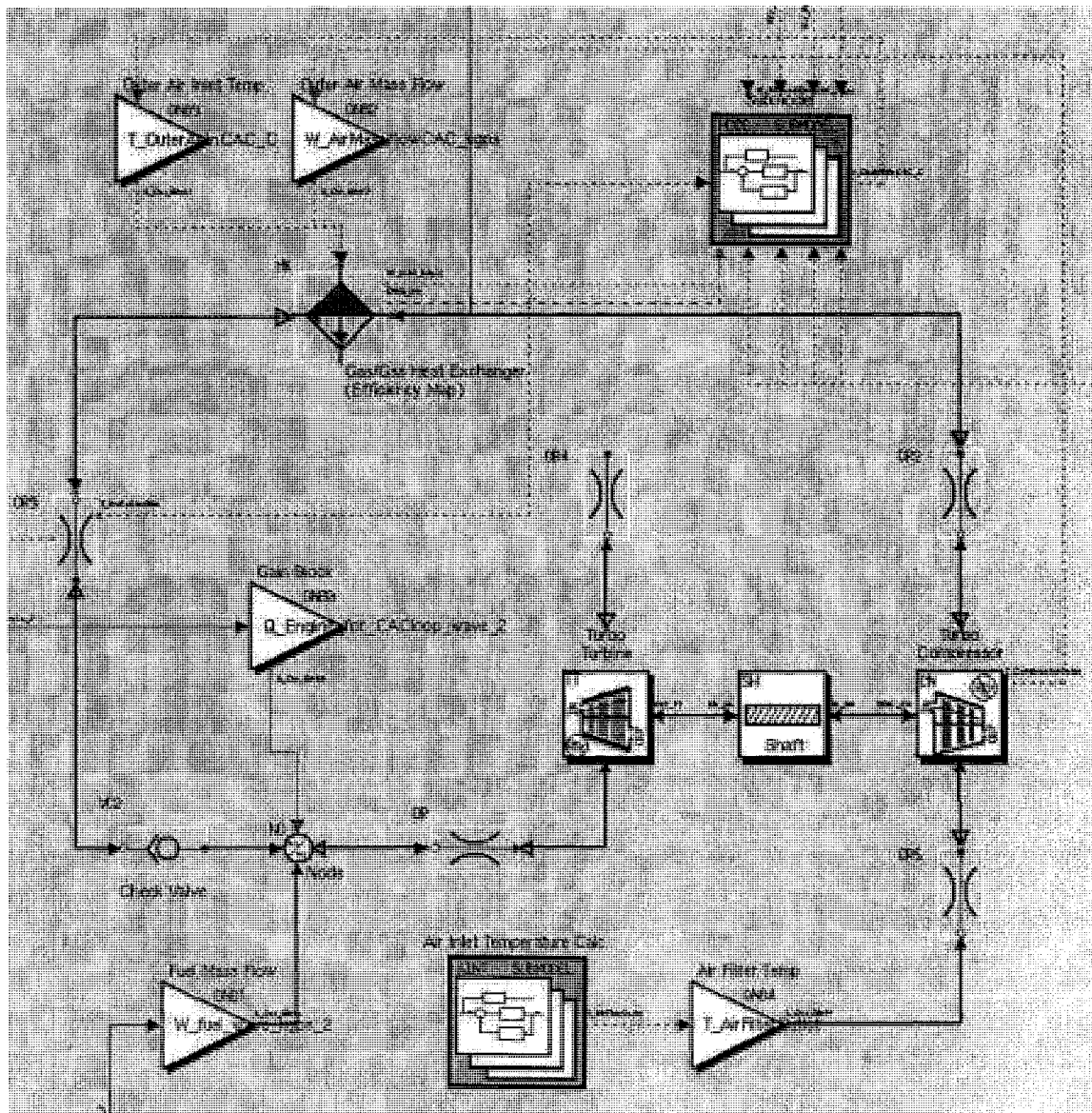


Figure 11. Easy5 model for the alternative CAC circuit

Approximations in alternative CAC circuit. Even though the energy exchange given in equation 2 is generally correct, there are other types of energies for the control volume that have not been accounted. As stated in Diesel Engine Fundamentals (2001): "For instance, any mass entering the control volume brings with it several forms of energy.

- internal energy; mainly due to its temperature which is generally very small
- kinetic energy; mainly due to injection characteristics which usually leads to important interactions between the fuel and the air within the control volume
- potential energy; generally associated with pressure admitting mass into the control volume
- flow energy; principally associated with the interrelation between the control volume and its pressure."

In this study, the forms of energies that are quoted above are neglected in calculating the heat for CAC circuit.

Transmission

In the tractor, 16-speed automatic power shift transmission (PST) is used. As it can be seen in Figure 12, there exist four levels of shafts in PST. The first level shaft is input from flywheel of the engine. The second level is used to obtain different gear ratios. The third level is the output shaft to front and rear axles. Finally the fourth one is output to PTO shaft.

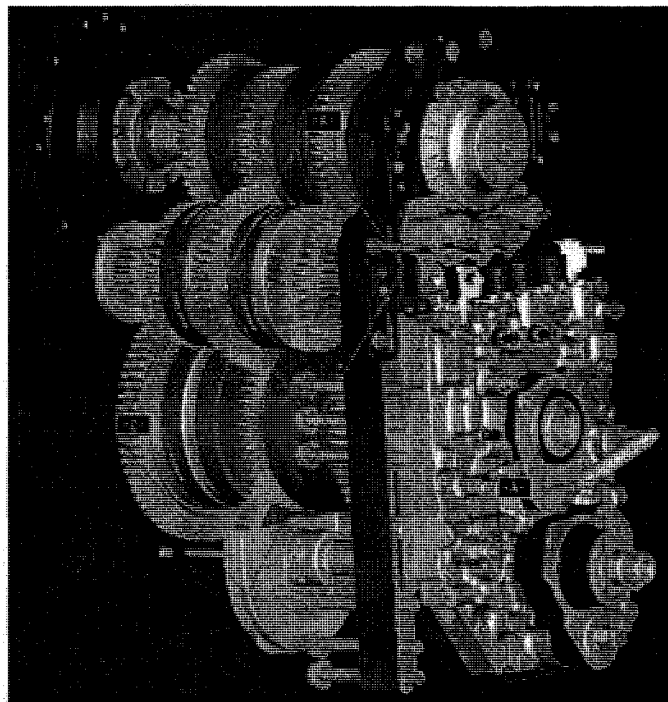


Figure 12. Power shift transmission for the tractor

Gear ratios are for each shift as well as PTO gear is given as table in Appendix B1. When the operator selects a

gear related clutches are engaged on the shafts to obtain corresponding gear ratios in the table. Only PTO gear is always engaged independent of selected gear, the operator has control to turn on and off the PTO through a clutch connecting level four shaft of transmission and PTO drives.

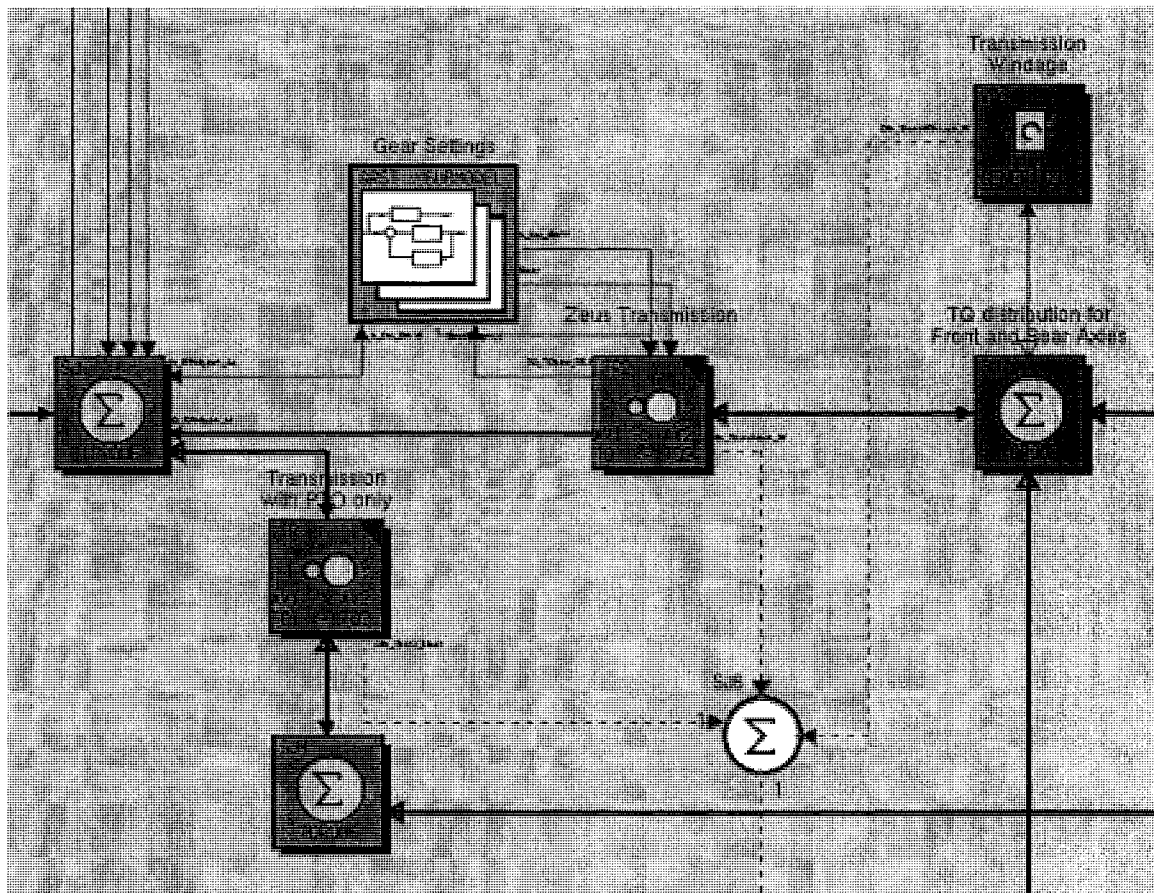


Figure 13. Easy5 model for power shift transmission

Easy5 model for the transmission. The transmission has been modeled with two sets of gear couples, namely

components TR and TR2 (see Figure 13). The component TR has only one gear setting (0.4545) for PTO. The component TR2 can be set to five reverse and sixteen forward gears. The transmission windage losses are introduced to the model with experimental results via WD3, the transmission windage component, which has table of torque losses with respect to transmission output rpm as an input (see Appendix B.2).

Inefficiencies (1- efficiency) in TR and TR2 are considered as source of heat increase in lubricating oil (see Equation 3).

$$Q_{\eta} = (1 - \eta) \cdot TQ \cdot AV \quad (3)$$

where,

Q_{η} : Heat due to gear inefficiency [W]

η : Gear efficiency

TQ : Output torque [Nm]

AV : Output angular velocity [rad/s]

It is assumed that the windage heat losses are also converted into heat increase in lubricating oil and calculated as in Equation 4.

$$Q_{Windage} = TQ \cdot AV \quad (4)$$

where,

$Q_{windage}$: Heat due to windage losses [W]

TQ : Output torque [Nm]

AV : Output angular velocity [rad/s]

PTO Drive

PTO drive has been modeled as a torque-summing junction (SJ3), which allows PTO torque generator connected when an output needed from it (see Figure 14). PTO clutch and shafts are neglected; instead their windage losses (component WD2) are introduced in the model.

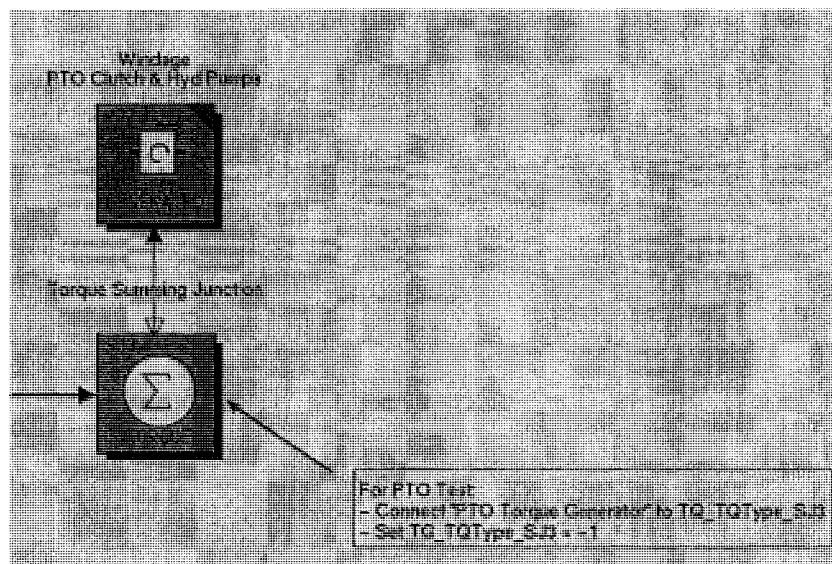


Figure 14. Easy5 model for PTO drive

Vistronic Fan Drive

The vistronic fan drive uses an electronically controlled variable speed fan control strategy. The feature

accepts up to six temperature inputs, one pressure or temperature input, and two switch inputs to determine a desired fan speed. The six temperature inputs use a PI control algorithm to set a desired fan speed while all other inputs use a simple table lookup or two-state logic to determine a desired fan speed. The maximum of these desired fan speeds is used as the desired fan speed (see Appendix C).

In this study, we have modeled four input parameters for fan speed control: three PI controlled temperature inputs and one two-state logic input.

The PI controlled input parameters are T_{optank} temperature, intake manifold temperature and oil cooler inlet temperature. For all PI controlled parameters the proportionality constant (KP) is set 120 and the integral constant (KI) is set to 2.

The control target for T_{optank} temperature depended on whether the PTO is running or not. If the PTO is engaged the target settings in Table 5, otherwise Table 6 is used. In between values in both tables are linearly interpolated.

Table 5

Target Toptank Temperature If PTO is Engaged

Engine Speed (rpm)	1000	1400	2000	2100	2200
Target Toptank temperature (°C)	98	104	99	98	97

Table 6

Target Toptank Temperature If PTO is Not Engaged

Engine Speed (rpm)	1000	1400	2000	2100	2200
Target Toptank temperature (°C)	94	95	95	94	93

The target temperature for the other two PI controlled parameters are set to constant number independent of the engine rpm. The intake manifold temperature is controlled at 75 °C, and the oil cooler inlet temperature is controlled at 90 °C.

The two-state logic input is used to control the fan speed for on and off state of air conditioning (A/C) unit. If the A/C is on the desired fan speed is set to 1200 rpm, otherwise 650 rpm.

The Easy5 model of vistronic drive is depicted in Figure 15.

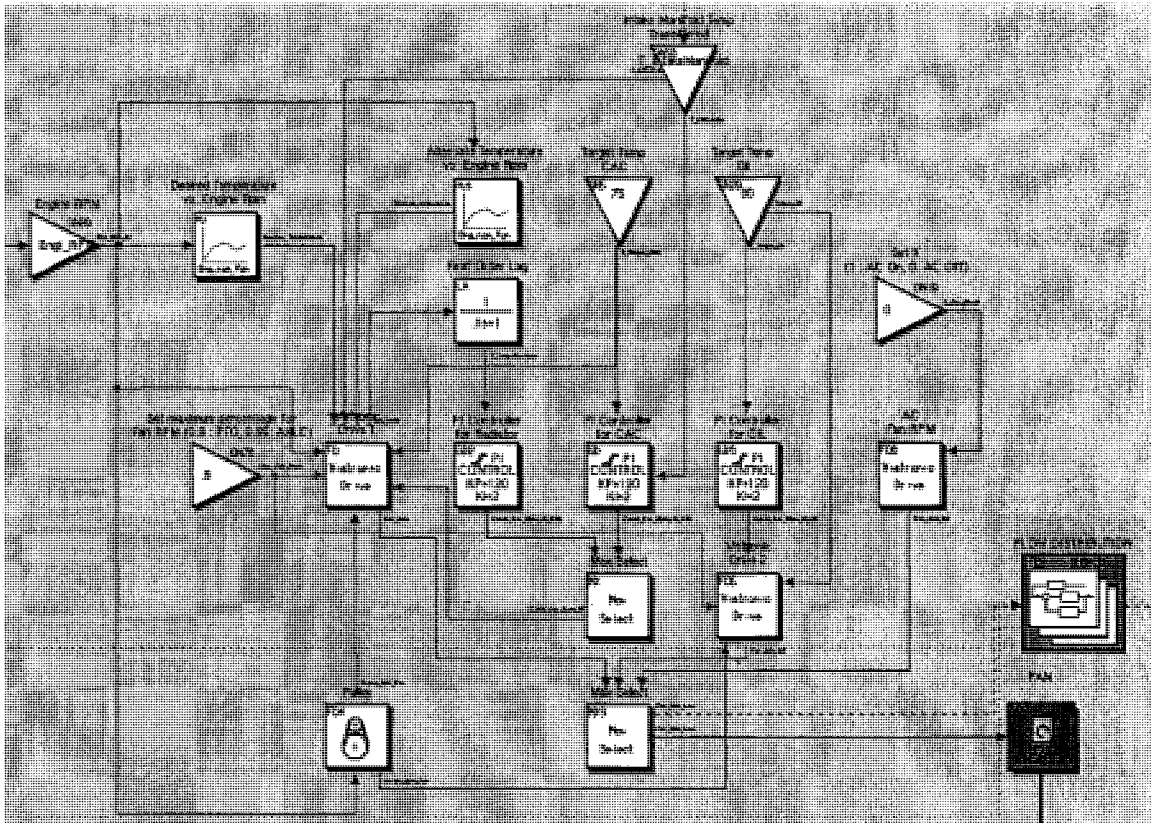


Figure 15. The Easy5 model for vistronic fan drive

Transmission Oil Circuit

A schematic for the oil circuit is given in Appendix D1. The oil circuit basically consists of five reservoirs, five hydraulic pumps, an oil cooler and their connecting pipes. The reservoirs are the transmission housing, the pump drive housing, differential housing, clean oil reservoir (COR) and independent link suspension (ILS). The pumps in the system are the scavenge pump, the charge pump, the steering and transmission pump, the implement pump and

the ground drive pump. At rated engine rpm (2200 rpm) the volumetric flow rates of the pumps in the oil circuit are listed in Table 7.

Table 7

Volumetric Flow Rates of Hydraulic Pumps

Pump	Volumetric Flow Rate at Rated Engine Rpm (l/s)
Scavenge pump	1.3
Charge pump	1.7
Steering and transmission pump	1.3
Implement pump	0.1

Note that, since the Ground drive pump is not modeled at this stage of CEM, it is not listed in the table. The flow rates for different engine speeds are linearly interpolated. The oil cooler is placed between the steering and transmission pump and transmission housing.

The Easy5 model of the oil cooler hydraulic circuit is illustrated in Figure 16.

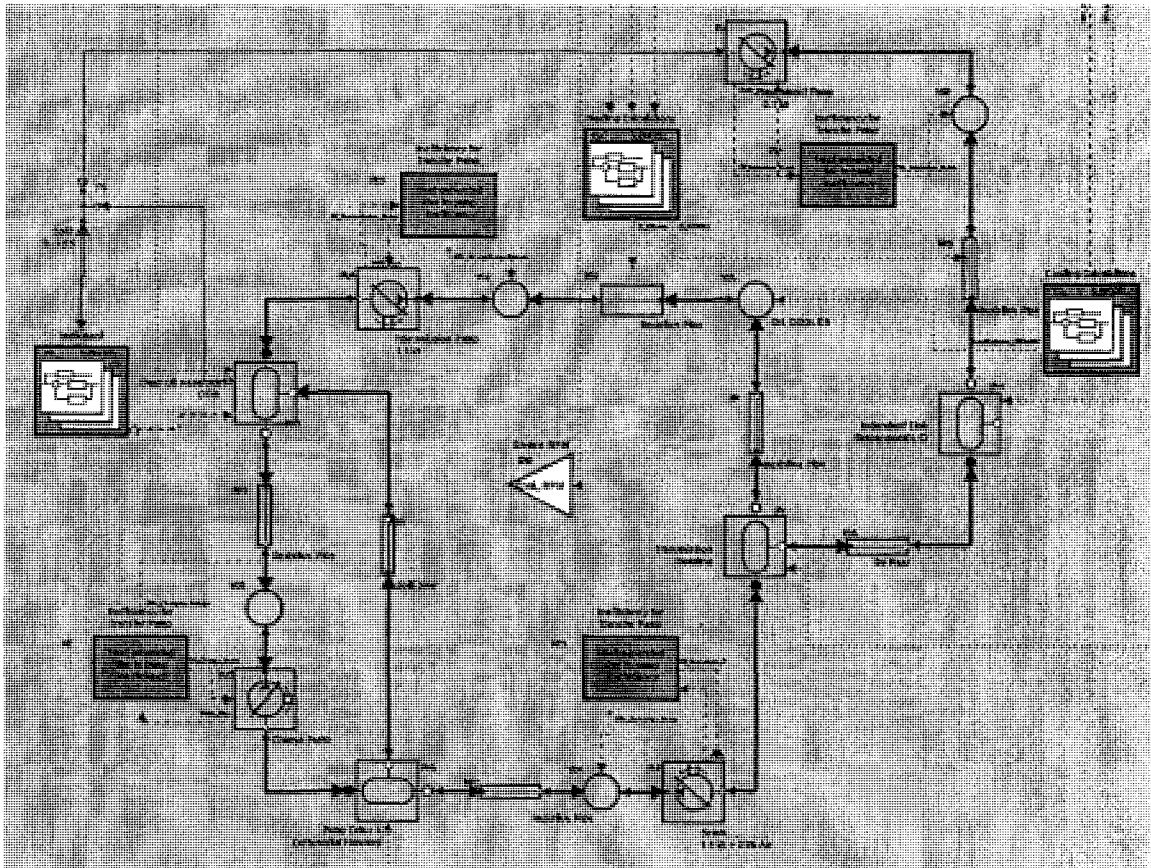


Figure 16. The Easy5 model for oil cooler hydraulic circuit

Implement Hydraulic Circuit. The flow rate for the implement pump in Table 7 is given as a leakage quantity if the implement hydraulic circuit is not used. Another implement pump is modeled to pressurize the implement hydraulic circuit as demonstrated in Figure 17. The schematic for implement hydraulic circuit is given in Appendix D2.

The theory behind the implement hydraulic circuit is: when raising the implement, SCV valve lets the pumped oil

into the piston-cylinder mechanism; and when lowering, SCV valve lets the oil in the piston-cylinder mechanism return to the clean oil reservoir.

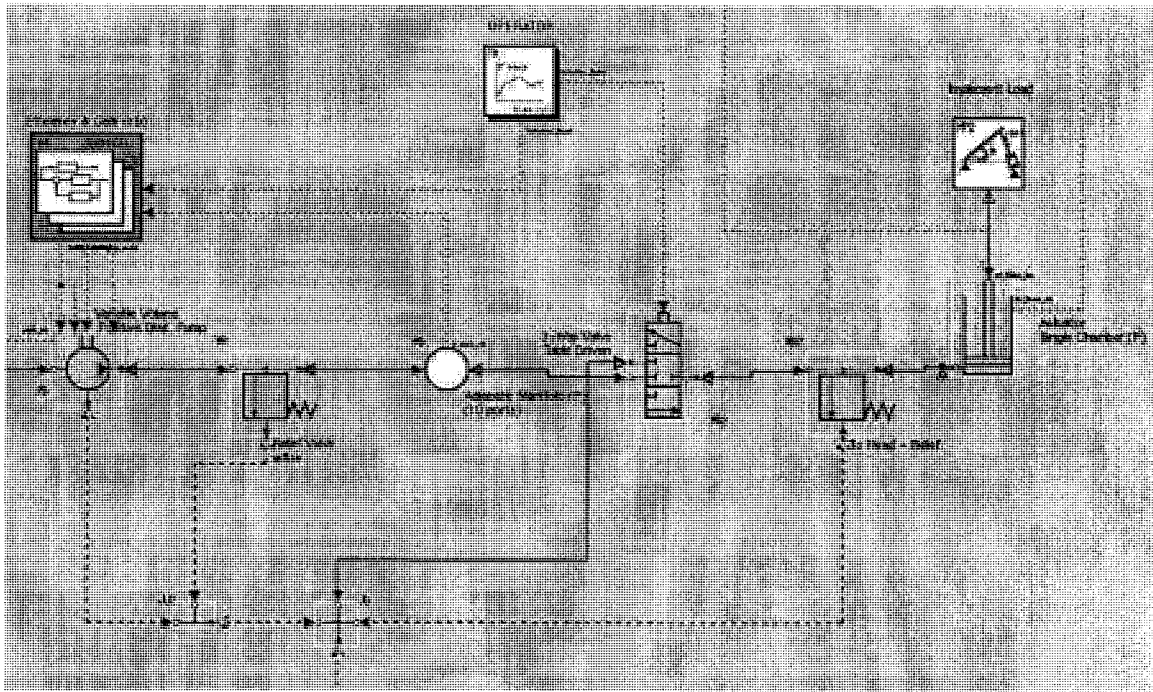


Figure 17. The Easy5 model for implement hydraulic circuit

Heat calculations for pumps. In the implement hydraulic circuit, there are two sources of heat introduced to the circuit; mechanical friction and inefficiency of hydraulic pumps. The heat due to mechanical friction is calculated as it was previously shown in the transmission model by using equation 3.

The generated heat due to the inefficiencies of pumps can be calculated as:

$$Q_{Pump} = (1 - \eta_{Vol}) \cdot POW_{Pump} \quad (5)$$

where,

- Q_{Pump} : Heat due to pump inefficiency [W]
 η_{Vol} : Volumetric efficiency of the pump
 POW_{Pump} : Power of the pump [W]

The power of pump can be calculated as:

$$POW_{Pump} = P \cdot q_{Vol} \quad (6)$$

where,

- P : Pressure [Pa]
 q_{Vol} : Volumetric flow rate [m³/s]

Combining equations 5 and 6

$$Q_{Pump} = (1 - \eta_{Vol}) \cdot P \cdot q_{Vol} \quad (7)$$

In CEM, the heat from inefficiency of pumps (Q_{Pump}) is applied to the components located to the outlet of each

pump. For instance the heat generated due to the pump inefficiency for the scavenge pump (component PU2) is applied to component VO4, which is used as the connecting volume.

Heat rejection calculation for the oil cooler. The oil cooler is an aluminum heat exchanger with 546 mm width, 357 mm height, and 76 mm depth. The heat rejection values for the oil cooler for 51 °C inlet outer flow temperature and 97 °C inlet inner flow temperature is given in Table 8. The outer flow for the oil cooler is ambient air, and the inner flow is oil in the circuit.

Table 8

Heat Rejection (kW) for the Oil Cooler

Speed of Outer Flow (m/s)	Volumetric Inner Flow (l/s)			
	1.00	1.25	1.50	1.75
6.16	25.7	26.9	27.9	28.9
6.94	27.3	28.6	29.7	30.8
7.62	28.6	30.0	31.1	32.2
8.40	30.1	31.5	32.7	33.9

For the convenience of the usage of the table in Easy5, the values of the inner and outer flows are

converted to mass flow [kg/s] (see equations 8 and 9), and the heat rejection values are converted to the heat per entrance temperature difference (ETD) [kW/°C] (see equation 10).

$$w_{outer} = v_{outer} \cdot A_{core} \cdot \rho_{air} \quad (8)$$

where,

- w_{outer} : Outer air mass flow [kg/s]
- v_{outer} : Velocity of outer air flow [m/s]
- A_{core} : Core area of the heat exchanger [m²]
- ρ_{air} : Density of air at 51 °C, 1.07491 [kg/m³]

$$w_{inner} = q_{inner} \cdot \rho_{oil} \quad (9)$$

where,

- w_{inner} : Inner oil mass flow [kg/s]
- q_{inner} : Inner oil volumetric flow [m³/s]
- ρ_{oil} : Density of oil at 97 °C, 826.85 [kg/m³]

$$Q_{ETD} = \frac{Q}{ETD} \quad (10)$$

where,

- Q_{ETD} : Heat rejection per ETD [kW/°C]

Q : Heat rejection values given in Table 8
[kW]

ETD : Entrance temperature difference (ETD)
between inner and outer flows [°C]

Table 9

Heat Rejection per ETD for the Fuel Cooler

Outer Mass Flow (kg/s)	Inner Mass Flow (kg/s)				
	0	0.827	1.034	1.240	1.447
0	0	0	0	0	0
1.291	0	0.559	0.585	0.607	0.628
1.454	0	0.593	0.622	0.646	0.670
1.600	0	0.622	0.652	0.676	0.700
1.760	0	0.654	0.685	0.711	0.737

Inner outer mass flows are obtained from the circuit. Corresponding heat rejection per ETD is read from Table 9. Linear interpolation is used between data values. Finally to calculate the heat rejected from the oil cooler, the heat rejection per ETD is multiplied by the entrance temperature difference. The calculated heat is rejected from the oil cooler volume (VO5) (see Figure 17, page 50).

Fuel Cooler Circuit

A schematic for the fuel circuit is given in Appendix D.3. There are two pumps in the circuit; transfer pump and supply pump. The transfer pump feeds the system with fuel from the fuel tank, and the supply pump maintains high pressure to facilitate the fuel injection into cylinders. The pressure in the common rail goes as high as 200 MPa, and it causes a considerable temperature increase. In order to make sure there is enough fuel for injectors, the supply pump is designed to deliver more fuel than needed. The excessive unburned high temperature fuel returns back to the fuel tank through the leakage lines. Even though the flow rate of the leak is not much, because of its high temperature, it causes temperature increase in the fuel tank. The fuel cooler prevents excessive temperature increase in the fuel tank. The Easy5 model of the fuel circuit is depicted in Figure 18.

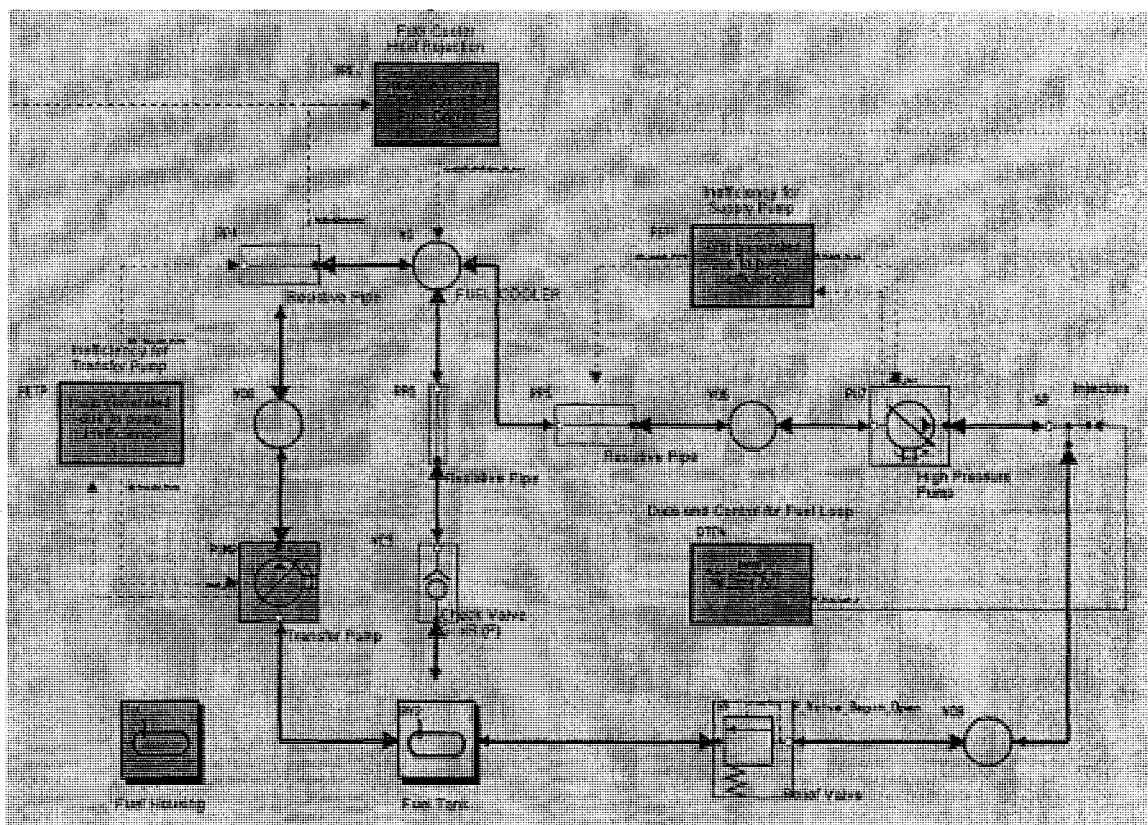


Figure 18. Easy5 model for the fuel circuit

In addition to the fuel tank, a fuel housing has been designed for the fuel circuit. The fuel housing is an external fuel supply with constant temperature. It is used for some of the wind tunnel tests to eliminate the effect of the temperature changes in the fuel tank on the other parameters. The fuel tank has to be disconnected from the transfer pump before connecting the fuel housing.

In this circuit, the injectors are modeled with a T-split. The fuel consumption rate that was calculated by WAVE engine model is applied to open end of the T-split as

mass flow rate, and the excessive fuel returns to the fuel tank after depressurized through a relief valve (RF).

Heat calculations for pumps. The pumps are the only heat sources for the fuel circuit. The generated heat due to the inefficiencies of pumps can be calculated by using equation 7. The heat calculated for the transfer pump and the supply pump have been applied to pipes RP4 and RP5, respectively.

Heat rejection calculation for the fuel cooler. The fuel cooler and AC condenser are combined together and called as the combo cooler. The core sizes of the combo cooler are 591 mm in width, 305 mm in height and 97.2 mm in depth. However the width, height and depth utilized for fuel cooling is given as 591 mm, 76 mm and 58 mm respectively. The heat rejection values for the fuel cooler for 51 °C inlet outer flow temperature and 80 °C inlet inner flow temperature is given in Table 10. The outer flow for the oil cooler is ambient air as in oil cooler, and the inner flow is diesel fuel in the circuit.

Applying similar conversions as the oil circuit heat rejection calculations Table 10 is transformed to mass flow inputs and the heat rejection per ETD for the output (see

Table 11). Linear interpolation is used between data values.

Table 10

Heat Rejection (kW) for the Fuel Cooler

Speed of Outer Flow (m/s)	Volumetric Inner Flow (l/min)				
	4.7	5.7	6.6	7.6	4.7
0	0	0	0	0	0
6.63	0	2.07	2.29	2.48	2.64
8.84	0	2.24	2.51	2.74	2.95
12.22	0	2.35	2.65	2.91	3.15
13.27	0	2.42	2.75	3.04	3.30

Table 11

Heat Rejection per ETD for the Fuel Cooler

Outer Mass Flow (kg/s)	Inner Mass Flow (kg/s)				
	0	0.827	1.034	1.240	1.447
0	0	0	0	0	0
1.291	0	0.559	0.585	0.607	0.628
1.454	0	0.593	0.622	0.646	0.670
1.600	0	0.622	0.652	0.676	0.700
1.760	0	0.654	0.685	0.711	0.737

The calculated heat rejected from the volume component (VO) that represents the fuel cooler in Figure 18, page 56.

Recirculation of Air Effect

The fan draws the ambient air through the grill screen and coolers, and pushes it out from side hood openings. Since this air is used to cool the circulating fluids in the cooling systems, its temperature is expected to be higher than the ambient temperature. Depending on the wind speed and direction, this heated air recirculates and causes temperature increase at the grill screen in front of the tractor. This phenomenon is called the recirculation of air effect, and a schematic of it is demonstrated in Figure 19.

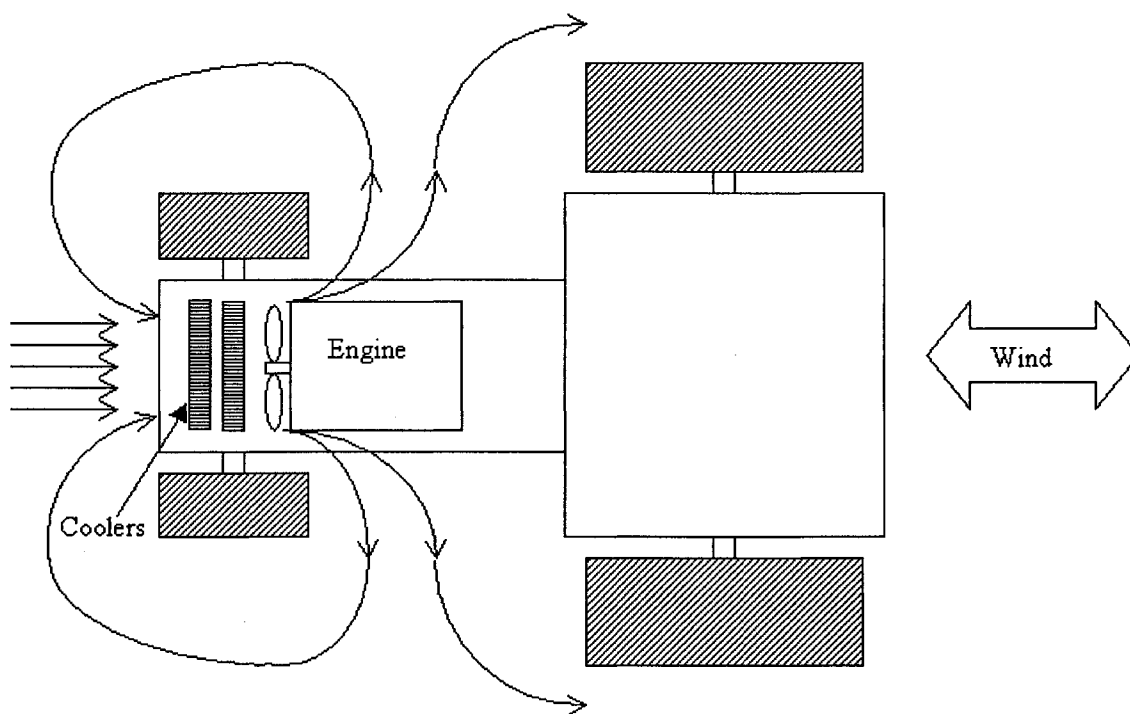


Figure 19. The top view of the schematic for recirculation of air effect for tractor

In modeling the recirculation of air effect, real test data are used. The tests have been conducted in wind tunnel with different wind speeds and wind directions, the difference between the ambient air and the air at the grill screen is measured, the test results are given in Appendix D.4 and D.5.

The tractor was let running for two hours to reach the steady state. Six measurements are taken in one-minute intervals by changing only the wind speed after two hours of run. Only two wind directions have been considered for these tests: tail wind and head wind. The tail wind is the

case when the wind blows from the rear to the front of the tractor; in this case, ambient temperature measurement is taken from the rear. As opposed to tail wind, the head wind is the case when the wind blows from the front to the rear of the tractor; apparently the ambient temperature measurement is taken from the front of the tractor. The test results are summarized in Table 12.

Table 12

Temperature Difference from the Ambient Because of Recirculation of Air Effect

Wind Direction (Head/Tail)	Wind Speed (km/h)	Ambient (°C)	Grill Temp (°C)	Temperature Difference (Grill - Ambient) (°C)	Estimated Temperature Difference (°C)
T	-11.0	40.5	52.4	11.9	11.9
T	-9.0	40.5	51.9	11.4	11.4
T	-7.0	42.6	52.4	9.8	9.8
T	-5.0	42.5	51.4	8.9	8.9
T	-3.0	45.1	51.6	6.5	6.5
	0				2.3
H	1.3	25.9	26.7	0.8	0.8
H	1.4	25.9	26.5	0.6	0.6
H	3.5	25.9	26.2	0.6	0
H	4.2	25.9	26.4	0.8	0
H	4.3	25.9	26.5	0.6	0
H	5.1	25.9	26.2	0.3	0

Test results are represented with a solid line in the graph illustrated in Figure 20. Negative wind speed represents the tail wind as positive one represents the head wind. Missing test values between -3.0 and 1.3 km/h wind speed are estimated as linear and depicted with a dashed line in Figure 20. Moreover the recirculation of air effect is estimated as zero for 3.4 km/h and more head wind speeds. The estimated temperature differences are also given in Table 12.

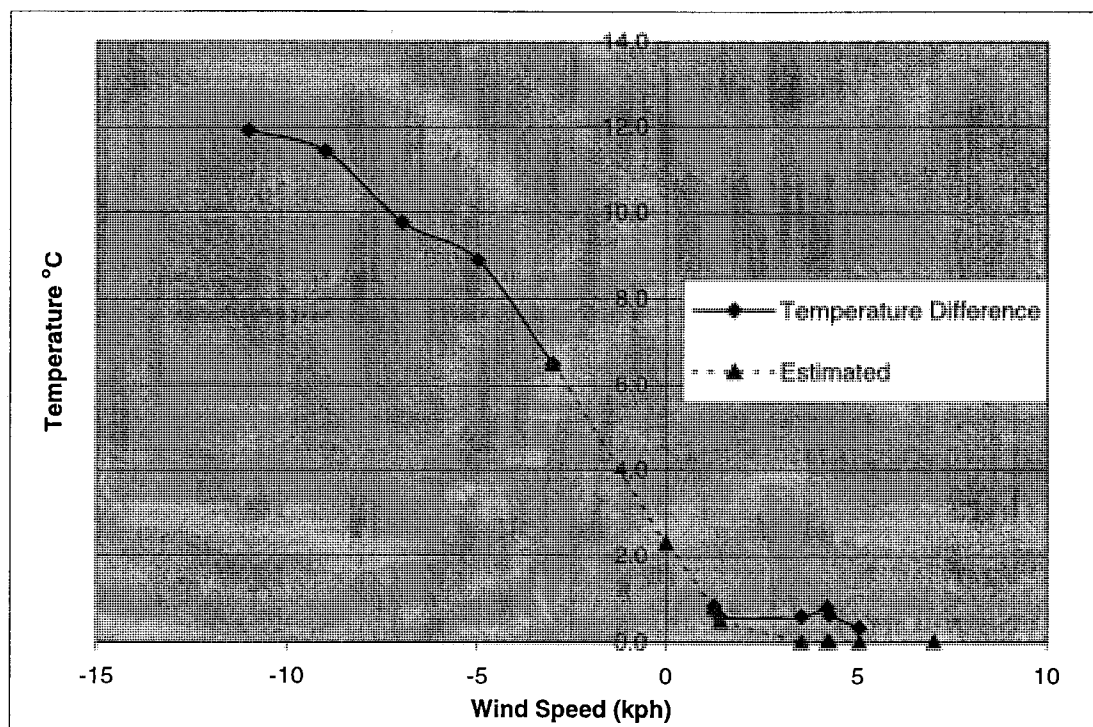


Figure 20. Recirculation Effect on Air Temperature at Grill Screen

As wind speed and direction are inputs to the comprehensive energy model, the corresponding estimated temperature difference from the Table 12 is added to ambient temperature to get the grill screen temperature.

Only two wind directions are considered in the scope of this study, however in real operating conditions the wind direction is much more complex than this. For a better understanding of the recirculation of air effect a computational fluid dynamics (CFD) analysis can be very helpful.

Controlled Torque Applied to PTO Shaft and Rear Axles

Two separate torque generators are created to facilitate the model run for PTO and Axle tests. They are named as PTO torque generator and the rear axle torque generator, respectively. Both use a PI controller with a proportional constant 20 and an integral constant 2. Normally they are not the part of the CEM, they are required to be connected by the user.

PTO torque generator. Figure 21 depicts a sample connection for PTO torque generator. The connection procedure is as follows:

- 1) Connect TQ_PTO_PI output of component GB to TQ_RPMtype_SJ3 input of component SJ3,

- 2) Set TG_RPMtype_SJ3 input of component SJ3 to negative one (-1),
- 3) Connect Engine RPM output of E3 simple engine model to REF_GB input of component GB,
- 4) Set input table A2T_T14 to the desired engine RPM as required in the test.

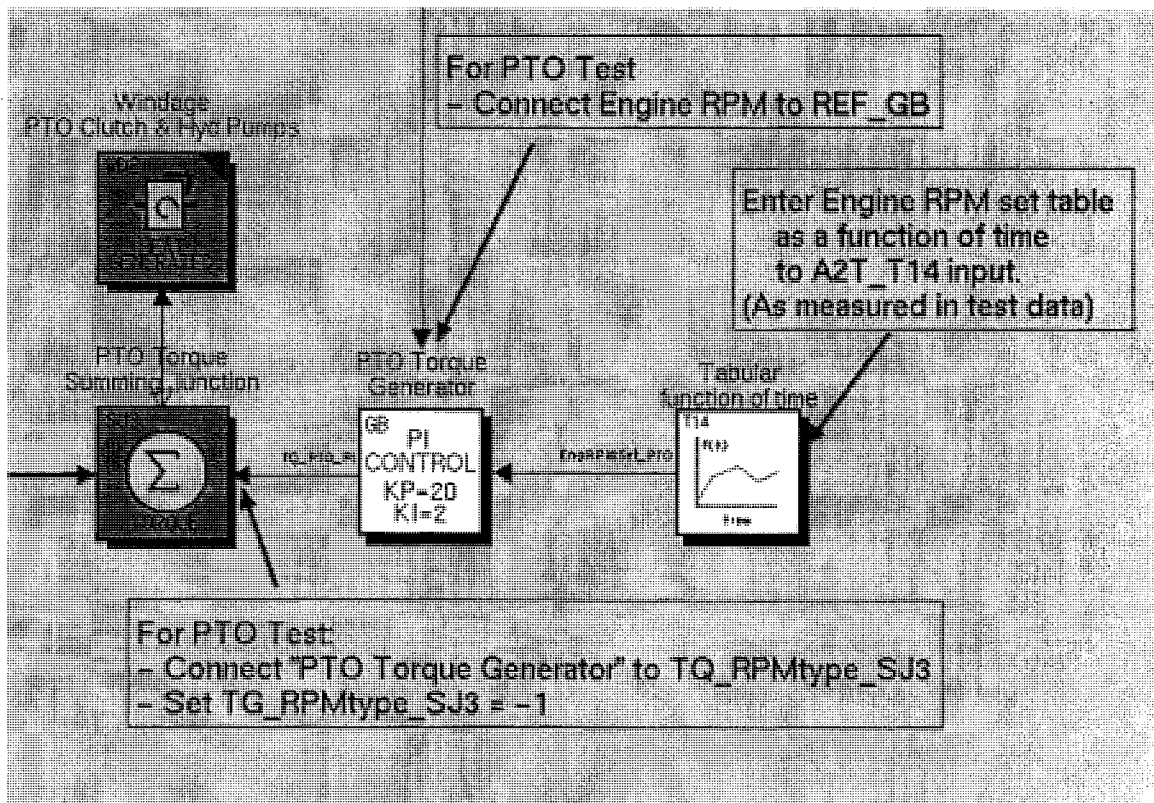


Figure 21. PTO torque generator connected to torque summing junction

The PTO Torque Generator compares the engine RPM with the desired one and generates the torque to be applied to

summing junction (SJ3). The PI controller's schematic and governing equations are given in Appendix D.6 ("Easy5 Library Documentation," 2002).

Rear AXLE torque generator. Figure 22 depicts rear axle with the rear tires connected; T2LR is the left rear tire and T3RR is the right rear tire.

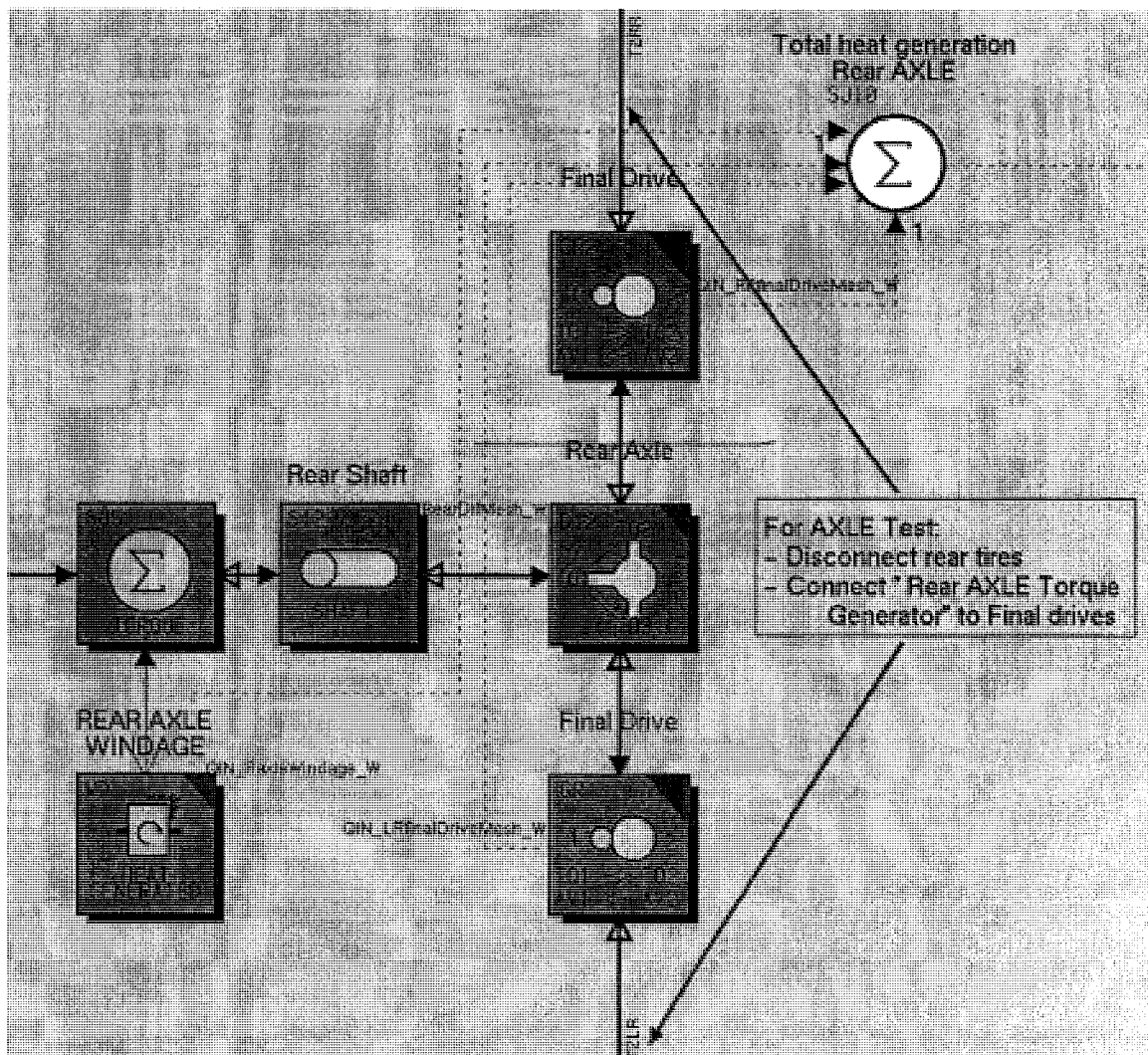


Figure 22. Rear AXLE connected with tires

Since gear couples GR and GR2 representing the final drives for rear axle do not have torque input, the axle torque generator has two rotating inertia components RI and RI2 addition to the PTO torque generator (See Figure 23).

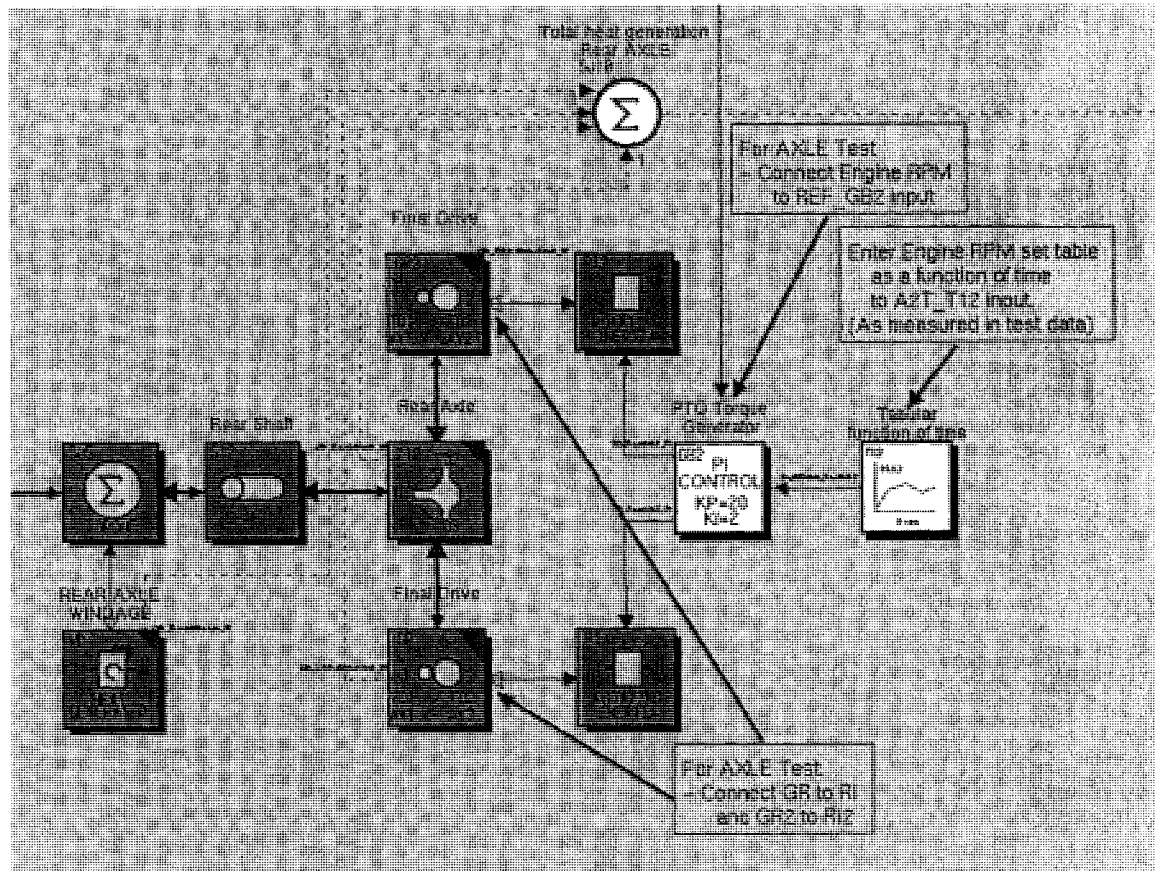


Figure 23. Axle torque generator is connected to the rear axle

The connection procedure of the rear AXLE torque generator as follows:

- 1) Disconnect the left and the right rear tires from the final drives,
- 2) Connect the final drives GB and GB2 to rotating inertias RI and RI2, respectively. GB and RI components have ported connection ability, therefore selecting GB and RI consecutively would be enough for a default connection ("Easy5 User Guide", 2003).
- 3) Connect Engine RPM output of E3 simple engine model to REF_GB2 input of component GB2,
- 4) Set input table A2T_T12 to the desired engine RPM as required in the test.

Similar to the PTO torque generator, the rear AXLE torque generator compares the engine RPM with the desired one and generates the torque to be applied to rotating inertias (RI and RI2). Note that the torques applied on the left and the right final drives are both equal.

Theory for the rotating inertia. RI component has four torque inputs. It generates an angular velocity depending on these torques. The governing equation is:

$$\frac{d\omega}{dt} = \frac{1}{J} \sum_{i=1}^4 TQ_i \cdot TG_i$$

where

ω : Angular velocity of rotating inertia
[rad/sec]

J : moment of inertia [kg.m²]

TQ_i : ith torque (i=1,...,4) [N.m]

TG_i : Gender of ith torque (i=1,...,4) [+1 or -1]

Front and Rear Differentials

Simple differential model D1 is used for both front and rear differential. The detailed D1 is given in appendix D.7. The torsional efficiencies are taken 0.98 for both front and rear differentials. The ratio of drive shaft to axle speed for the rear differential is 5.2727 and for the front shaft 3.7273.

Final Drives

The final drives have been simulated by gear couple. The efficiencies and the gear ratios for four final drives are listed in Table 13.

Table 13

Efficiencies and Gear Ratios for the Final Drives

Location	Efficiency	Gear Ratio
Front-Left	0.975	6.0
Front-Right	0.975	6.0
Rear-Left	0.975	6.4286
Rear-Right	0.975	6.4286

Vehicle Dynamics

M3 component is used for the vehicle model (see Figure 24). M3 is a planar vehicle dynamics model, which is developed in the Midwest tractor company. A schematic of the vehicle model depicting the forces and moments applied to the tractor body is given in Figure 25.

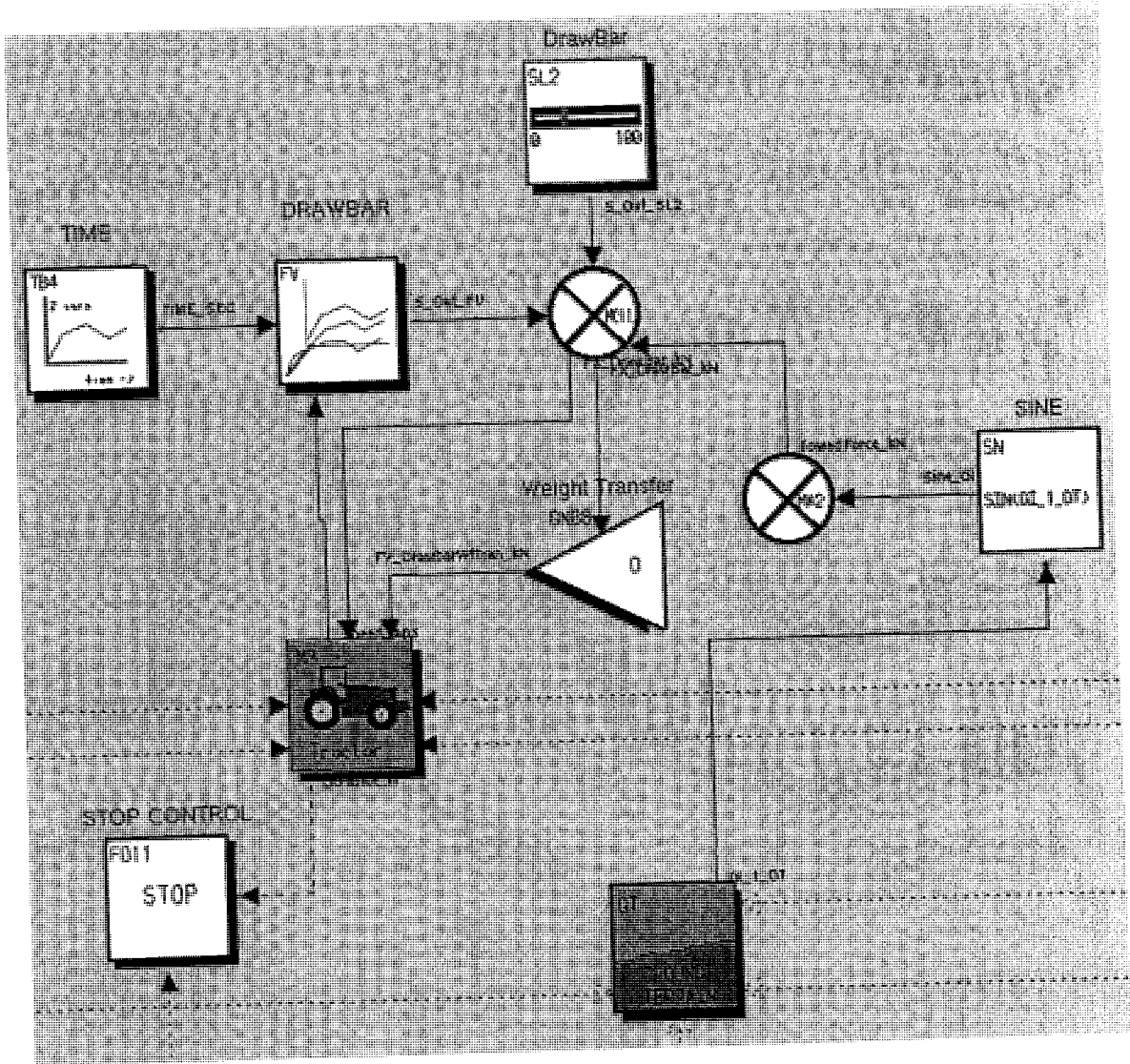


Figure 24. The usage of M3 and GT in the CEM

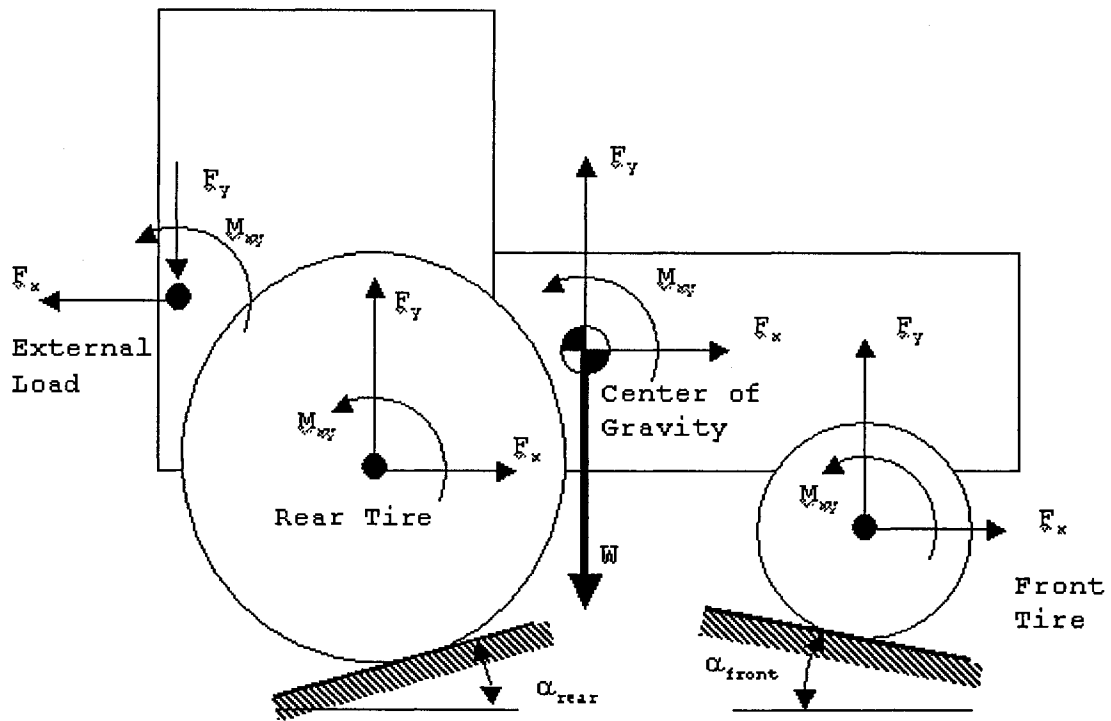


Figure 25..The schematic of planar vehicle dynamics

In this figure;

W : Gross weight of the tractor

F_x : Horizontal force

F_y : Vertical force

M_{xy} : Moment in x-y plane

α_{rear} : Average rear angle

α_{front} : Average rear angle

where

$$\alpha_{rear} = \frac{\alpha_{rear-left} + \alpha_{rear-right}}{2}, \text{ and } \alpha_{front} = \frac{\alpha_{front-left} + \alpha_{front-right}}{2}.$$

Geometric dimension and physical inputs to M3 component are given in Table 14.

Table 14

Geometric Dimension and Physical Inputs to M3 Component

Input	Value	Unit	Description
PMI_M3	25,000	kN.m ²	Polar pitch moment of inertia
GVM_M3	15,000	kg	Gross vehicle mass
XFV_M3	2.991	m	Horizontal position of front axle wrt rear axle
YFV_M3	-0.3	m	Vertical position of front axle wrt rear axle
XCV_M3	1.0469	m	Horizontal position of center of gravity wrt rear axle
YCV_M3	0.125	m	Vertical position of center of gravity wrt rear axle
XLV_M3	-1.0	m	Horizontal position of load point wrt rear axle
YLV_M3	-0.2	m	Vertical position of load point wrt rear axle

In addition, M3 has four inputs for each tire; horizontal force, vertical force, moment and angle of the ground with respect to horizontal line. These inputs are not supposed to be entered manually, since they are directly connected to the tires.

The last three inputs are horizontal and the vertical forces, and the moment of the load point, which will be used when a trailer is attached to the body of the tractor. Otherwise they will be set to zero.

Ground and Terrain

GT component is used for the ground and terrain model (see Figure 24, page 70). The Midwest tractor company has also developed GT component, which is a planar ground and terrain model. A schematic of the model is demonstrated in Figure 26.

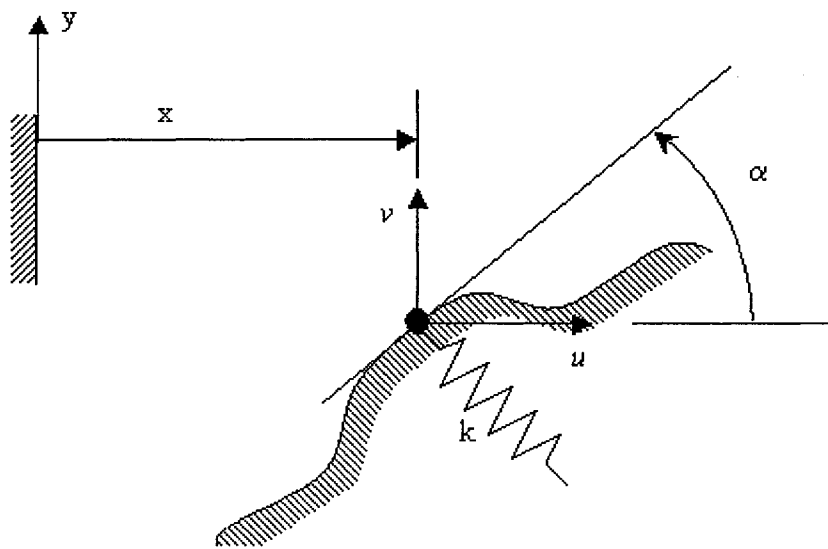


Figure 26. The schematic for ground and terrain model

In this figure;

x : the horizontal distance from the starting point[m]

y : the vertical distance from the starting point[m]

- u : the horizontal velocity [m/s]
- v : the vertical or the climbing velocity [m/s]
- α : the climbing angle at distance x [degree]
- k : the cone index of the soil at distance x

The horizontal velocity and vertical velocity can be calculated as:

$$u = \frac{dx}{dt}$$

$$v = \frac{dy}{dt} = u \cdot \tan\left(\frac{2\pi\alpha}{360}\right)$$

TCI_GT is the input table, which the cone index physical property of the soil is given depending on the distance traveled. Cone index value for a hard surface (e.g. asphalt) is taken as 9999 kPa. Cone index values for different soil types are given in Table 15 (Saarilahti, 2002). To improve the understanding of cone index terminology, the vehicle operability for different levels of cone indexes are also given in Appendix D.8.

Table 15

Cone Index for Different Soil Types

Soil description	Cone Index (kPa)
Gravel, dry	300-700
Gravel, moist	400-800
Sand, dry	150-250
Sand, moist	300-500
Clay, dry	400-1200
Clay, moist	200-300
Clay, wet	50-150

The other inputs to GT macro are horizontal position and velocities of for wheels, which are connected to tire macros.

Tires

Two dimensional traction model is used for tire simulation. Similar to M3 and GT macros, the Midwest tractor company has developed T2 macro to simulate two-dimensional traction. The usage of T2 macro for four tires is illustrated in Figure 28.

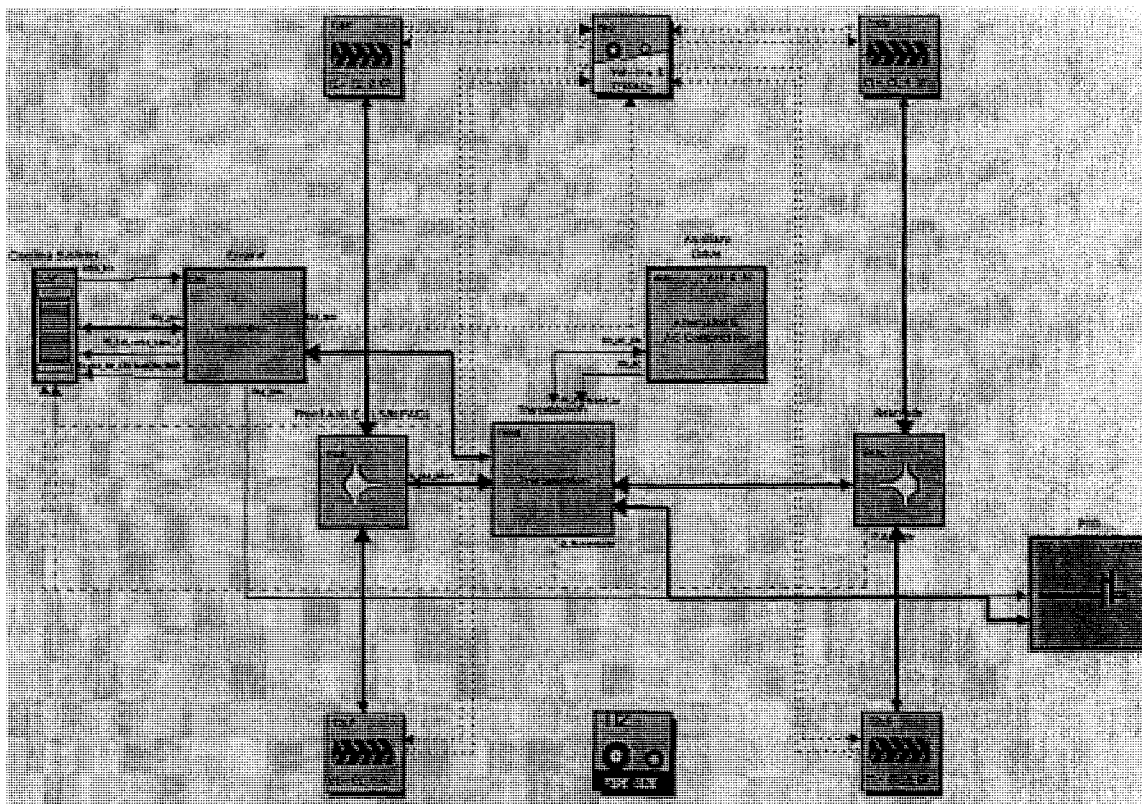


Figure 27. An overall view to comprehensive energy model the tractor

In order to use T2-tire traction macro, the simulation model should also include TI- the tire size macro, which allows the user to choose one or more of the tires that are already defined. For the Tractor model for CEM the tire selection codes are determined as 28 for the front tires and 29 for the rear tires. The tire selection codes and the basic dimensions of the tires are listed in Table 16.

Table 16

Tire Selection Codes and Tire Dimensions for the Tractor

	Front Tire	Rear Tire
Tire Selection Code	28	29
Overall tire diameter (m)	1.59	2.0498
Tire section width (m)	0.419	0.5309
Tire section height (m)	0.3373	0.4407
Tire Pressure (psi)	2 - 41	9 - 29

Implement Load

Implements are connected to three-point hitch mechanism at the rear of the tractor. A simplified schematic of the three-point hitch is given in Figure 29. MP (pivoting mechanical load) macro in hc - thermal hydraulics library represents a similar mechanism to the one in Figure 28. Detailed information on MP - macro is given in Appendix D.9 ("MSC.Easy5 Thermal," 2003).

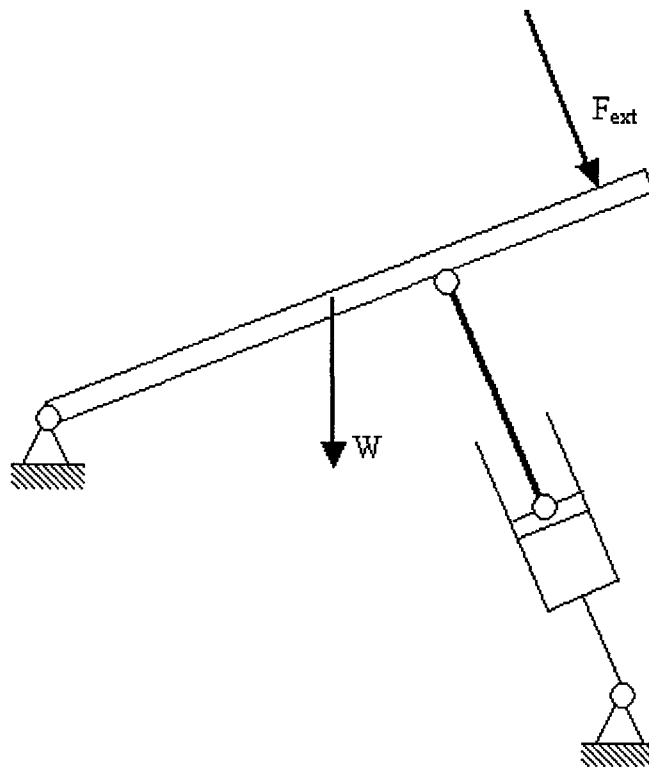


Figure 28. A schematic for three-point hitch mechanism for tractor

The hydraulic cylinder is a single chamber actuator, and the thermal hydraulics library has AX - macro to represent it. The implement load modeled by connecting AX and MP macros (see Figure 18, page 56).

Verification of the Developed Model

Ramanata (1998, chap. 2) has validated his vehicle simulation model by comparing against Smith & Starkey's (1995) results. He has selected the parameters that Smith had graphed, and reproduced the same graphs with his model. After a visual comparison, he concluded by stating "the three-degree-of-freedom model is valid since the response of this model closely follows the response generated by Smith. Therefore, the vehicle model of this study is concluded to be acceptable and valid".

Fritz (1999) has followed a similar way to Ramanata. He has created a dynamic model of the gear-cam mechanism with the EASY5 macros that he had developed, and compared its results against the results of the kinematics analysis of the same mechanism that he had published in an earlier article with his colleagues (Fritz, ElSawy, Modler & Goldhan, 1997). Obviously there were oscillations around the kinematics analysis results since dynamics were involved. However, since it was observed that both cases were following the same pattern, he concluded that the Easy5 model of the gear-cam mechanism and the developed macros are valid. Fritz has continued his validation process by creating a servomotor model with the developed

macros and comparing against experimental and theoretical results of other researchers (Chern, Chang & Chang, 1997; Dulger & Uyan, 1997).

Once the comprehensive energy model was developed it was necessary to verify it with the test data. In this verification, the test data and the results of the simulation model have been plotted and their relation was observed as many of researchers had suggested (Assanis et al., 2000; Day, 1996; Fritz et al., 1999; Ramanata, 1998). The most of the available test data for the selected tractor model was for the earlier versions of the tractor. The company has upgraded some components as conclusions of those tests. Therefore the test data available for the CEM was limited. This section describes the strategy, and three sets of test data used for comparison to verify CEM.

Comparison with PTO Test Data

As it was described in chapter 3, page 23, the PTO test is a six-minute run after a two-hours of warm-up session. Measurements are taken at the end of each minute during the six-minute run. Table 17 lists the PTO test data for the selected parameters. In order to run the simulation model for the PTO test, the PTO torque generator was connected, as it is described in pages 59 through 60.

Table 17

The PTO Test Data for Selected Parameters

Test Parameter	Reading Minutes					
	1	2	3	4	5	6
Engine Speed (rpm)	2203	2201	2202	2202	2202	2198
Fan Speed (rpm)	1591	1636	1626	1628	1632	1699
Wind Speed (km/h)	1.4	3.5	1.3	4.2	4.3	5.1
Air, Ambient Front of Tractor (°C)	25.9	25.6	25.9	25.6	25.9	25.9
Air, Ambient Rear of Tractor (°C)	31.9	31.4	31.8	32.1	31.8	31.9
Toptank Temperature (°C)	96.8	96.8	96.8	97.0	97.0	96.9
Air, Ave. Grill Screen Temp. (°C)	26.5	26.2	26.7	26.4	26.5	26.2
Intake manifold temperature (°C)	56.7	56.8	56.1	56.3	56.4	56.2
Oil Cooler Inlet Temperature (°C)	66.5	66.5	66.5	66.5	66.5	66.5
Oil Cooler Outlet Temperature (°C)	58.6	58.5	58.5	58.5	58.5	58.3
Fuel Cooler Inlet Temperature (°C)	48.8	49.0	48.9	49.1	48.9	48.9
Fuel Cooler Outlet Temperature (°C)	37.4	37.7	37.4	37.2	37.8	37.3
PTO shaft velocity (rpm)	1011	1010	1011	1011	1011	1009
PTO Torque (Nm)	1850	1849	1849	1849	1848	1848

In order to acquire results from the CEM, three consecutive steps of simulation runs have been followed.

First, CEM was run 5 minutes of real time to obtain steady state torque applied to E3 the simple engine due to the load in PTO. The estimated heat rejection from charge air cooler was also recorded. Secondly, these two parameters were used as inputs to WAVE engine model, which was run for 120 seconds of real time to obtain the estimated fuel consumption rate and the estimated heat rejection from radiator. And finally, the CEM was run again by inputting the estimated fuel consumption rate and the estimated heat rejection from radiator. The comparison graphs are depicted in Figures 29 through 36.

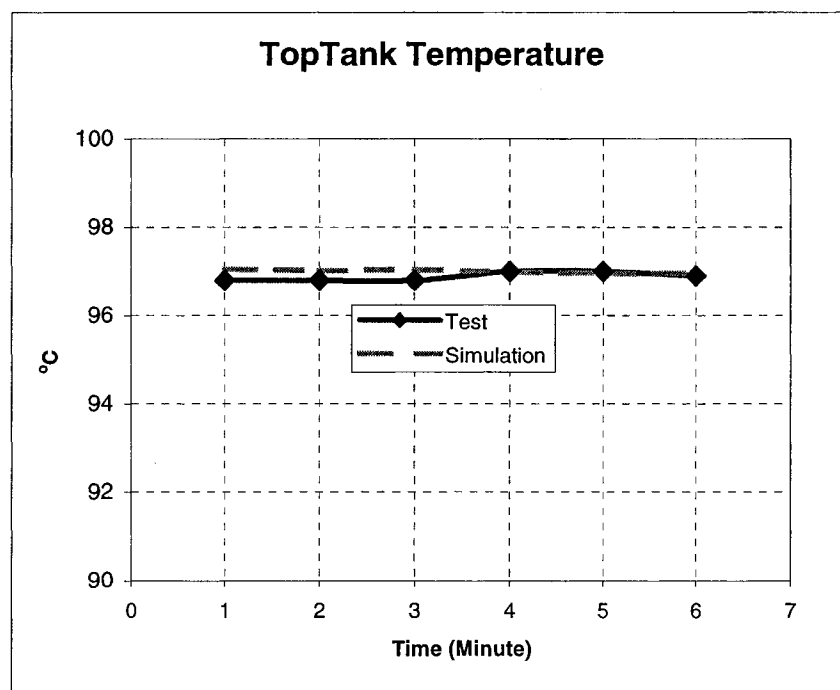


Figure 29. Comparing the simulation against the PTO test for Toptank temperature

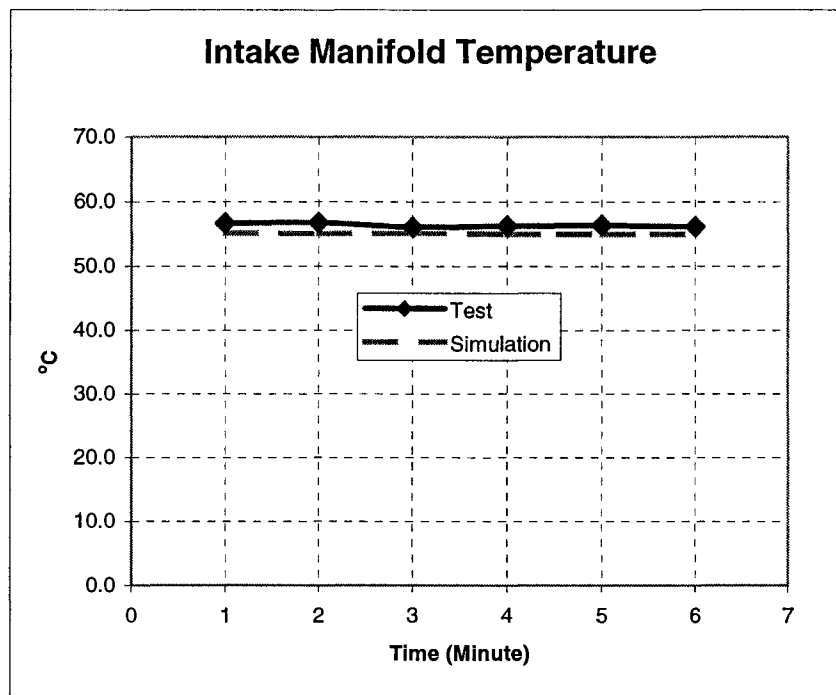


Figure 30. Comparing the simulation against the PTO test for intake manifold temperature

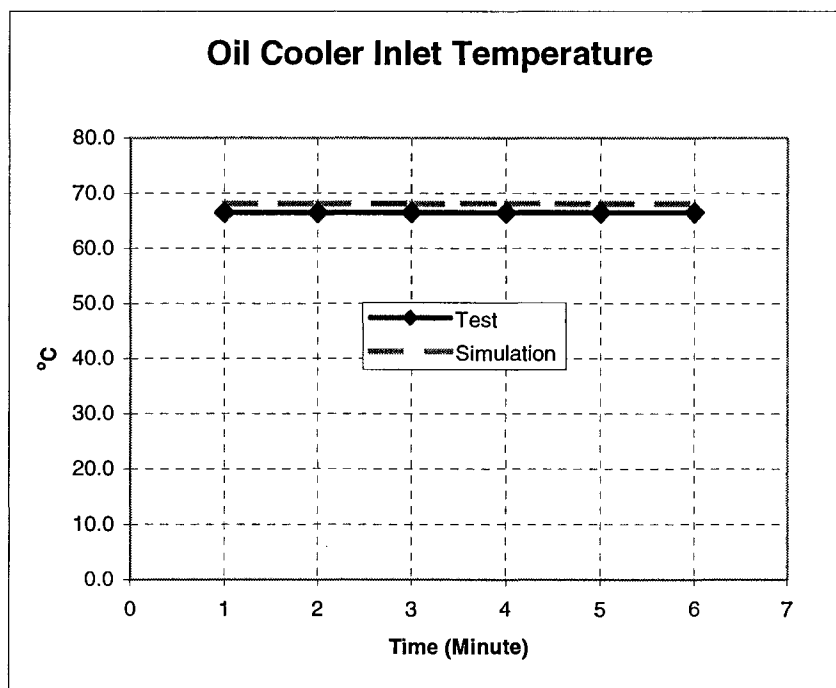


Figure 31. Comparing the simulation against the PTO test for oil cooler inlet temperature

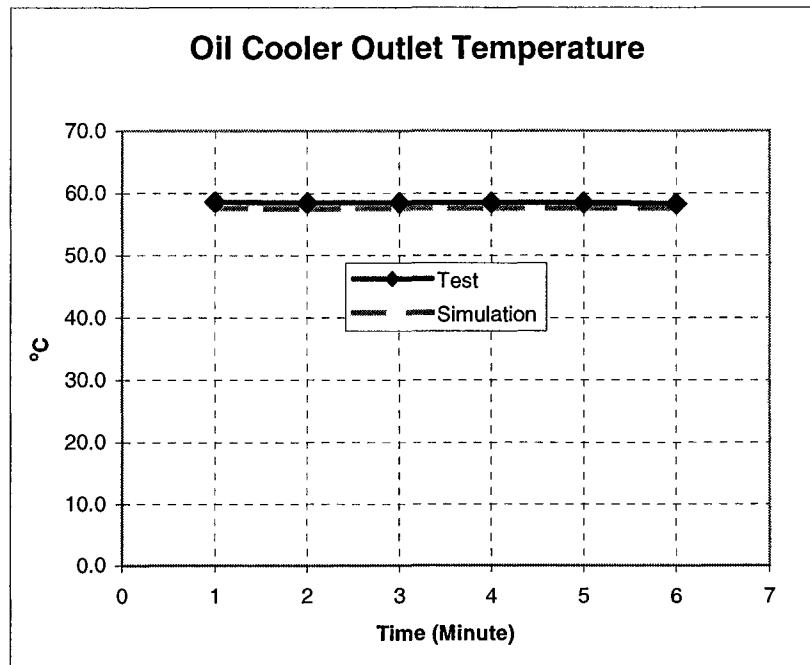


Figure 32. Comparing the simulation against the PTO test for oil cooler outlet temperature

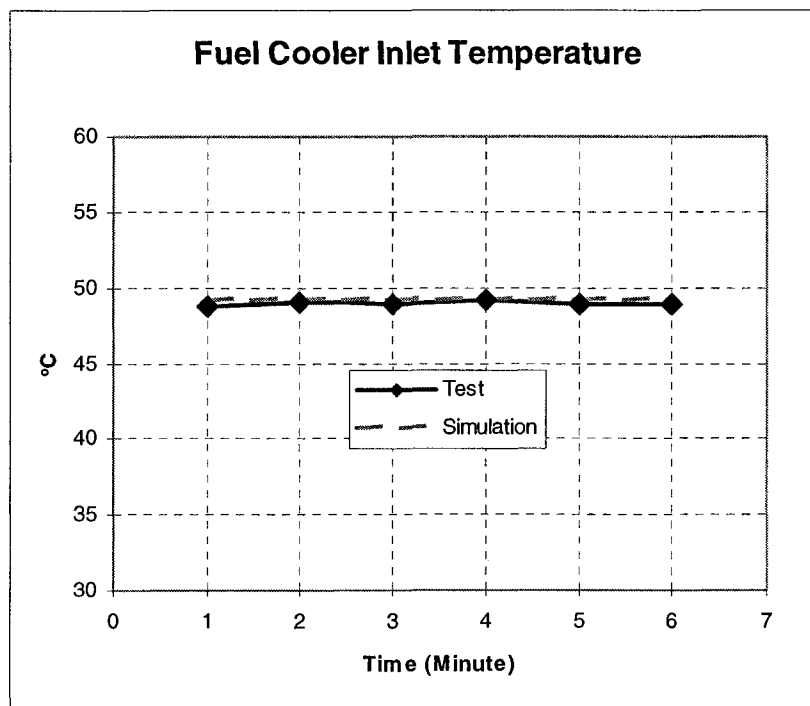


Figure 33. Comparing the simulation against the PTO test for fuel cooler inlet temperature

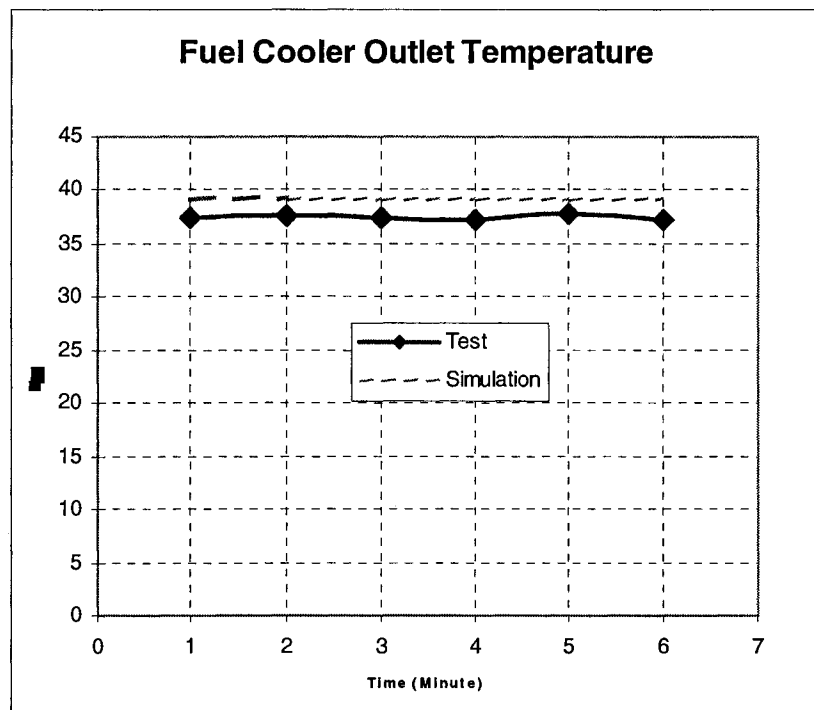


Figure 34. Comparing the simulation against the PTO test for fuel cooler outlet temperature

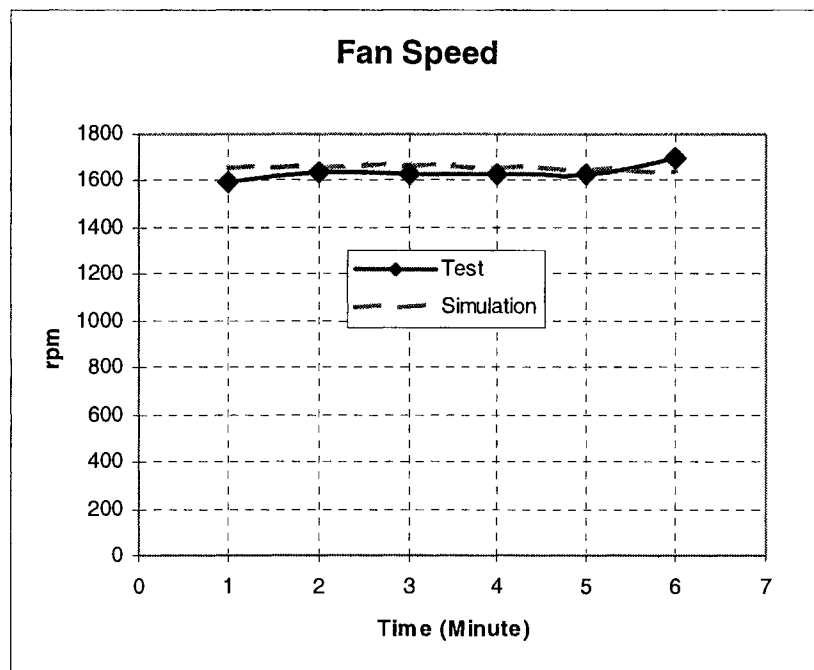


Figure 35. Comparing the simulation against the PTO test for fan speed

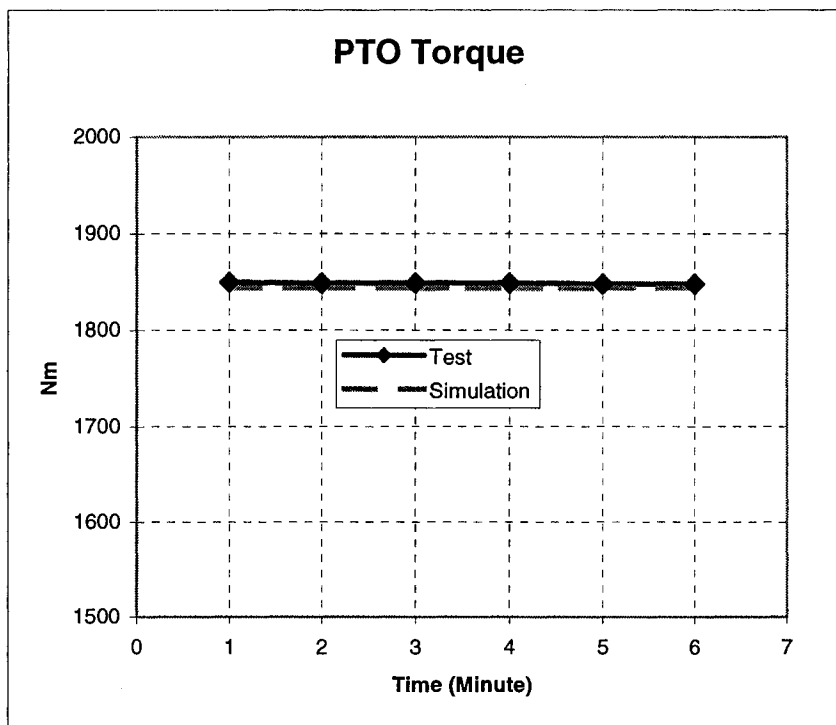


Figure 36. Comparing the simulation against the PTO test for PTO torque

Table 18

Percentage Errors of the Simulation Results from the PTO Test Data

Parameters	Average Test Data	Average of CEM	Percentage Error
Top Tank Temperature	96.88	97.00	0.12%
Intake Manifold Temperature	56.42	55.07	2.39%
Oil Cooler Inlet Temperature	66.50	68.07	2.36%
Oil Cooler Outlet Temperature	58.48	57.55	1.59%
Fuel Cooler Inlet Temperature	48.93	49.20	0.54%
Fuel Cooler Outlet Temperature	37.47	39.10	4.36%
Fan Speed (rpm)	1635.33	1651.83	1.01%
PTO torque (Nm)	1848.83	1843.95	0.26%

Averages of the six readings for the test results and simulation model were compared to find out the percentage differences. The results are listed in Table 18. As rule of thumb, the simulation modelers are satisfied about the results of the simulation when the results are in the margin of $\pm 3\%$ of the actual test data (Gessel, G., Gilmore, B., Volfson, B., Zhang, H.-Y., personal communication, July 22, 2004). By using this criterion, the only parameter that exceeds the limits is the fuel cooler outlet temperature with a value of 4.36%. This indicates that the model for the fuel circuit requires to be revised. The errors in the remaining parameters are within the acceptable limits.

Comparison with AXLE Test Data

As it was described in chapter 3, page 24, the AXLE test is also a six-minute run after a two-hours of warm-up session. Measurements are taken at the end of each minute during the six-minute run. Table 19 lists the AXLE test data for the selected parameters.

In order to run the simulation model for the AXLE test, the rear tires were disconnected and the axle torque generator was connected to rear final drives, as it is described in pages 61 through 63.

Table 19

The AXLE Test Data for Selected Parameters

Selected Test Parameters	Reading Minutes					
	1	2	3	4	5	6
Engine Speed (rpm)	2214	2212	2197	2195	2202	2208
Fan Speed (rpm)	2406	2408	2392	2390	2395	2402
Wind Speed (km/h)	11.8	11.1	12.2	10.4	11.9	10.8
Air, Ambient Front of Tractor (°C)	44.0	44.3	43.4	43.3	43.7	44.3
Air, Ambient Rear of Tractor (°C)	41.4	40.8	39.8	39.6	40.3	41.0
Toptank Temperature (°C)	108.7	109.3	108.8	108.7	108.7	108.7
Air, Ave. Grill Screen Temp. (°C)	51.9	52.0	52.2	52.0	53.0	53.3
Intake manifold temperature (°C)	70.1	70.3	69.3	69.2	69.8	70.0
Oil Cooler Inlet Temperature (°C)	88.1	88.1	88.2	88.2	88.2	88.2
Oil Cooler Outlet Temperature (°C)	77.4	77.6	77.1	77.0	77.2	77.3
Fuel Cooler Inlet Temperature (°C)	72.9	73.1	73.4	73.5	73.5	73.6
Fuel Cooler Outlet Temperature (°C)	61.8	61.8	61.6	61.7	62.1	62.5
Average Rear Axle Torque (kNm)	31.46	30.53	30.32	29.36	29.22	29.13

The simulation model was run in three steps as it was described in "Comparison with PTO Test Data", p. 75. The comparison graphs for selected parameters are depicted in Figures 37 through 44.

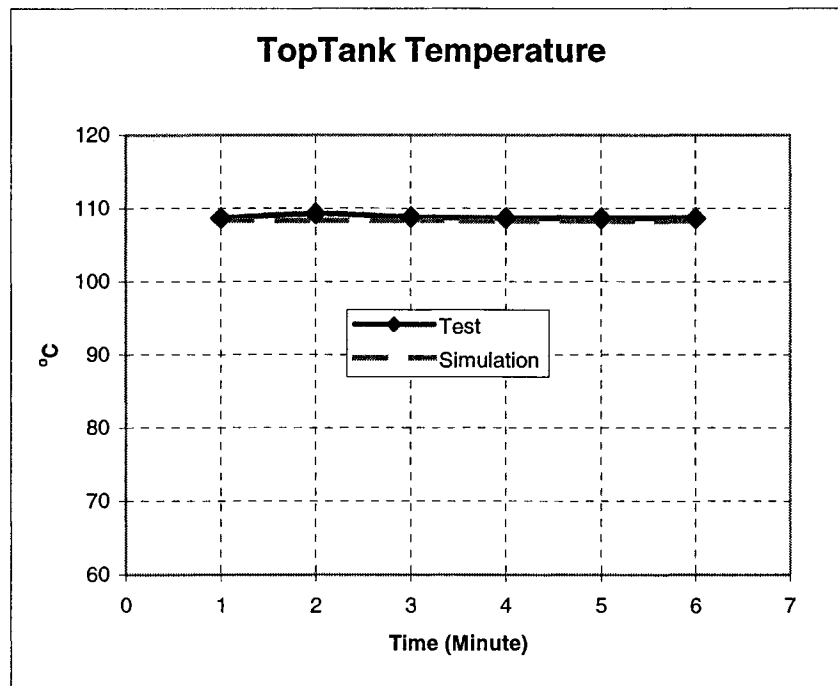


Figure 37. Comparing the simulation against the AXLE test for Toptank temperature

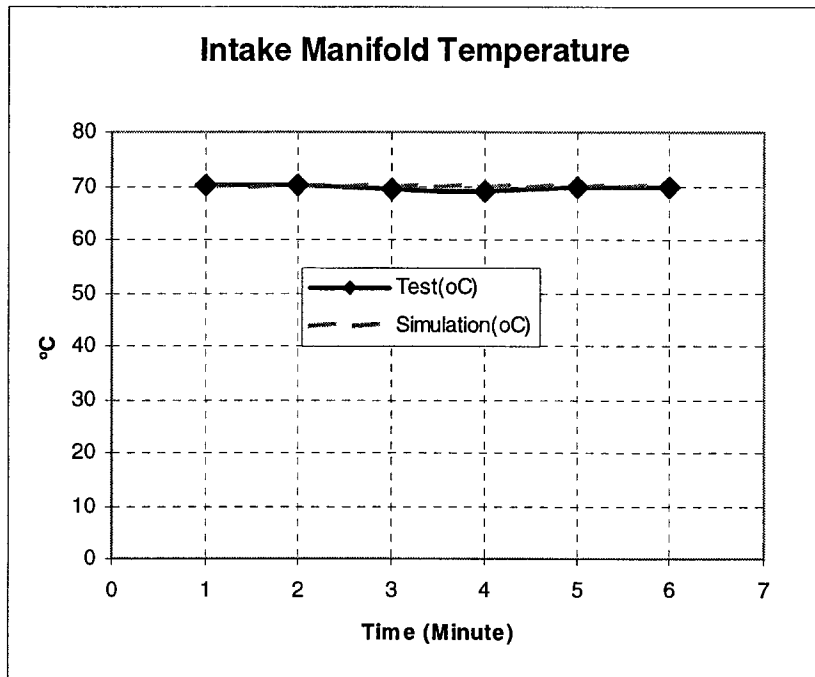


Figure 38. Comparing the simulation against the AXLE test for intake manifold temperature

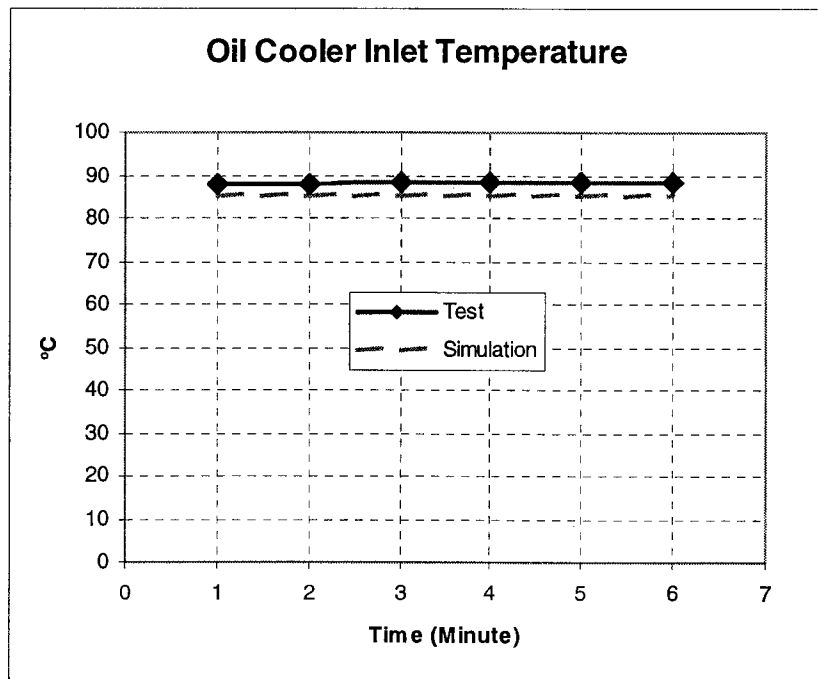


Figure 39. Comparing the simulation against the AXLE test for oil cooler inlet temperature

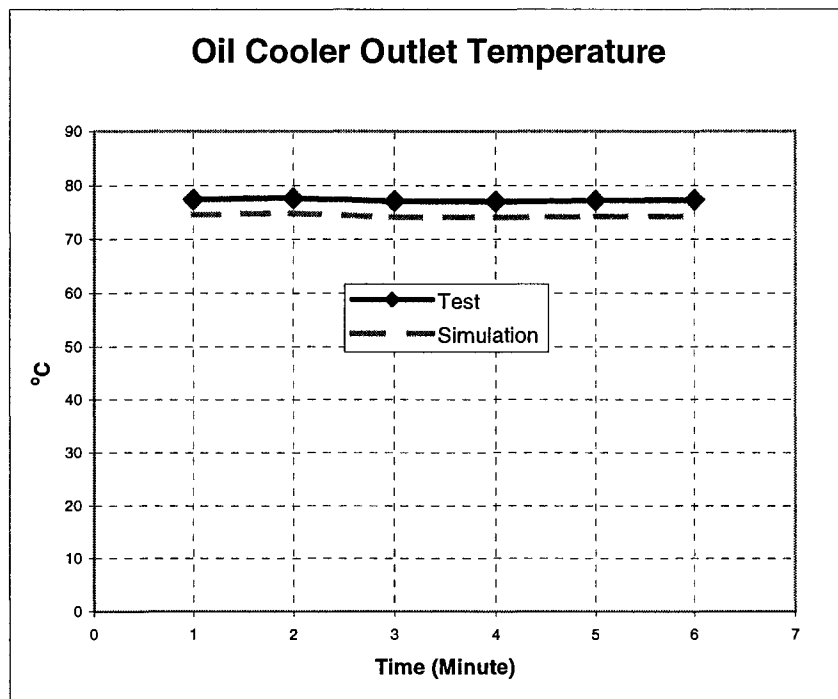


Figure 40. Comparing the simulation against the AXLE test for oil cooler outlet temperature

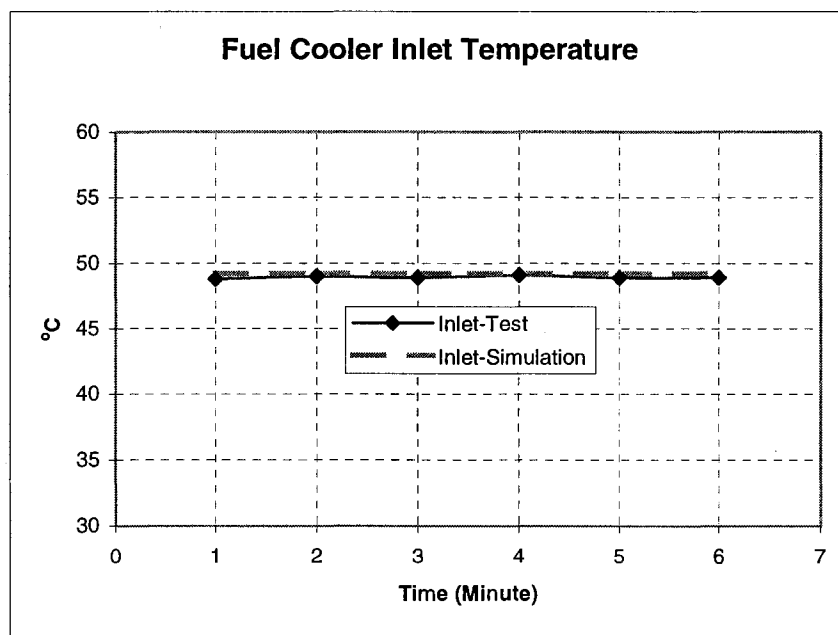


Figure 41. Comparing the simulation against the AXLE test for fuel cooler inlet temperature

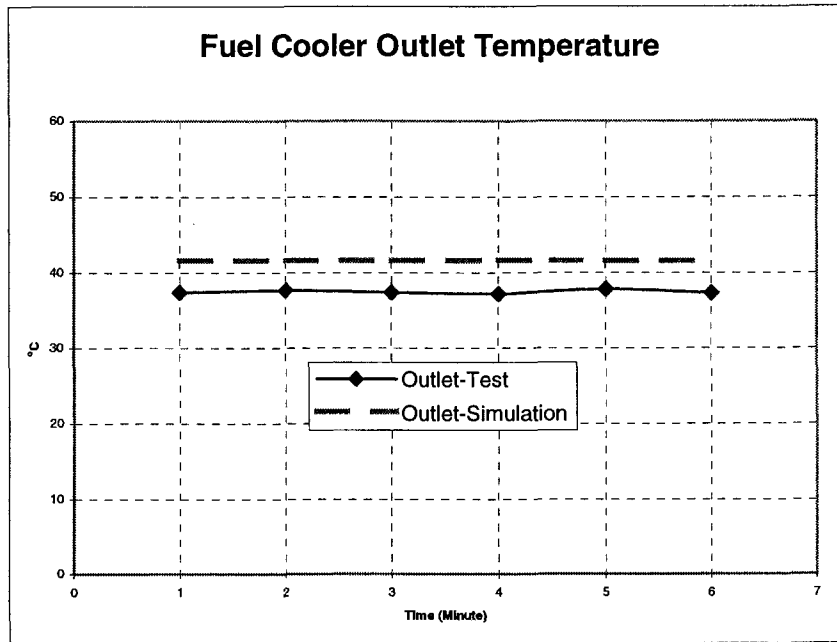


Figure 42. Comparing the simulation against the AXLE test for fuel cooler outlet temperature

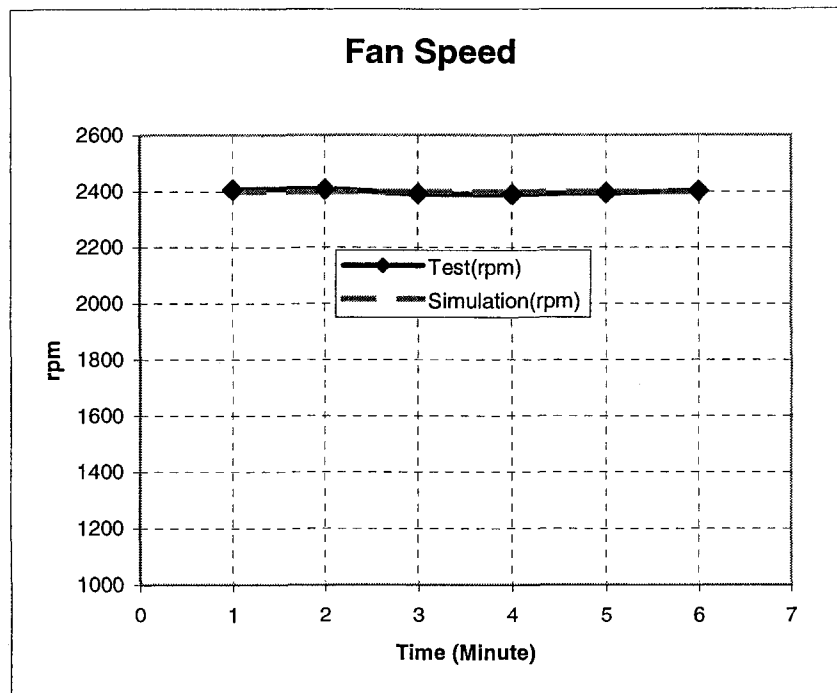


Figure 43. Comparing the simulation against the AXLE test for fan speed

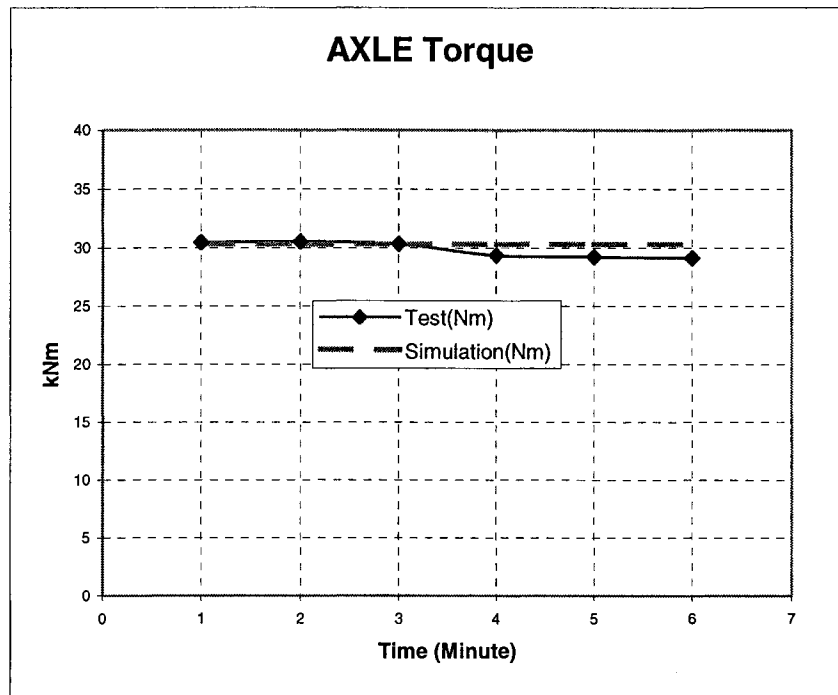


Figure 44. Comparing the simulation against the AXLE test for axle torque

Table 20

Percentage Errors of the Simulation Results from the AXLE Test Data

Parameters	Average Test Data	Average of CEM	Percentage Error
Top Tank Temperature	108.8	108.3	0.46%
Intake Manifold Temperature	69.8	69.9	0.21%
Oil Cooler Inlet Temperature	88.2	86.1	2.34%
Oil Cooler Outlet Temperature	77.3	75.8	1.90%
Fuel Cooler Inlet Temperature	73.3	71.5	2.50%
Fuel Cooler Outlet Temperature	61.9	58.5	5.52%
Fan Speed (rpm)	2399	2398	0.03%
AXLE Torque (kNm)	29.83	30.28	1.50%

Averages of the six readings for the AXLE test results and simulation model were compared to find out the percentage differences. The percentage errors are listed in Table 20. By using the $\pm 3\%$ margin criteria, the only parameter that exceeds the limits is the fuel cooler outlet temperature with a value of 5.52%.

Comparison with High Speed Wind Tunnel Transport Test Data

As it was described in chapter 3, page 24, the high-speed wind tunnel transport test is also a six-minute run after a two-hours of warm-up session. Measurements are taken at the end of each minute during the six-minute run. Table 21 lists the wind tunnel high-speed transport test data for the selected parameters.

Table 21

The High-speed Wind Tunnel Transport Test Data for Selected Parameters

Selected Test Parameters	Reading Minutes					
	1	2	3	4	5	6
Engine Speed (rpm)	2139	2139	2139	2139	2139	2138
Fan Speed (rpm)	2326	2325	2326	2326	2325	2326
Wind Speed (km/h)	23.7	22.1	23.0	21.5	22.1	18.9
Air, Ambient Front of Tractor (°C)	39.5	39.3	39.5	39.4	39.6	39.5
Air, Ambient Rear of Tractor (°C)	44.3	44.2	44.7	44.4	44.6	44.4
Toptank Temperature (°C)	94.7	94.7	94.7	94.7	94.7	94.7
Air, Ave. Grill Screen Temp. (°C)	40.1	40.0	40.2	39.8	40.0	40.0
Intake manifold temperature (°C)	59.2	59.2	59.2	59.0	59.2	59.2
Oil Cooler Inlet Temperature (°C)	100.1	100.1	100.1	100.1	100.1	100.1
Oil Cooler Outlet Temperature (°C)	81.8	81.8	81.8	81.8	81.8	81.8
Fuel Cooler Inlet Temperature (°C)	44.4	44.4	44.0	44.5	44.2	44.0
Fuel Cooler Outlet Temperature (°C)	44.5	44.5	44.7	44.6	44.6	44.6

In order to run the simulation model for the wind tunnel high-speed transport test, the tires were kept connected. The application of torque is simulated by setting the slope of the ground to 0.72 degree and adding a

wagonload of 25 kNm. These values are selected to obtain 2150 engine rpm. Even though the test was set to reach to 2200 engine rpm, the engine is software protected at the 16th gear; it can reach up to 2150 rpm.

The simulation model was run in three steps as it was described in "Comparison with PTO Test Data", p. 75. The comparison graphs for selected parameters are depicted in Figures 45 through 52.

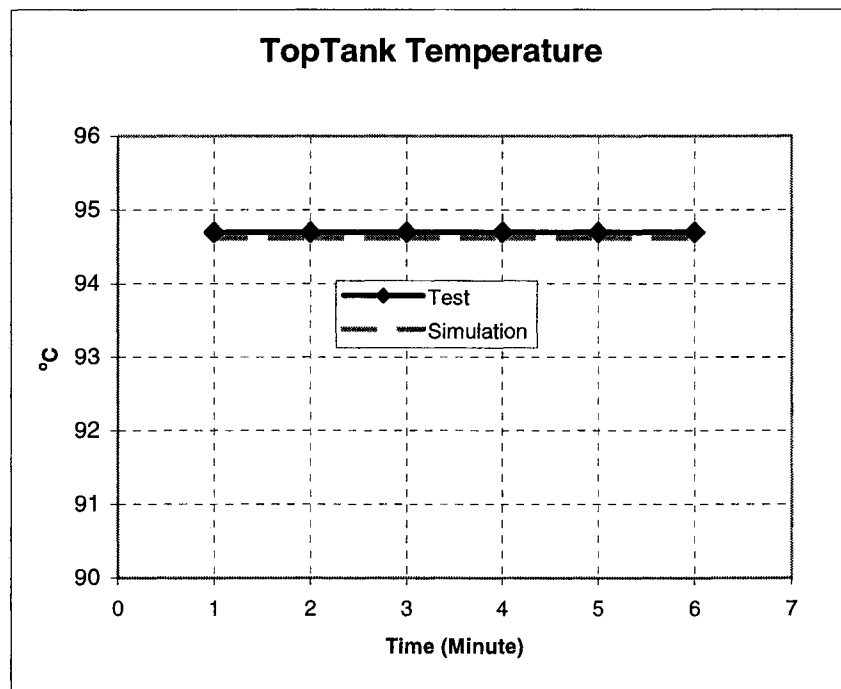


Figure 45. Comparing the simulation against the high-speed wind tunnel transport test for Toptank temperature

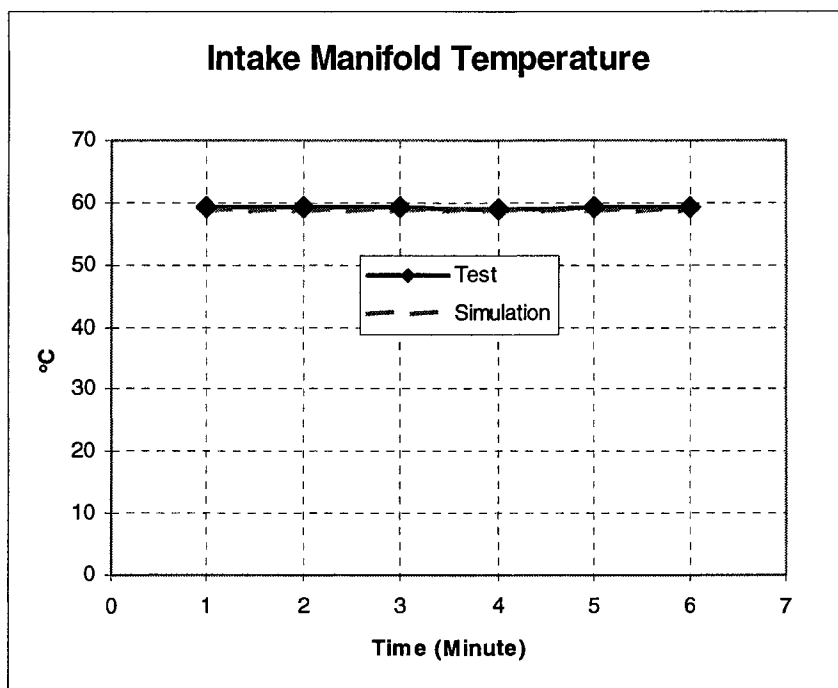


Figure 46. Comparing the simulation against the high-speed wind tunnel transport test for intake manifold temperature

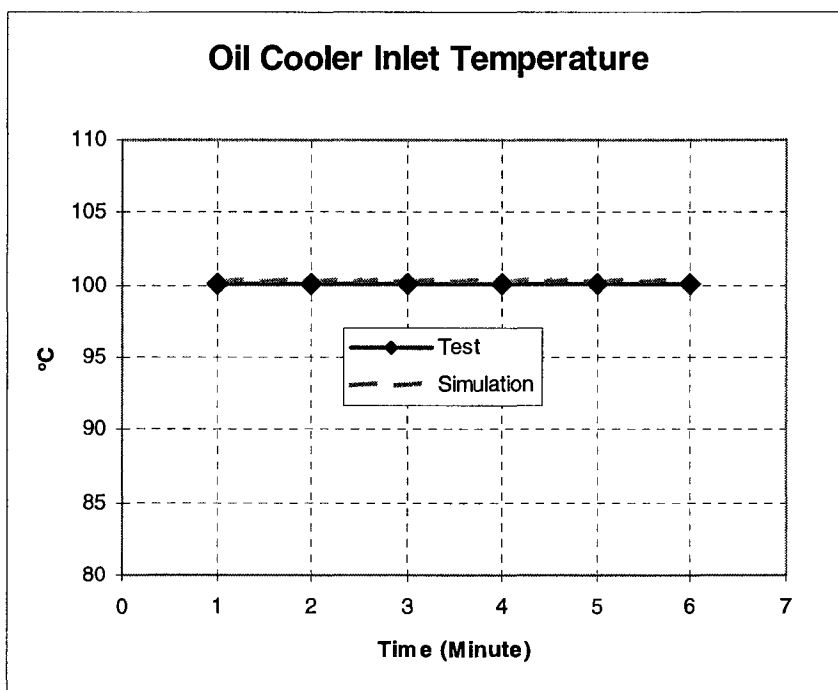


Figure 47. Comparing the simulation against the high-speed wind tunnel transport test for oil cooler inlet temperature

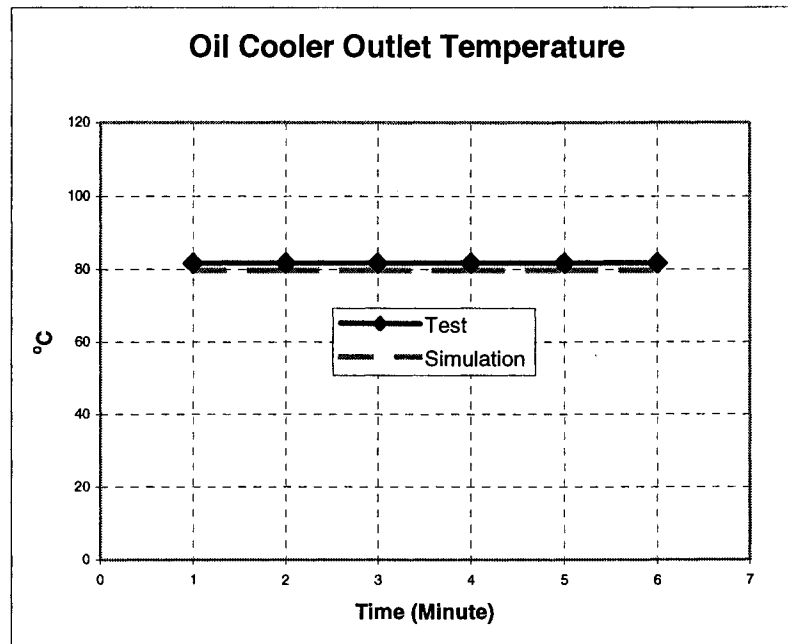


Figure 48. Comparing the simulation against the high-speed wind tunnel transport test for oil cooler outlet temperature

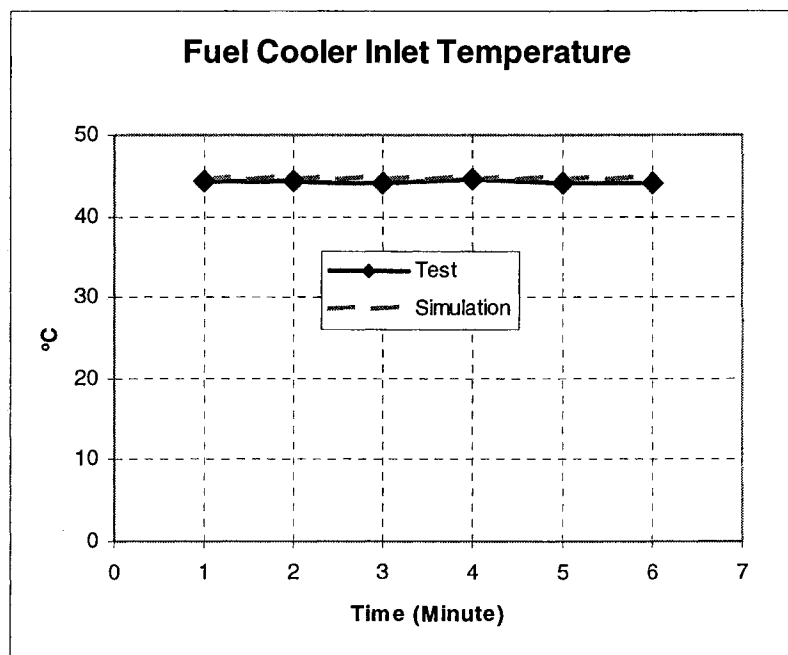


Figure 49. Comparing the simulation against the high-speed wind tunnel transport test for fuel cooler inlet temperature

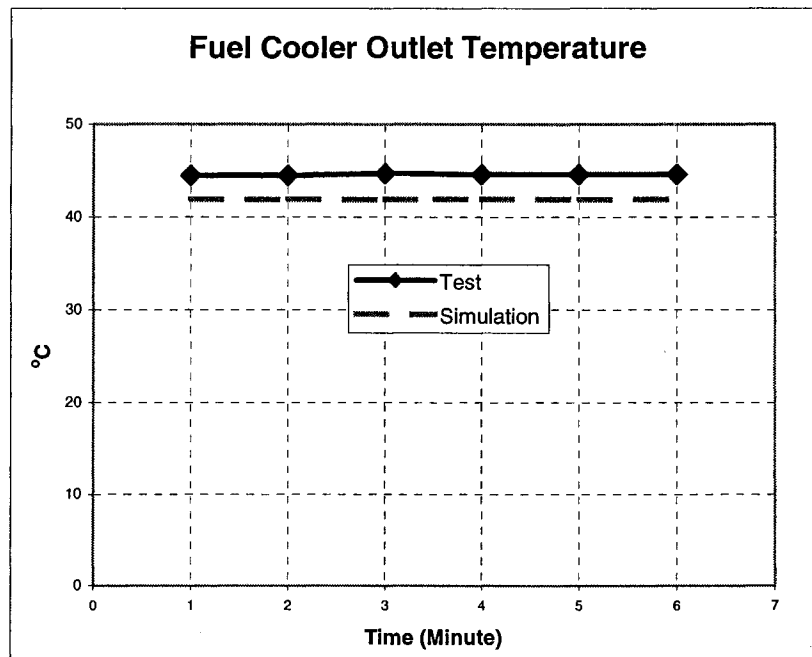


Figure 50. Comparing the simulation against the high-speed wind tunnel transport test for fuel cooler outlet temperature

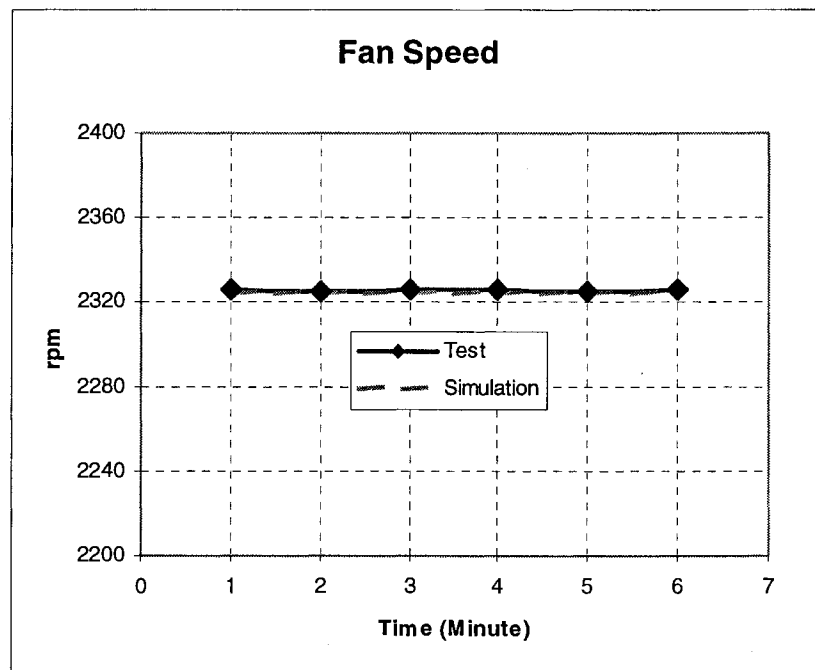


Figure 51. Comparing the simulation against the high-speed wind tunnel transport test for fan speed

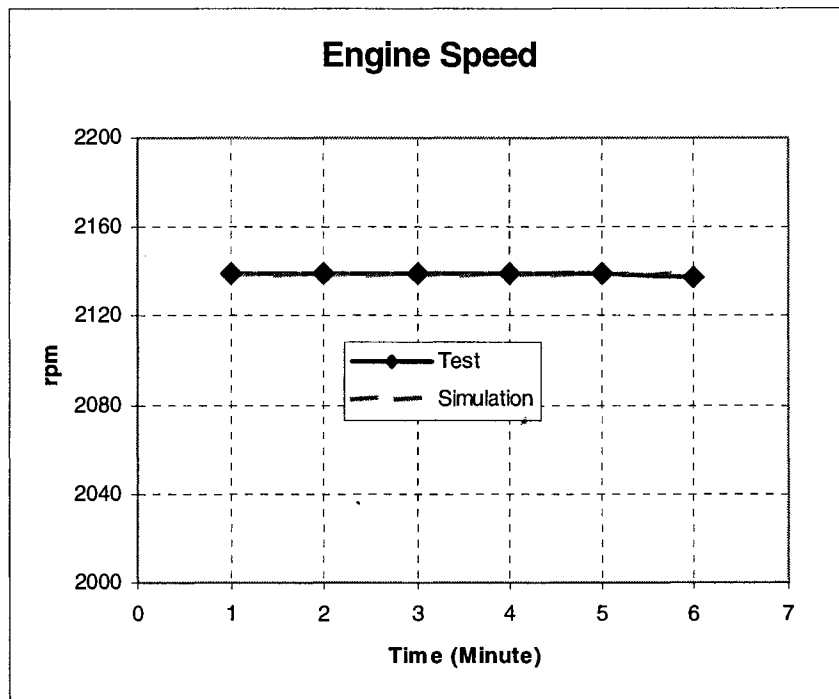


Figure 52. Comparing the simulation against the high-speed wind tunnel transport test for the engine speed

Averages of the six readings for the high-speed wind tunnel transport test results and simulation model were compared to find out the percentage differences. The percentage errors are listed in Table 22. By using the $\pm 3\%$ margin criteria, the only parameter that exceeds the limits is the fuel cooler outlet temperature with a value of 6.09%.

Table 22

Percentage Errors of the Simulation Results from the AXLE Test Data

Parameters	Average Test Data	Average of CEM	Percentage Error
Top Tank Temperature	94.7	94.62	0.08%
Intake Manifold Temperature	59.18	58.52	1.12%
Oil Cooler Inlet Temperature	100.1	100.28	0.18%
Oil Cooler Outlet Temperature	81.8	79.7	2.57%
Fuel Cooler Inlet Temperature	44.25	44.55	0.68%
Fuel Cooler Outlet Temperature	44.58	41.87	6.09%
Fan Speed (rpm)	2326	2324	0.07%
Engine speed (rpm)	2138.83	2138.70	0.01%

CHAPTER 5.

CONCLUSIONS, RECOMMENDATIONS AND SUMMARY

In the previous chapter, the findings were discussed and supporting data were reported. The results of abovementioned tests suggest that the comprehensive energy model representing the actual vehicle adequately.

In Chapter 5, the accuracy of this representation will be discussed in the guidance of the research questions. This chapter includes the following headings: Research Questions of the Study, Recommendations for Future Work, and Summary of the Study.

Research Questions of the Study

A set of two research questions was used as the basis of this study. The goal of this study was to create a comprehensive energy model for a tractor with certain accuracy.

The research questions were:

1. Is EASY5 simulation package adequate to create a comprehensive energy model for off-highway vehicles?
2. With what accuracy the comprehensive energy model represents the off-highway machines?

Based on the experience in the modeling process, the standard EASY5 component libraries supplied by MSC.Software and the EASY5 component libraries created in the Midwest off-road machinery manufacturing company were found reasonably adequate. Some additional programming effort needed in modeling the fan control mechanism and in incorporating the WAVE engine with the comprehensive energy model. Extremely slow simulation speed was observed when WAVE engine model integrated with the comprehensive energy model. This was because of the extremely small integration steps (in some cases 10^{-19} sec) that the WAVE engine model had to run in order to calculate the highly dynamic nature of the engine.

Based on comparison of the test data and the comprehensive energy model outputs for selected critical parameters, the $\pm 3\%$ margin of error was found to be reasonable for the accuracy of the model. Only the fuel cooler outlet temperature was out of this margin, which leads the author to conclude that a further refinement on the fuel cooling circuit was required. However, for the accuracy of the relatively more important critical parameters, such as the top tank temperature and the fan

speed (Burk, R., personal communication, June 1, 2004), the margin of error was even observed as less than $\pm 1\%$.

Recommendations for Future Work

Several recommendations can be made on how to use the comprehensive energy model for cost reduction:

1. Some of the components in the model can be replaced by the models of less costly ones in the market, to examine the effect on the rest of the components without actually buying and assembling them.
2. Removal of some whole subsystems, such as fuel cooler system, can be studied with the comprehensive energy model (Lafferty, C., personal communication, September 3, 2004).

It is recommended that there is a need for future research on increasing the speed of the EASY5 simulation model when it is incorporated with the WAVE engine model. Hence the model could be run at once.

Future research could include three-dimensional computational fluid dynamic analysis for a better understanding of the recirculation of air effect phenomenon.

Additional research is suggested in more and higher fidelity levels of each subcomponent of the model to investigate detailed information on the specific component. This will help the researcher to analyze the differences of each fidelity level of the component and utilize the most convenient one for the research.

It is also recommended that different fidelity levels of subcomponents can be brought together to investigate their effects on the simulation speed, the critical parameters, and so on. Hence, the researcher can optimize the simulation speed while acquiring more accurate data from the model.

Further research could include modeling the vehicle by using different simulation packages to investigate the performance differences in terms of simulation speed as well as model development time.

Summary of the Study

Utilizing machine and thermal system simulations (vehicle energy models) can be very helpful for vehicle manufacturing companies to develop a machine with acceptable component temperatures, less heat loads to the vehicle cooling systems, and reduced emissions that will also reduce overall product development cycle.

Energy models of vehicles were developed mostly in the automotive industry, and most of these studies were based on partial energy models.

The aim of this research study was to create a comprehensive energy model for agricultural machinery, which will be a basis for future work on similar products. A tractor model from a Midwest off-road machinery manufacturing company was selected as a starting point for modeling. The work in creating the model has been presented in detail. Verification of the simulation model has been carried out using the results from three different wind tunnel tests that have been conducted by the Midwest company; namely the PTO test, the AXLE test, and the high-speed wind tunnel transport test.

The critical parameters selected to be analyzed for each test were the top tank Temperature, the intake

manifold temperature, the oil cooler inlet temperature, the oil cooler outlet temperature, the fuel cooler inlet temperature, the fuel cooler outlet temperature, the fan speed, the engine speed, the PTO torque and the axle torque.

Based on the analysis of data, it was concluded that the comprehensive energy model is adequately representing the selected tractor model from the energy distribution and the component temperatures point of view. Therefore, it can be used for specific field missions that are not easy to conduct in a wind tunnel set up to acquire data for the critical parameters.

REFERENCES

- A Joint Venture of Industry and Government. (2001). *Off-Highway Vehicle Technology Roadmap*. U.S. Department of Energy. DOE/EE-0261, December 2001.
- Assanis, D., Bryzik, W., Chalhoub, N., Filipi, Z., Henein, N., Jung, D., et al. (1999). Integration and use of diesel engine, driveline and vehicle dynamic models for heavy duty truck simulation. *SAE Technical Paper Series*, No: 1999-01-0970.
- Assanis, D., Filipi, Z., Gravante, S., Grohnke, D., Gui, X., Louca, L. et al. (2000). Validation and use of Simulink integrated, high fidelity, engine-in-vehicle simulation of the international class VI truck. *SAE Technical Paper Series*, No: 2000-01-0288.
- Chern, T.L., Chang, J., & Chang, G.K. (1997). DSP-based integral variable structure model following control for brushless dc motor drives. *IEEE Transactions on Power Electronics*, 12(1), 53-63.
- Day, T. D. (1996). Validation of the EDVSM 3-dimensional vehicle simulator. *SAE Technical Paper Series*, No: 970958, p. 251-287.
- Diaz-Calderon, A. (2000). *A Composable Simulation Environment to Support the Design of Mechatronic Systems*. Unpublished doctoral dissertation, Carnegie Mellon University, Pittsburg, Pennsylvania.
- Diesel Engine Fundamentals, (2001). Retrieved September 13, 2004, from <http://www.DieselNet.com/tech/diesel-fund.html>
- Diesel & Gas Turbine Publications, (2000). Advances in engine analysis software. *Diesel Progress North American Edition*. 66(2).
- Dulger, L.C.T., & Uyan, S. (1997). Modeling, simulation and control of a four-bar mechanism with a brushless servomotor. *Mechatronics: Mechanics, electronics, control*, 7(4), 369-383.
- Dvorak, P. (2003). A better way to model fluid-power systems. *Machine Design*, 75(19).

- Easy5 Library Documentation (2002). General Purpose & Interactive Simulation Libraries Manual. MSC.Software Corporation, Bellevue, WA. p. GB1 - GB2.
- EASY5 Overview. (n.d.). Retrieved August 29, 2004, from <http://www.adams.com/easy5/overview.html>
- Easy5 User Guide (2003). MSC.Software Corporation. Bellevue, WA.
- Fales, R. (2004). *Robust Control Design for an Electrohydraulic Wheel Loader System with a Human-in-the-loop Assessment in a Virtual Environment*. Unpublished doctoral dissertation, Iowa State University, Ames, IA.
- Favate, S. (2002). MSC.Software/Boeing - 2: Buys Model, Simulation Software. *Dow Jones News Service*. Newswires, 201-938-5400.90
- Federal Register, (1998). Retrieved September 21, 2004, from <http://www.epa.gov/fedrgstr/EPA-AIR/1998/December/Day-11/a32304.htm>
- Fritz, N., ElSawy, A., Modler, H., and Goldhahn, H. (1997). Development of an analysis software to synthesize gear-cam-disc mechanisms. *International Mechanical Engineering Congress*, Dallas, TX.
- Fritz, N., ElSawy, A., Modler, H., and Goldhahn, H. (1999). Simulation of mechanical drives with EASY5. *Computers & Industrial Engineering*, 37(1,2), 231-234.
- Fritz, N. (1999). *Simulation of Optimal Drive Systems Consisting of Gear-Cam Mechanisms with Brushless DC Servomotors*. Unpublished doctoral dissertation, University of Northern Iowa, Cedar Falls, IA.
- Gould, L.S. (2003). What auto can learn from aero: Simulating without prototypes. *Automotive Design & Production*, 115(10).
- Harbach, A. (1999). Development of extended systems models for GKN Westland Helicopters Simulation Facility. Retrieved August 29, 2004, from http://www.informatics.bangor.ac.uk/~dewi/ci_grp/UGrad_Dissertations/andy_dissertation.PDF

- HyperDictionary.com, (2003). Retrieved September 22, 2004, from <http://www.hyperdictionary.com/dictionary/windage>
- Johnson, J.L. (2000). The final chapter on simulation programs. *Hydraulics & Pneumatics*, 53(5).
- Joshi, A., and Jayan, PG. (2002). Modeling and simulation of aircraft hydraulic system. *AIAA Modeling and Simulation Conference and Exhibit*, 05-08 August, Monterey, California, USA.
- Miller, M. (1997, June). Integrated design environment for mixed electronic-mechanical systems. *Electronic Engineering*, 24.
- MSC.Easy5 Thermal Hydraulic Library Guide, (2003). MSC.Software Corporation. Bellevue, WA.
- Ramanata, P. (1998). *Optimal vehicle path generator using optimization methods*. Unpublished master thesis, Virginia Polytechnic Institute and State University, Blacksburg, Virginia.
- Saarilahti, M. (2002). *Development of a Protocol for Ecoefficient Wood Harvesting on Sensitive Sites: Project Deliverable D2 on Soil Interaction Model*. Department of Forest Resource Management, University of Helsinki.
- Sandberg, T. (2001). *Heavy truck modeling for fuel consumption simulation and measurements*. Unpublished master's thesis, Linköping University, Linköping, Sweden.
- Smith, D.E., and Starkey, J.M. (1995). Effects of Model Complexity on the Performance of Automated Vehicle Steering Controllers: Model development, Validation and Comparison. *Vehicle System Dynamics*, 24, 163-181.
- Society of Automotive Engineers, (1992, November). Dynamic system development tool. (Boeing Co.'s Easy5x software) (Simulation products/applications). *Automotive Engineering*, 58.
- Soil Science Society of America (2004). Retrieved October 13, 2004, from http://www.soils.org/cgi-bin/gloss_search.cgi?QUERY=cone+index&SOURCE=3

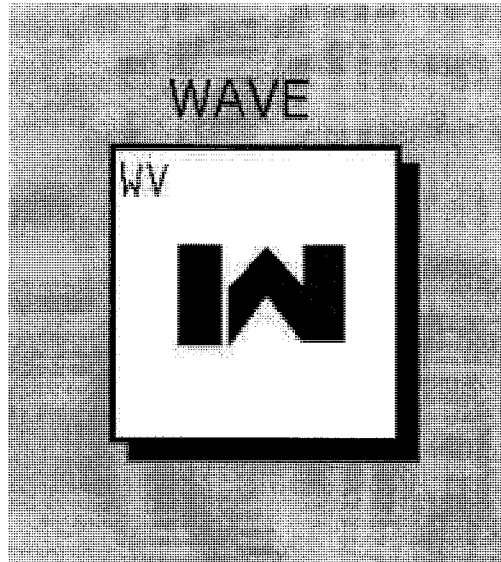
Valeo (2002). *Valeo Advanced Thermal Systems to be featured on future Chrysler group vehicle*. Retrieved August 29, 2004, from http://www.valeo.com/gb/news/news_admin.asp?news_id=278

Yang, Z., Bozeman, J., Shen, F.Z. and Acre, J.A. (2003). *CFRM Concept at Vehicle Idle Conditions*. *SAE Technical Paper Series*, No: 2003-01-0613.

APPENDIX A

HELP DOCUMENT FOR RS LIBRARY USED CONNECTING WAVE AND EASY5

WV - WAVE Link



Description

This block starts and connects to a WAVE model, which runs as a separate process on the same machine running EASY5. Simulation data are exchanged with the WAVE model once per EASY5 time step. During data exchanges, WAVE's actuators are passed values from EASY5 and the values of WAVE's sensors are passed to EASY5.

Only one WAVE component is allowed in an EASY5 model.

Parameters

Component Dimension:

M: The Number of actuators in the WAVE model
N: The number of sensors in the WAVE model

Inputs:

ACT(M): Instantaneous actuator values
WIF: WAVE input file name prefix (see below)
MAP: WAVE map mode for map-based running
 0=none (Normal transient run)
 1=new (Make new interpolation maps)
 2=merge (Merge with existing maps)
 3=old (Use existing maps)
AP(M): Actuator pin numbers to connect to in WAVE
SP(N): Sensor pin numbers to connect to in WAVE

Outputs:

SEN(N): Instantaneous sensor values

Since there are no useable text fields within a macro component to store a WAVE input file name, input prefixes are restricted to integer numbers, giving rise to input file names such as 1.dat, 54321.dat etc.

APPENDIX B

POWER SHIFT TRANSMISSION AND PTO

B1 Gear Ratios and Mechanical Efficiencies for PST

Gear	Ratio	Efficiency
5 Reverse	-0.7016	0.956
4 Reverse	-0.7016	0.956
3 Reverse	-0.2492	0.956
2 Reverse	-0.2162	0.956
1 Reverse	-0.0807	0.956
1 Forward	0.0863	0.951
2 Forward	0.1156	0.951
3 Forward	0.1538	0.951
4 Forward	0.2061	0.951
5 Forward	0.2311	0.97
6 Forward	0.2664	0.97
7 Forward	0.3095	0.97
8 Forward	0.3569	0.97
9 Forward	0.4121	0.97
10 Forward	0.4751	0.97
11 Forward	0.5519	0.97
12 Forward	0.6364	0.97
13 Forward	0.75	0.97
14 Forward	1.0045	0.97
15 Forward	1.3374	0.97
16 Forward	1.7913	0.97
PTO	0.4545	0.985

B2 Windage Losses for PST

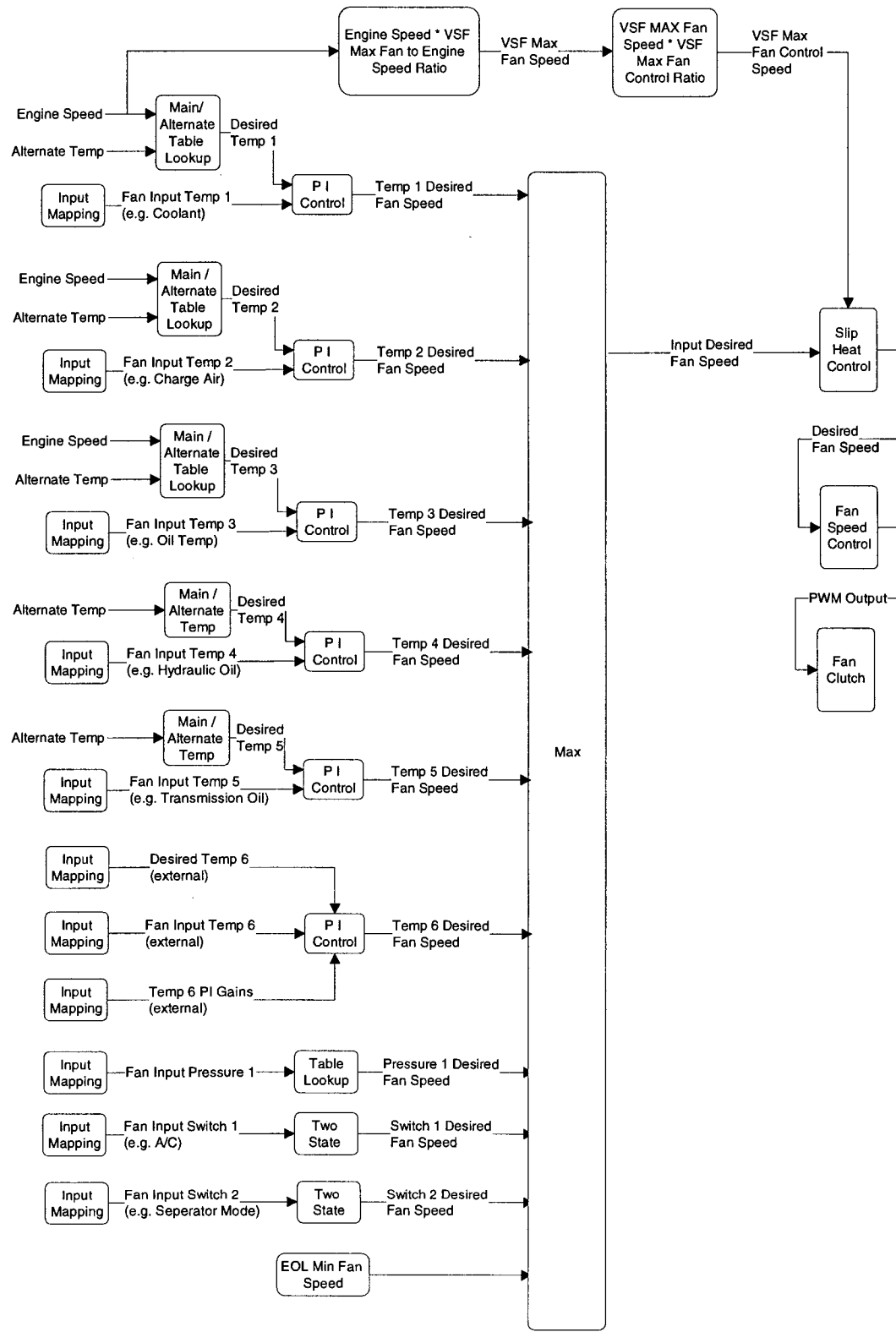
Transmission Speed (rpm)	Windage Loss (Nm)
0	0
500	4.78
1000	9.56
1500	15.93
2000	21.5
2500	28.67
2775	32.02
3000	35.04
3242	38.31
3500	42.32
4000	49.17
4163	57.27
4500	70.67

B3 Windage Losses for PTO Drive and Clutch

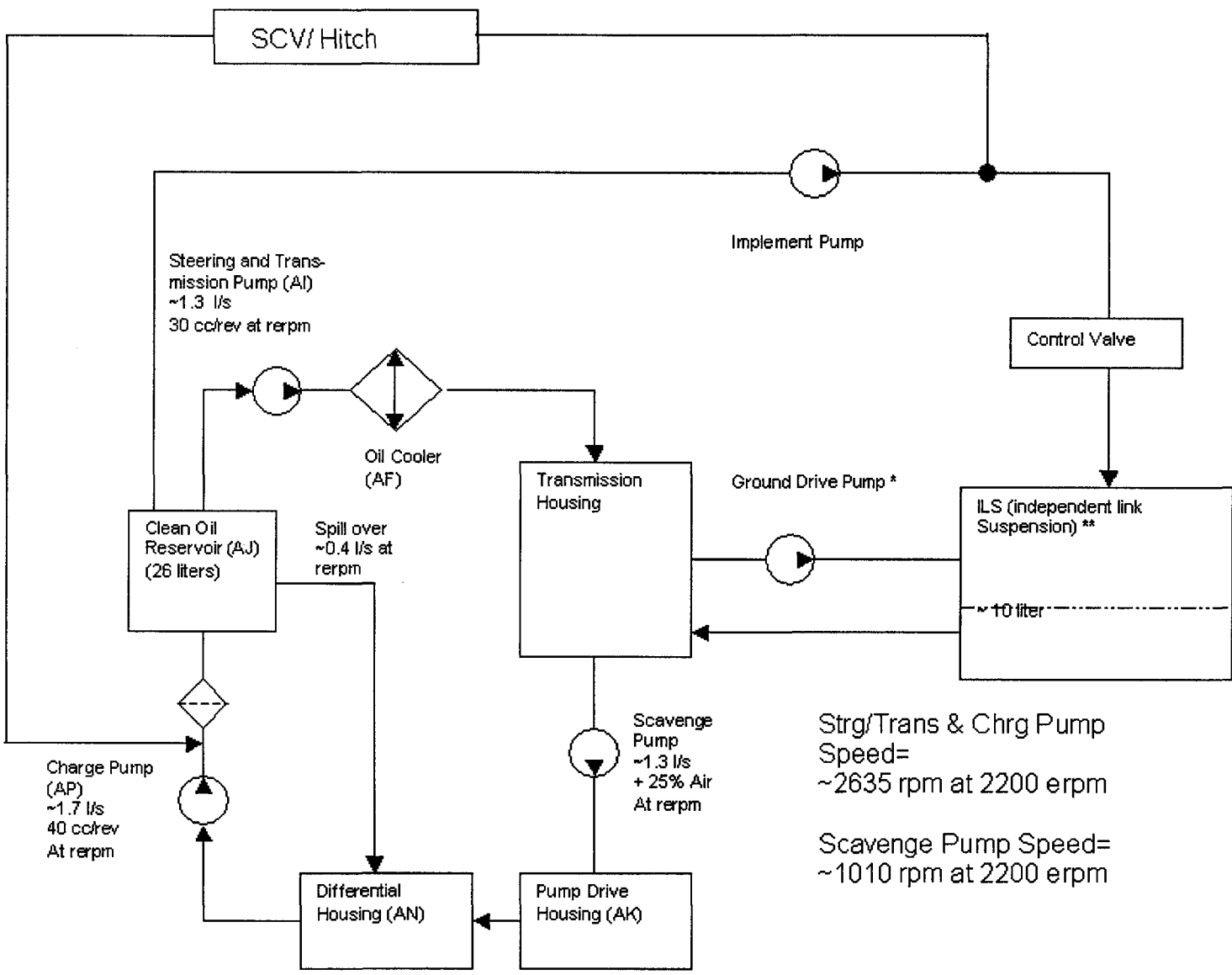
PTO Speed (rpm)	Windage Loss (Nm)
0	0
500	4.78
1000	9.56
1500	14.65
2000	19.11
2500	23.7
2775	26.51
3000	28.4
3242	30.1
3500	30.85
4000	32.12
4163	33.3
4500	34.6

APPENDIX C

OVERALL STRATEGY DIAGRAM OF THE VARIABLE SPEED FAN CONTROL

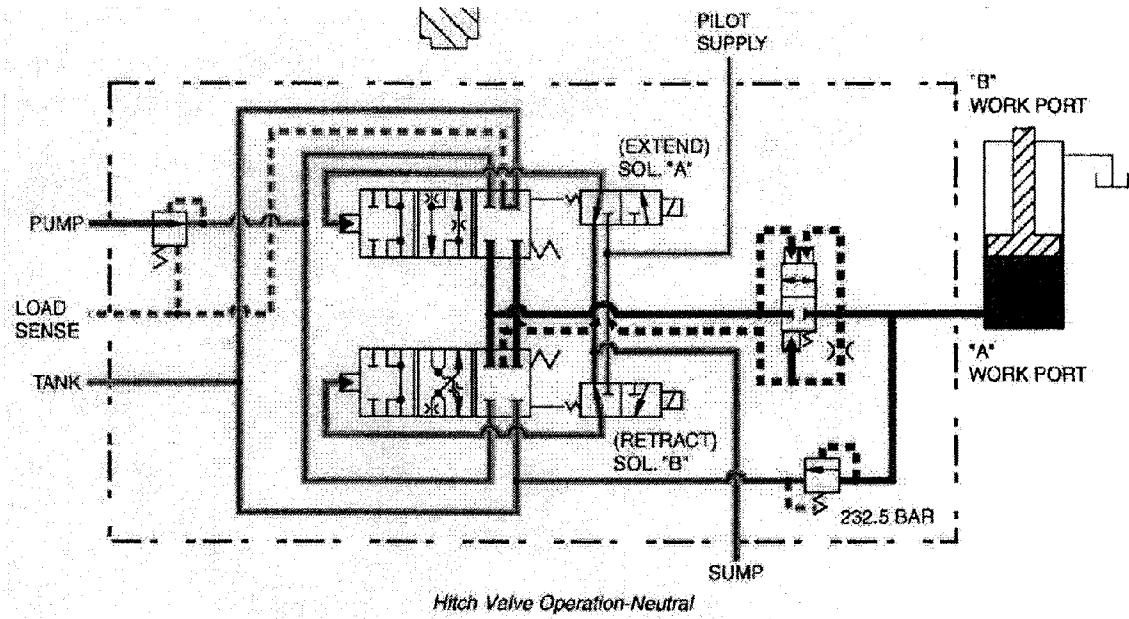


APPENDIX D
TRANSMISSION AND HYDRAULIC OIL CIRCUIT

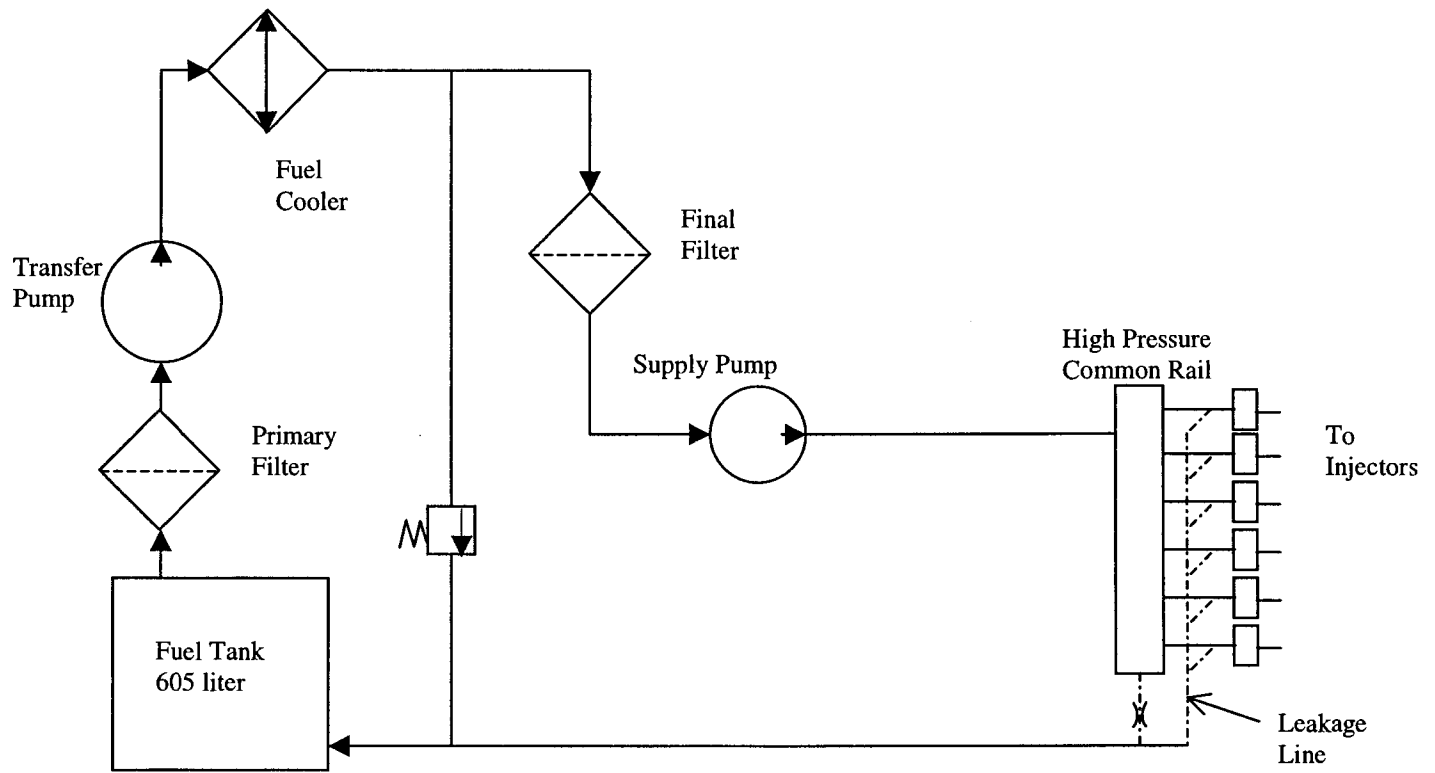


D1 The Schematic for Transmission Oil Circuit

D2 The Schematic for Implement Oil Circuit



D3 The Schematic for the Fuel Circuit



D4 The Test Results for Recirculation of Air Effect
for Tail Wind

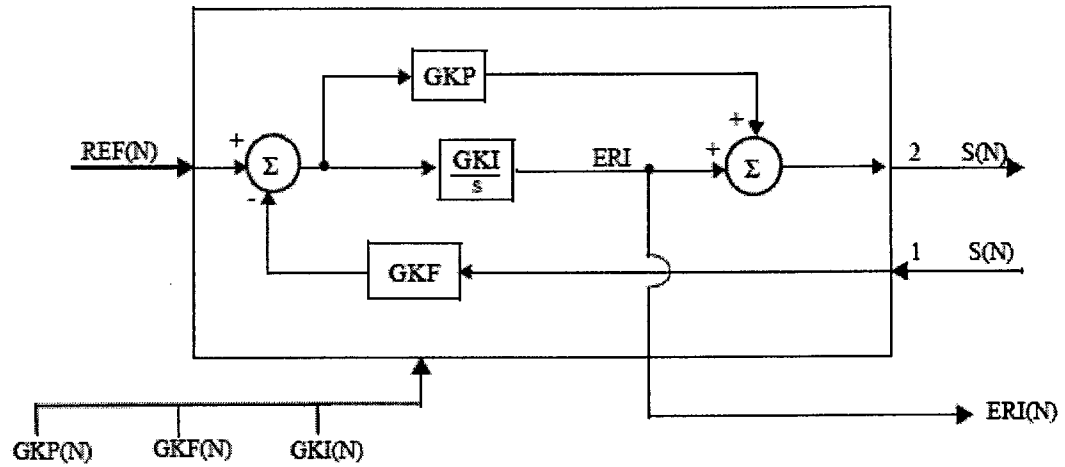
Run #	Wind Direction (T/H)	Wind Speed (kph)											
				AVG	MIN	MAX	1	2	3	4	5	6	
8	T	11											
			Air, Ambient Front of Tractor(WEST)	°C	43.8	43.3	44.3	44.0	44.3	43.4	43.3	43.7	44.3
			Air, Ambient Rear of Tractor(EAST)	°C	40.5	39.6	41.4	41.4	40.8	39.8	39.6	40.3	41.0
		Air, Avg Grille Screen	°C	52.4	51.9	53.3	51.9	52.0	52.2	52.0	53.0	53.3	
10	T	9											
			Air, Ambient Front of Tractor(WEST)	°C	43.9	43.1	44.7	43.9	44.7	44.3	43.5	43.1	43.7
			Air, Ambient Rear of Tractor(EAST)	°C	40.5	39.6	41.5	40.9	41.5	40.8	39.8	39.6	40.3
		Air, Avg Grille Screen	°C	51.9	51.4	52.3	52.1	52.3	52.1	51.9	51.4	51.6	
12	T	7											
			Air, Ambient Front of Tractor(WEST)	°C	45.8	45.4	46.1	45.4	45.8	45.9	45.9	46.1	45.9
			Air, Ambient Rear of Tractor(EAST)	°C	42.8	42.6	43.1	42.6	42.6	42.8	43.1	43.1	42.8
		Air, Avg Grille Screen	°C	52.4	51.6	52.8	52.0	52.2	52.7	52.8	52.8	51.6	
14	T	5											
			Air, Ambient Front of Tractor(WEST)	°C	46.5	45.8	47.5	46.0	45.9	47.1	47.5	46.4	45.8
			Air, Ambient Rear of Tractor(EAST)	°C	43.4	42.5	44.3	42.8	43.7	44.3	44.3	42.6	42.5
		Air, Avg Grille Screen	°C	51.4	50.1	52.8	51.0	52.8	52.4	51.6	50.1	50.4	
16	T	3											
			Air, Ambient Front of Tractor(WEST)	°C	50.3	49.0	51.1	50.7	51.1	50.1	49.0	49.9	51.1
			Air, Ambient Rear of Tractor(EAST)	°C	46.7	45.1	47.9	47.6	47.6	45.1	45.4	46.5	47.9
		Air, Avg Grille Screen	°C	51.6	48.7	52.8	52.7	52.6	48.7	50.7	52.1	52.8	

D5 The Test Results for Recirculation of Air Effect

for Head Wind

		AVG	MIN	MAX	1	2	3	4	5	6
Air, Ambient Front of Tractor(WEST)	Deg C	25.8	25.6	25.9	25.9	25.6	25.9	25.6	25.9	25.9
Air, Ambient Rear of Tractor(EAST)	Deg C	31.8	31.4	32.1	31.9	31.4	31.8	32.1	31.8	31.9
Air, Avg Grille Screen	Deg C	26.4	26.2	26.7	26.5	26.2	26.7	26.4	26.5	26.2
Wind Speed Km/Hr	Km/Hr	3.29	1.25	5.05	1.41	3.54	1.25	4.21	4.27	5.05

D6 Theory for PI controller



INPUTS

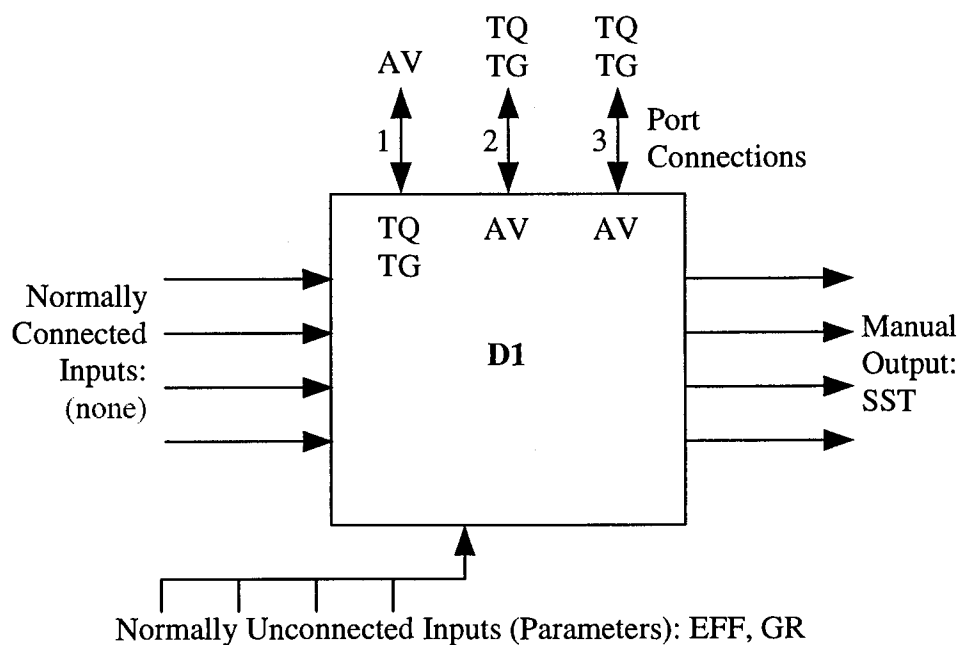
NAME	PORT NO.	DESCRIPTION	UNITS
REF(N)		Controller input variable (Input command)	
S(N)	1	Controller feedback variable	
GKP(N)		Proportional control gain	
GKF(N)		Feedback gain	
GKI(N)		Integral control gain	

OUTPUTS

NAME	PORT NO.	DESCRIPTION	UNITS
ERI(N)		Integrated error signal (Continuous state)	
S(N)	2	Controller output (Variable)	

Equations: $ERI = GKI [REF - GKF \cdot S1]$
 $S2 = ERI + GKP [REF - GKF \cdot S1]$

D7 Simple Differential (D1)



INPUTS

NAME	PORT	DESCRIPTION	UNITS
TQ	1	Input torque on drive shaft	N-m
TG	1	Sign convention of TQ1 (+Drives, -Loads)	-
AV	2	Angular velocity of axle shaft 2	rpm
AV	3	Angular velocity of axle shaft 3	rpm
EFF	-	Torsional efficiency	-
GR	-	Ratio of drive shaft (1) to driven (2 & 3)	-

OUTPUTS

NAME	PORT	DESCRIPTION	UNITS	TYPE
SST	-	Powering/braking switch	-	Switch
AV	1	Angular velocity of drive shaft	rpm	Variabl e
TQ	2	Torque delivered to shaft 2	N-m	Variabl e
TQ	3	Torque delivered to shaft 3	N-m	Variabl e
TG	2	Sign convention of TQ2	+1, Drives	Variabl e
TG	3	Sign convention of TQ3	+1, Drives	Variabl e

DESCRIPTION

This component provides a simple differential representation. Axle shaft speeds are averaged to provide the driven shaft speed. Input torque is ratio up/down per the input parameter GR, reduced per the efficiency parameter EFF, and split evenly between the two output shafts.

EQUATIONS

In the following equations, a distinction is made between *braking* and *driving*. This status is discern from the product

$$SST = \text{sgn} ((AV2 + AV3) * TQ1 * TG1) \text{ (direction switch)}$$

If the average shaft speeds are in the same sense as the applied torque, then the torque is *driving* the load.

Otherwise the torque is *braking*, or retarding, the load.

Therefore,

$$SST = \begin{cases} -1 & \text{if } \textit{braking} \\ +1 & \text{if } \textit{driving} \end{cases} \quad (1)$$

$$AV1 = 0.5 GR (AV2 + AV3) \quad (2)$$

The torque throughput of this component is affected by its inefficiency. During *driving*, the traditional product is used ($EFF < 1$) to reduce the effective throughput torque. During *braking*, the throughput is increased by dividing by the efficiency parameter. The physical justification for this is that the torsional losses aid the input torque (are additive with) when the drivetrain is retarding the load and reduce the throughput torque in normal operation.

$$TQ2 = \begin{cases} \frac{GR * TQ1}{EFF} & \text{if } \textit{braking} \\ GR * TQ1 * EFF & \text{if } \textit{driving} \end{cases} \quad (3)$$

$$TQ3 = TQ2 \quad (4)$$

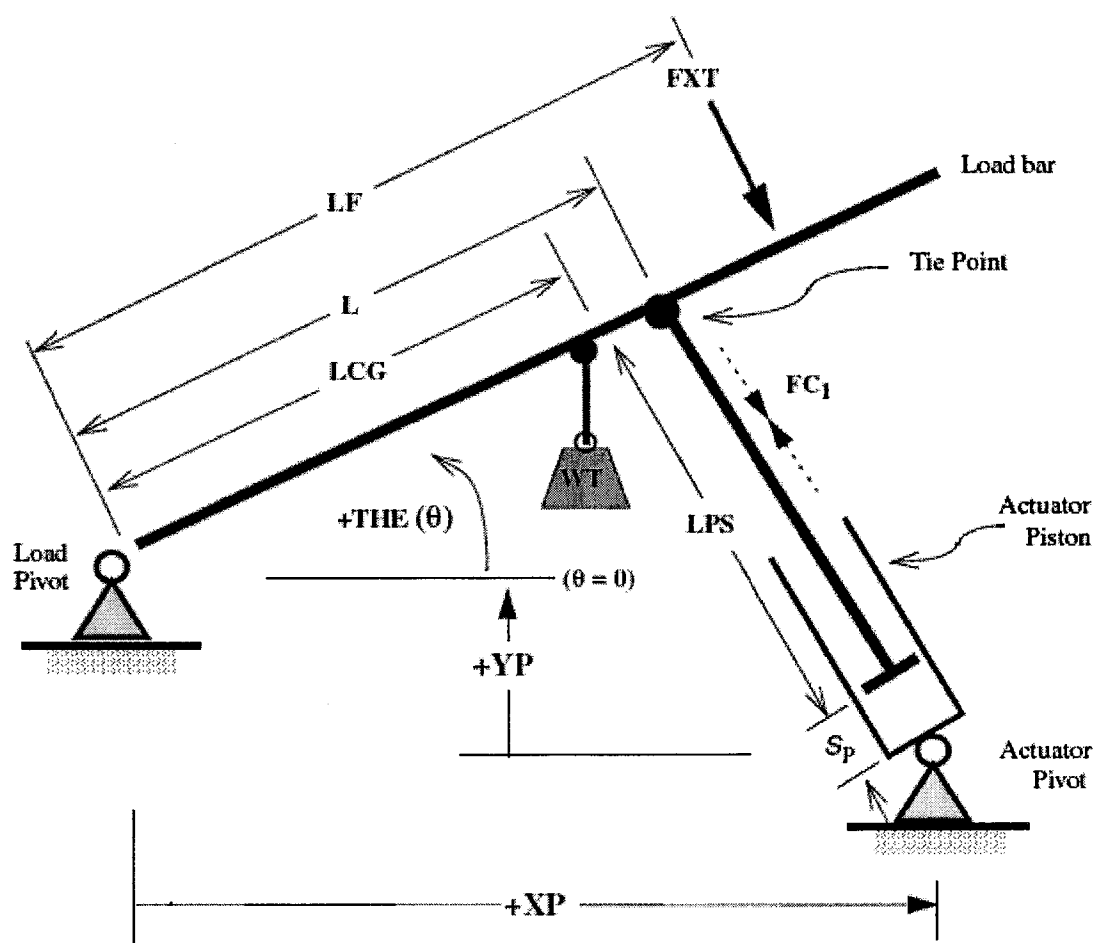
$$TG2 = TG1 \quad (5)$$

$$TG3 = TG1 \quad (6)$$

D8 Cone Index Properties of Soil vs. Vehicle
Operability

Cone Index (kPa)	Bearing description
0 to 21	Approximately at the liquid limit. No practical bearing value
40 to 62	A man has difficulty on the soil without sinking
103 to 165	A special tracked vehicle can travel
186 to 228	A small tractor can travel
276 to 352	A large tractor can travel
372 to 497	A jeep can travel
517 to 662	Track mounted heavy bulldozers
683 to 935	Passenger cars can travel
1034 plus	Any land vehicle can travel

D9 MP - Pivoting Mechanical Load Body Dynamics

General Discussion

This component is one of a group of mechanical load components designed to connect to actuator components. MP represents an offset rigid bar connected by a pivoting tie point to an actuator piston. A typical example of this sort of arrangement is using a linear actuator to elevate a control arm or truck bed.

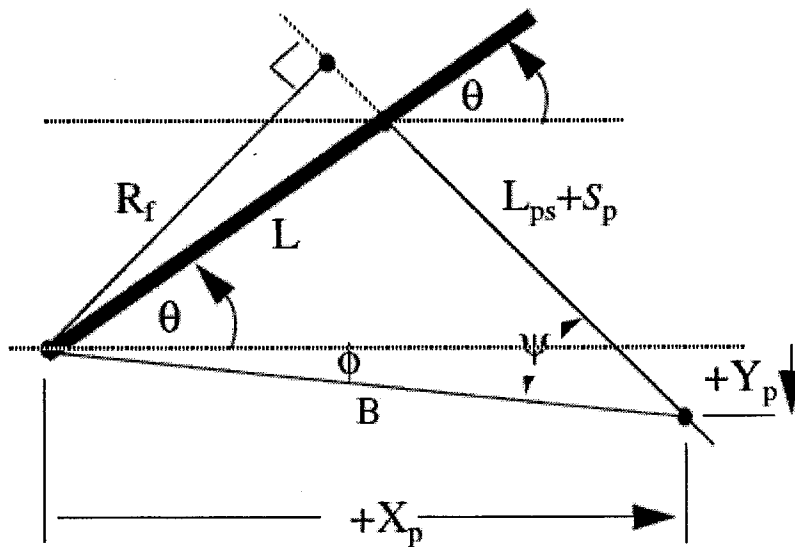
Input FP_1 represents the net static force from the connected actuator. A positive value of FP_1 tends to extend the connected actuator and rotate the MP load bar counterclockwise. FP_1 does not account for the acceleration of the actuator piston mass. The acceleration of the piston mass is however considered in the MP component logic that calculates force FC_1 .

Note: Parameter MP should have the same value as parameter MP of the connected actuator component. In addition, you MUST set the minimum travel limit for the actuator to a reasonable number (usually zero), as the connected output SP from the actuator is the position relative to the minimum travel position of the piston. If this limit is left at the default number (-10^{20}), the MP output position will remain at 90 degrees.

MP offers an alternative to the usual approach of using a very stiff spring or compliance to model a rotating inertial load rigidly connected to an actuator piston mass. The stiff spring approach is somewhat undesirable as it often adds a high frequency eigenvalue pair with a low damping ratio.

Geometry Considerations

For convenience, the constant angle ϕ is defined as the angle between the horizontal and the line B. S_p represents the actuator piston displacement (input SP_1).



From the geometry,

$$2LB \cos(\theta + \phi) = L^2 + B^2 - (L_{ps} + S_p)^2$$

$$L \sin(\theta + \phi) = (L_{ps} + S_p) \sin \psi$$

$$B^2 = X_p^2 + Y_p^2$$

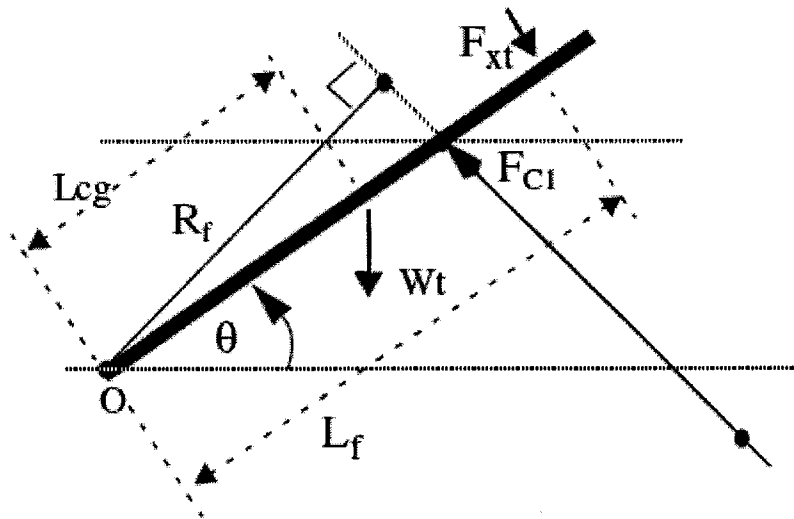
Additionally,

$$LB \dot{\theta} \sin(\phi + \theta) = \dot{S}_p (S_p + L_{ps}), \text{ and}$$

$$LB [\ddot{\theta} \sin(\phi + \theta) + \dot{\theta}^2 \cos(\phi + \theta)] = \ddot{S}_p + \dot{S}_p (S_p + L_{ps})$$

Load Bar Dynamics

The angular acceleration of the load bar is given by summing the torques about the load pivot O.



From the load diagram above, a summation of torques about the pivot O yields:

$$J\ddot{\theta} = F_{C1}R_f - F_{XT}L_f - W_T L_{CG} \cos \theta$$

$$R_f = B \sin \psi$$

If component MP is connected to an actuator from the HC library, the force F_{C1} is related to input force F_{P1} by:

$$F_{C1} = F_{P1} - m_p \ddot{S}_p,$$

where m_p is the actuator piston mass. If MP is not connected to an actuator component, $F_{C1} = F_{P1}$. Substituting

for F_{C1} and S_p , the torque summation equation yields

expressions for $\dot{\theta}$ and F_{C1} :

$$\dot{\theta} = \frac{M_a + M_b}{J_{\text{net}}}, \text{ where}$$

$$M_a = F_{P1}R_f - F_{XT}L_F - W_T L_{CG} \cos \theta$$

$$M_b = \frac{m_p R_f}{(S_p + L_{ps})} \cdot [S_p'^2 - LB \dot{\theta}^2 \cos(\phi + \theta)]$$

$$J_{\text{net}} = J + \frac{m_p R_f}{(S_p + L_{ps})} \cdot LB \sin(\phi + \theta)$$

The quantities S_p (input AV_1) and S_p' represent the piston velocity and acceleration respectively.

The force F_{C1} is then given by:

$$F_{C1} = F_{P1} - m_p S_p', \text{ where}$$

$$S_p' = \frac{[LB[\ddot{\theta} \sin(\phi + \theta) + \dot{\theta}^2 \cos(\phi + \theta)] - S_p'^2]}{(S_p + L_{ps})}, \text{ and}$$

$$\dot{\theta} = \frac{S_p'(S_p + L_{ps})}{LB \sin(\phi + \theta)}$$

Note: The value for the piston mass m_p is obtained internally by searching for the assumed name (MP) of the attached actuator piston mass in the list of model parameter names. To enable this approach, the name of the piston mass in the attached actuator component must not be redefined with a user-defined name. If the piston mass

parameter name is not found internally, the value of parameter MP of this component is used for the piston mass. Otherwise, parameter MP of this component is not used.

Note 2: Observe that the distances XP and YP are defined so that positive distances are in the direction of the arrows on the diagram. L_{PS} must be in the range

$$B-L < L_{PS} < B+L-S_{pmax} .$$